KATHOLISCHE UNIVERSITÄT
EICHSTÄTT-INGOLSTADT

Mathematische Modelle und Metaheuristiken zur Optimierung der Transportplanung von Drohnen: Fallbeispiele in der Paketauslieferung und im Gesundheitswesen

Mathematical models and metaheuristics for optimizing the transportation planning of drones:
Case studies in parcel delivery and healthcare services

Alexander Rave

Kumulative Dissertation
zur Erlangung des akademischen Grades
Doctor rerum politicarum (Dr. rer. pol.)

November 2023

Referent: Prof. Dr. Pirmin Fontaine

Korreferent: Prof. Dr. Alena Otto

Danksagung

Für die vorliegende Dissertation möchte ich mich im Folgenden für die Unterstützung bedanken, die ich von vielen Seiten erhalten habe. Zunächst möchte ich mich ganz herzlich bei meinem Doktorvater Prof. Dr. Pirmin Fontaine für seine exzellente Betreuung, die mir gewährte Forschungsfreiheit und das Vertrauen in meine Promotion bedanken. Ich konnte stets auf sein schnelles, konstruktives und kritisches Feedback zählen, welches meine Forschung maßgeblich weiterentwickelt hat. Außerdem möchte ich Prof. Dr. Heinrich Kuhn für die Möglichkeit der Mitarbeit an seinem Lehrstuhl und die hervorragende Zusammenarbeit während dreier Publikationen danken. Mein besonderer Dank gilt auch Prof. Dr. Harry Wagner für die abwechslungsreiche Zusammenarbeit im MEDinTime Projekt. Ich danke auch Prof. Dr. Alena Otto für die Übernahme des Zweitgutachtens.

Außerdem danke ich Birgit Jürgens dafür, dass sie mir stets tatkräftig zur Seite stand und mich bei organisatorischen Aufgaben unterstützte. Zudem danke ich meinen Kollegen für die wertvollen Anregungen und Ideen bei gemeinsamen Forschungsworkshops: Dr. Stefan Voigt, Dr. Markus Frank, Tobias Potoczki, Daniel Müllerklein, Simon Mader, Johannes Gückel, Moritz Hundhammer, Dr. Sandra Zajac und Tamara Beschler.

Mein herzlicher Dank gilt auch meinen Eltern Maria und Ulrich, meinem Bruder Christian und seiner Frau Katja, meinem Sohn Jonathan sowie Josey und Armani, die mir stets beistanden und mich aufmunterten, sodass ich sehr viel Freude auf meinem Weg zur Promotion hatte.

Zuletzt gilt mein herzlichster Dank meiner langjährigen Partnerin und Verlobten Linda, die neben ihrer eigenen Promotion stets ein offenes Ohr für mich hatte. Nach diesem Lebensabschnitt freue ich mich auf viele weitere Jahre voller gemeinsamer Erlebnisse und Glück!

Alexander Rave

Kurzzusammenfassung

Die vorliegende kumulative Dissertation befasst sich mit vier Problemstellungen der Transportplanung im Falle der Übernahme des Paket- und Medikamententransports durch Lieferwagen und Drohnen. Folgende vier Artikel sind Hauptbeiträge der Dissertation:

1. Rave, A., Fontaine, P., Kuhn, H., 2023. Drone location and vehicle fleet planning with trucks and aerial drones. European Journal of Operational Research 308 (1), 113–130.
2. Rave, A., 2023. Two-indexed formulation of the traveling salesman problem with multiple drones performing sidekicks and loops. Working paper.
3. Rave, A., Fontaine, P., Kuhn, H., 2023. Cyclic stochastic inventory routing with reorder points and recourse decision for an application in medical supply. Working paper.
4. Rave, A., Fontaine, P., Kuhn, H., 2023. Drone fleet planning and battery allocation for emergency resupply of pharmacies and ambulances. Working paper.

   Die veröffentlichten bzw. eingereichten Versionen der Beiträge können sich leicht von den Versionen in dieser Dissertation unterscheiden (z.B. Gestaltung der Tabellen). Inhalte bleiben hiervon unberücksichtigt, mit Ausnahme weiterer Anpassungen von Beiträgen während des Review Prozesses.

Der erste Beitrag thematisiert die Fahrzeugflottenplanung und Zuweisung von Drohnen zu Mikrodepots, wenn Lieferwagen und Drohnen den Transport von Paketen in der letzten Meile übernehmen. Im Vordergrund stehen die taktischen Entscheidungen, welche Kombination von Auslieferungsformen mit Lieferwagen und Drohnen optimal wäre sowie die Ausgestaltung der Fahrzeugflotte. Die Problemstellung wird als gemischt-ganzzahliges lineares Programm (MILP) modelliert. Zudem wird eine adaptive große Nachbarschaftssuche (ALNS) eingeführt, die neue problemspezifische Operatoren beinhaltet.

Der zweite Beitrag fokussiert sich auf die operative Tourenplanung eines Lieferwagens, welcher mit mehreren Drohnen ausgerüstet ist. Hierfür wird ein effizientes MILP entwickelt, welches ein kommerzieller Solver schneller lösen kann als vergleichbare MILPs für eine Ein-Drohnen Problematik aus der Literatur.

Der dritte Beitrag optimiert die simultane Bestands- und Tourenplanung für die Belieferung von Krankenhäusern unter der Berücksichtigung ihrer Lagerhaltungspolitiken. Es wird analysiert, welchen Einfluss Drohnen als Vehikel für Notfalltransporte zur Vermeidung von Fehlmengen haben. Die Problemstellung wird als zweistufiges stochastisches Programm präsentiert und eine problemspezifische ALNS wird entwickelt, welche einen innovativen Algorithmus zur Bestimmung von Bestellpunkten innerhalb der Lagerhaltungspolitiken beinhaltet.

Der vierte Beitrag thematisiert die Ausgestaltung der Drohnenflotte für die Belieferung von Apotheken und Krankenwagen im Einsatz durch einen Großhändler. Hierfür wird die Drohnenflotte in einer ereignisdiskreten Simulationsstudie hinsichtlich der Kosten bzw. der CO_2-Emissionen optimiert.

Abstract

This cumulative dissertation addresses four problems in transportation planning in the case of delivery trucks and drones taking over parcel and medicine delivery. The following four articles are the main contributions of the dissertation:

1. Rave, A., Fontaine, P., Kuhn, H., 2023. Drone location and vehicle fleet planning with trucks and aerial drones. European Journal of Operational Research 308 (1), 113–130.
2. Rave, A., 2023. Two-indexed formulation of the traveling salesman problem with multiple drones performing sidekicks and loops. Working paper.
3. Rave, A., Fontaine, P., Kuhn, H., 2023. Cyclic stochastic inventory routing with reorder points and recourse decision for an application in medical supply. Working paper.
4. Rave, A., Fontaine, P., Kuhn, H., 2023. Drone fleet planning and battery allocation for emergency resupply of pharmacies and ambulances. Working paper.

   The published or submitted versions of the papers may differ slightly from the versions in this dissertation (e.g., design of tables). Contents are not affected, with the exception of further adjustments to working papers during the review process.

The first paper covers vehicle fleet planning and assignment of drones to microdepots when both trucks and drones can handle the last-mile delivery of packages. The focus is on tactical decisions as to which combination of delivery methods with trucks and drones is optimal, as well as the number of trucks, drones, and microdepots used. The problem is modeled as a mixed-integer linear program (MILP). In addition, an adaptive large neighborhood search (ALNS) is introduced, which includes new problem-specific operators.

The second paper focuses on optimizing the operational routing of a truck that is equipped with multiple drones. For this purpose, an efficient MILP has been developed, which a commercial solver can solve faster than comparable MILPs from the literature for a one-drone problem.

The third paper simultaneously optimizes inventory and routing for clinic supplies, while taking their inventory policies into account. The influence of drones as vehicles for emergency transport to avoid shortages is analyzed. The problem is presented as a two-stage stochastic program, and a problem-specific ALNS is developed, which includes an innovative algorithm for determining reorder points within the inventory policies.

The fourth paper covers the design of drone fleets for deliveries to pharmacies and ambulances at service by a wholesaler. For this purpose, the cost- or CO_2-emission-minimal drone fleet is determined in a discrete-event simulation optimization.

Einleitung

Der kommerzielle Pakettransport mit Lieferwagen ist kosten-, zeit- und CO_2-intensiv (z.B. Roberti and Ruthmair 2021, Perboli and Rosano 2019). Daher ist die Entwicklung alternativer Auslieferungskonzepte im Transport der letzten Meile bedeutsam. Ein vielversprechendes Konzept zur Erhöhung der Effizienz und Effektivität des Transports der letzten Meile ist der Einsatz von Flugdrohnen (kurz: Drohnen). Drohnen können mit hoher Geschwindigkeit und unabhängig vom Straßennetz autonom operieren. Aufgrund dieser leistungssteigernden Effekte gewinnen Drohnen auch im Gesundheitswesen an Relevanz. So sind Drohnen ideal geeignet, um schnell, dringend benötigte medizinische Produkte an für herkömmliche Bodenfahrzeuge schwer erreichbare Ziele zu transportieren (z.B. Zipline 2022). Der Transport von Produkten mit Drohnen ist daher aktuell Forschungsgegenstand sowohl in der Wissenschaft (z.B. El-Adle et al. 2021, Tiniç et al. 2023) als auch in der Praxis (z.B. Mims 2022, Quantum Systems 2020).

Damit Drohnen sowohl im kommerziellen Pakettransport als auch im Gesundheitswesen optimal eingesetzt werden können, bedarf es an Entscheidungen sowohl auf taktischer Ebene bzgl. der Fahrzeugflottenplanung, der Ausgestaltung von Belieferungskonzepten und der Netzwerkstruktur als auch auf operativer Ebene bzgl. der Tourenplanung. Die folgenden Beiträge adressieren diese taktischen und operativen Problemstellungen mit Anwendungsfällen im Pakettransport (Beiträge 1 und 2) und Gesundheitswesen (Beiträge 3 und 4). Zunächst beschäftigt sich Beitrag 1 mit der Fahrzeugflottenplanung und der Wahl von Auslieferungskombinationen auf taktischer Ebene. Beitrag 2 evaluiert die operative Tourenplanung einer Auslieferungskombination mit einem Lieferwagen, der mit mehreren Drohnen ausgerüstet ist. Basierend auf einer neuen Fallstudie aus der Praxis werden in Beiträgen 3 und 4 ein Krankenhaus bzw. ein Großhändler mit einer Drohnenflotte ausgerüstet, um umliegende Krankenhäuser bzw. zusätzlich Krankenwagen im Einsatz zu beliefern (Beitrag 4). Im Fokus stehen bei diesen beiden Beiträgen die simultane Bestands- und Auslieferungsplanung (Beitrag 3) und die Ausgestaltung der Drohnennflotte (Beitrag 4).

Für die komplexen Problematiken werden Entscheidungs- und Unterstützungsmodelle bzw. ein Bewertungsmodell vorgestellt, die einem Paketdienstleister oder Großhändler bei der Problemlösung helfen. In den Beiträgen 1, 2 und 3 werden die Problemstellungen als gemischt-ganzzahlige lineare Programme (MILP) formuliert, welche mit einem kommerziellen Solver (z.B. CPLEX Optimization Studio) optimal gelöst werden können. In den Beiträgen 1 und 3 wird zusätzlich jeweils eine problemspezifische adaptive große Nachbarschaftssuche (ALNS) entwickelt, welche größere Probleminstanzen lösen kann. Zuletzt optimiert Beitrag 4 die Ausgestaltung der Drohnenflotte in einer ereignisdiskreten Simulationsstudie.

Sowohl die betrachteten Problemstellungen, die entwickelten Methodiken als auch die präsen-

tierten Forschungsergebnisse tragen innovativ zur Literatur bei und knüpfen am wissenschaftlichen Diskurs zum Thema Drohnentransporte an. Dies gilt konzeptionell insbesondere für die Entscheidungsprobleme auf taktischer Ebene, methodisch für die innovativen MILP Formulierungen und der problemspezifischen Komponenten der ALNSs sowie für die Ergebnisse zur neuen Fallstudie aus der Praxis.

Im Folgenden wird zunächst ein Überblick der Dissertationsbeiträge gegeben. Anschließend werden die vier Beiträge ausführlicher zusammengefasst.

Überblick der Dissertationsbeiträge

Die vorliegende Dissertation thematisiert auf konzeptioneller und methodischer Ebene vier Transportplanungsprobleme mit Drohnen. Die Beiträge 1 und 2 betrachten neue Entscheidungsprobleme im Pakettransport, wenn Drohnen für den Transport der letzten Meile hinzugezogen werden. Die Beiträge 3 und 4 analysieren den Einsatz von Drohnen im medizinischen Bereich, wenn Drohnen anstelle von Lieferwagen den Medikamententransport übernehmen. Zur Lösung der Entscheidungsprobleme werden in den Beiträgen 1, 2 und 3 neuartige MILP Formulierungen vorgestellt. Die Beiträge 1 und 3 entwickeln zudem jeweils eine ALNS Heuristik mit neuen problemspezifischen Komponenten. In Beitrag 4 wird methodisch eine Optimierung in einer ereignisdiskreten Simulationsstudie durchgeführt. Die Beiträge 3 und 4 liefern zudem Daten und Ergebnisse zu einer neuen Fallstudie aus der Praxis.

Beitrag 1 - Drone location and vehicle fleet planning with trucks and aerial drones

Während autonome Drohnen durch ihre höhere Geschwindigkeit und Unabhängigkeit vom Straßennetz den Transport effektiver gestalten können, haben Lieferwagen den Vorteil der großen Tragfähigkeit, sodass Konsolidierungseffekte im Transport der letzten Meile genutzt werden können. Eine Kombination von Lieferwagen mit Drohnen bietet die Möglichkeit, die Vorteile beider besser zu nutzen und kann folgende Ausprägungen annehmen: Zum einen können Lieferwagen und Drohnen synchronisiert zusammenarbeiten, indem die Drohnen direkt vom Lieferwagen aus starten. Dies ist Vorteilhaft, da der Lieferwagen günstige Start- und Landepunkte für die Drohne wählen kann. Zum anderen können Drohnen von Mikrodepots oder dem zentralen Lager aus starten und agieren somit unabhängig von der Tour des Lieferwagens. Dies hat insbesondere den Vorteil, dass größere und effizientere Drohnen gewählt werden können, da Mikrodepots und das zentrale Lager mehr Kapazität zur Verfügung haben als Lieferwagen. Zusätzlich entfallen potentielle Wartekosten des Lieferwagens, die durch die Synchronisation von Lieferwagen und Drohne entstehen. Beide genannten Auslieferungsmöglichkeiten können zudem beliebig kombiniert werden. So kann der Lieferwagen sowohl mit eigenen Drohnen ausgestattet sein, als auch Mikrodepots beliefern, von denen aus eine eigene Drohnenflotte agiert.

Dieser Beitrag stellt sich den zentralen Fragen auf taktischer Ebene, wie die kostenoptimale Auslieferungsmethode ausgestaltet ist. Dazu gehört die Anzahl an Lieferwagen, Drohnen und Mikrodepots und die Zuweisung von Drohnen zu jedem Lieferwagen, jedem Mikrodepot und dem zentralen Lager. Hierbei von Bedeutung ist zudem die Berücksichtigung der operativen Tourenplanung und

der daraus resultierenden Kosten. An dieser Stelle knüpft dieser Beitrag am wissenschaftlichen Diskurs zum Thema Drohnen an, da bisher in der Literatur verschiedene Auslieferungskonzepte mit Lieferwagen und Drohnen nur in wesentlich geringerem Umfang gemeinsam betrachtet wurden. Zudem lag der Fokus der Literatur bisher nicht auf taktischen, sondern vielmehr auf operativen Planungsproblemen.

Methodisch wird in dem Beitrag die Problemstellung zunächst als two-echelon location routing problem with drones als MILP formuliert. Aufgrund der Komplexität der Problematik wird zusätzlich eine ALNS mit problemspezifischen Operatoren entwickelt, welche größere Instanzen lösen kann. Die gute Performance der ALNS wird zunächst für kleine Instanzen gezeigt, welche mit dem entwickelten MILP optimal gelöst werden können. Für Tests mit größeren Instanzen wird anschließend auf Benchmark-Instanzen aus der Literatur zurückgegriffen, welche die Tourenplanung einer kombinierten Auslieferung von mehreren Lieferwagen mit jeweils einer Drohne heuristisch lösen. Hierbei konnte nicht nur gezeigt werden, dass die entwickelte ALNS vergleichbare Ergebnisse erzielt, sondern zudem noch 17 neue bessere Lösungen findet.

Eine numerische Studie mit Kunden im ländlichen Raum zeigt, dass eine Kombination bzw. ein Mix beider Auslieferungsmethoden in 58% aller betrachteten Szenarien kostenoptimal ist. Dadurch lassen sich die gesamten Lieferkosten um durchschnittlich 33,3% im Vergleich zu einem Szenario ohne Drohnen und 14,1% reduzieren, wenn Lieferwagen, welche mit mehreren Drohnen ausgerüstet sind, für die Lieferung in Betracht gezogen werden.

Beitrag 2 - Two-indexed formulation of the traveling salesman problem with multiple drones performing sidekicks and loops

Dieser Beitrag thematisiert die operative Tourenplanung eines Lieferwagens in der Belieferung der letzten Meile, wenn dieser mit mehreren Drohnen ausgerüstet ist (TSPmD). Im Fokus steht die Analyse der folgenden beiden Möglichkeiten eines Drohnenflugs: Drohnen können an einen späteren Ort innerhalb der Lieferwagentour (Sidekick) oder zum selben Ort zurückkehren, von dem aus sie gestartet wurden (Loop). Dies wird näher untersucht, da die Berücksichtigung von Loops zu einer komplexeren Problemstellung und somit zu längeren Laufzeiten führt. Bisher wurde dieses TSPmD mit Sidekicks und Loops in der Literatur nicht definiert und dementsprechend fehlte auch eine MILP Formulierung.

Dieser Beitrag definiert das TSPmD mit Sidekicks und Loops und liefert eine MILP Formulierung, welche besonders effizient zu lösen ist, sodass optimale Lösungen für Instanzen mit bis zu 28 Knoten gefunden werden. Zudem wird die Performance des MILPs im Vergleich zu zwei state-of-the-art MILP Formulierungen aus der Literatur für eine Tourenplanungsproblematik mit nur einer Drohne gezeigt, welche in einem Standard Solver implementiert wurden. Durch diese Effizienzsteigerung der mathematischen Formulierung können neue Lösungen für Benchmark Instanzen generiert werden. In der numerischen Studie wird gezeigt, dass die Berücksichtigung von Loops zu einer durchschnittlichen Reduktion der maximalen Zykluszeit von bis zu 2,7% führt.

Beitrag 3 - Cyclic stochastic inventory routing with reorder points and recourse decision for an application in medical supply

Für die Versorgung von Patienten ist es entscheidend, dass Kliniken ausreichend Medikamente zur Verfügung haben. Da die Medikamentennachfrage stochastisch ist, entstehen hohe Lagerhaltungskosten und Notfalllieferkosten zur Vermeidung von Fehlmengen. Diese Notfalllieferungen beinhalten in der Praxis nur wenige Medikamente und erfolgen in einer Pendeltour. Basierend auf einer realen Fallstudie wird in diesem Beitrag analysiert, welchen Einfluss eine Drohne als Vehikel für die Notfalllieferungen auf die Kosten und Medikamentenbestände hat.

Typischerweise übernimmt in Deutschland eine zentrale größere Klinik sowohl die Beschaffung als auch die Verteilung von Medikamenten an kleinere umliegende Kliniken. Innerhalb dieser zweistufigen Netzwerkstruktur planen die Kliniken nach individueller Lagerhaltungspolitik, bei welcher die mögliche Notwendigkeit von Notfalllieferungen fest eingeplant ist. Während die zentrale Klinik nach Bedarf bestellt, werden die umliegenden Kliniken stets an festgelegten Tagen innerhalb eines Zyklus (z.B. eine Woche) beliefert. Daher ist es möglich, bei der Belieferung der umliegenden Kliniken ebendiese zu konsolidieren. Im Beitrag werden die zyklischen Bestellzeitpunkte und Routen für die Belieferung der umliegenden Kliniken sowie die Bestellpunkte aller Kliniken optimiert. Hierfür werden die Lagerhaltungspolitiken mit mehreren verschiedenen Produkten, welche eine stochastische Nachfrage aufweisen, berücksichtigt. In der Literatur fehlen bisher integrierte Planungsansätze, die zwei Lagerhaltungspolitiken parallel betrachten. Zudem stellen die hier betrachteten Lagerhaltungspolitiken eine Besonderheit dar, da Drohnen zur Vermeidung von Fehlmengen eingesetzt werden. Dieser Beitrag schließt diese Forschungslücke und modelliert die Problemstellung als zweistufiges stochastisches Programm, bei welcher die Höhe der Bestellpunkte und die Tourenplanung in der ersten Stufe, und die resultierenden Notfalllieferungen in der zweiten Stufe entschieden werden. Zusätzlich wird eine problemspezifische ALNS entwickelt, welche in jeder Iteration einen innovativen Algorithmus zur Bestimmung lokal-optimaler Bestellpunkte ausführt. Die gute Performance der ALNS wird mit optimalen Lösungen für kleine Instanzen sowie mit Benchmark Instanzen aus der Literatur gezeigt.

In einer neuen Fallstudie mit dem Klinikum Ingolstadt wird aufgezeigt, dass die simultane Planung - im Vergleich zum Status Quo - die Transport- und Lagerhaltungskosten der umliegenden Kliniken um 58,4% und der zentralen Klinik um 15,9% senken kann. Zudem wird gezeigt, dass der Einsatz von Drohnen den durchschnittlichen Medikamentenbestand in den umliegenden Kliniken bei teuren und selten benötigten Medikamenten reduzieren kann, sodass Gesamtkosteneinsparungen von 29,8% entstehen. Für die zentrale Klinik hingegen hat der Einsatz der Drohne für den Notfalltransport keinen merklichen Effekt auf die Gesamtkosten.

Beitrag 4 - Drone fleet planning and battery allocation for emergency resupply of pharmacies and ambulances

Basierend auf der Fallstudie des vorherigen Beitrags *Cyclic stochastic inventory routing with reorder points and recourse decision for an application in medical supply* thematisiert dieser Beitrag die Ausgestaltung einer Drohnenflotte für einen Großhändler. Diese Drohnenflotte soll den Notfalltransport zu Apotheken beschleunigen und kosten- und CO_2-effizienter gestalten. Zudem erschließt

sich ein neues Geschäftsmodell, Krankenwagen im Einsatz zu beliefern. Ziel des Beitrags ist die Bestimmung der kosten- bzw. CO_2-minimalen Drohnenflotte, sodass ein gewünschter Servicelevel und eine Belieferungsrate durch Drohnen sichergestellt werden. Zentrale Entscheidungen sind hierbei sowohl die Flottenplanung, bestehend aus der Anzahl an Drohnen, Batterien und Transportboxen, als auch die Platzierung von zusätzlichen Batterien bei den Apotheken. Diese Problemstellung wurde insbesondere mit dem Detaillierungsgrad der Drohnenflotte in der Literatur bisher nicht betrachtet.

Zur Bewertung von Ausprägungen der Drohnenflotte anhand ökonomischer, ökologischer und service-orientierter Key Performance Indices (KPIs) präsentiert dieser Beitrag eine ereignisdiskrete Simulationsstudie, welche eine Optimierung der Flotte beinhaltet. Zudem wird ein Framework zur Bewertung neuer Geschäftsideen auf die Problemstellung angewandt. Zunächst werden alle Stakeholder identifiziert und ihre wirtschaftlichen Verbindungen sowie der Wettbewerb zueinander aufgezeigt. Anschließend werden die KPIs und relevante Parameter eingeführt, die Lieferketten der Notfalllieferung analysiert und zuletzt die Simulationsstudie durchgeführt. Der Beitrag zeigt, dass eine kostenoptimale Drohnenflotte zu Kosteneinsparungen von bis zu 19,6% führt, wenn ein Servicelevel und eine Belieferungsrate von mindestens 90% eingehalten werden sollen. Wird andererseits ein Servicelevel bzw. eine Belieferungsrate von 95% angestrebt, können keine Kosteneinsparungen erzielt werden.

Inhaltsverzeichnis

Abbildungsverzeichnis

Tabellenverzeichnis

Abkürzungsverzeichnis

ALNS adaptive large neighborhood search

BMC business model canvas

CDC central distribution center

DP delivery patterns

FCFS first-come-first-serve

FLP facility location problem

IRP inventory routing problem

KPI key performance indicator

LNS large neighborhood search

MILP mixed-integer linear program

OPL Open Programming Language

PVRP periodic vehicle routing problem

SIRP inventory routing problem with stochastic demands

2E-LRP two-echelon location routing problem

2E-LRPD two-echelon location routing problem with drones

2E-SIRP cyclic multi-product two-echelon inventory routing problem with stochastic demand and inventory policies

2E-VRP two-echelon vehicle routing problem

TSP traveling salesman problem

TSPD traveling salesman problem with drone

TSPmD traveling salesman problem with multiple drones

TTRP truck-and-trailer routing problem

VFP vehicle fleet planning

VRP vehicle routing problem

VRPD vehicle routing problem with drones

Contribution 1 - Drone location and vehicle fleet planning with trucks and aerial drones

1 Drone location and vehicle fleet planning with trucks and aerial drones

Alexander Rave, Pirmin Fontaine, Heinrich Kuhn

Abstract In the context of parcel delivery, aerial drones have great potential that particularly applies in rural areas. In these areas drones mostly operate faster than trucks. As drones are limited in their payload, a combination of trucks and drones can be beneficial in reducing last-mile delivery costs. There are two different delivery methods that combine truck and drone delivery: trucks and drones collaborating with each other with drones launched from trucks, and trucks and drones serving customers independently of each other with drones launched from microdepots or the central distribution center.

We develop a tactical planning model that decides on the cost-optimal vehicle fleet and the location of dedicated drone stations of a logistics service provider that minimizes total costs. The problem setting is modeled as a mixed-integer linear program that allows the assessment of benefits of different transport concepts as well as the impact of mixing different delivery modes. To solve larger instances we develop a specialized adaptive large neighborhood search.

We present a numerical study for parcel delivery in a rural area where customers live in scattered settlements, e.g., villages or hamlets. The case study shows that it is best to launch drones both from trucks and dedicated drone stations in 58% of all scenarios considered. This fleet mix leads to average cost savings of 33.3% compared to an only truck scenario and 14.1% if trucks and drones launched from trucks are considered for delivery. Moreover, we find 17 new best-known solutions for benchmark instances from the literature.

Published: European Journal of Operational Research
URL: `https://doi.org/10.1016/j.ejor.2022.10.015`

1.1 Introduction

Parcel delivery with unmanned aerial vehicles, in the following also called drones, has the potential to revolutionize classic parcel delivery since drone delivery can both reduce costs as well as increase the speed of last-mile logistics (Aurambout et al. 2019, Joerss et al. 2016, Campbell et al. 2017). Because drones can fly over obstacles on the ground and do not have to avoid them, they can take more direct routes and perform the direct delivery of parcels in shorter times than conventional trucks (Caraballo et al. 2017, Scott and Scott 2017). In addition, drones typically fly at higher speeds than conventional trucks can normally travel (Otto et al. 2018). Drone delivery is therefore an innovative, fast and above all cost-effective development. So, for example, Amazon introduced drone delivery service under the name Prime Air in America (Mims 2022) and JD.com serves customers in some rural areas in China via drones since 2016 (Gartner 2016). Due to technological progress, disadvantages such as a maximum transport weight or a high noise level of drones are expected to reduce or even vanish (Wingcopter GmbH 2020). But contrary to conventional trucks, drones may not consolidate customers due to their restrictive payload and are therefore not suitable to serve all regions. For example, if many customers are located close to each other the consolidation effect of a truck can compensate for the lower speed, and a mix of both trucks and drones leads to an economic advantage.

We consider a tactical planning problem that aims to find the cost-optimal last-mile delivery system. This includes deciding on locations for dedicated drone stations (microdepots) from where drones can start as well as deciding on the fleet of conventional trucks, trucks equipped with drones, and drones. We therefore develop a decision-support model that determines both the best truck-and-drone delivery concept as well as the number of different vehicles within a tactical planning horizon. We introduce a mixed-integer linear program (MILP) and develop an adaptive large neighborhood search (ALNS) to solve larger instances. The ALNS is compared to optimal solutions for small instances and to the benchmark instances by Sacramento et al. (2019) for the vehicle routing problem with trucks and drones. In a sensitivity analysis we generate multiple managerial insights.

We contribute to the literature as follows: Our paper is the first that mixes a truck-and-drone concept with stationary drones with focus on fleet planning which means that the delivery methods and the fleet mix is not predetermined. We develop a comprehensive and consolidated model that allows the combination or mix of truck and drone delivery and derive both a MILP and an ALNS with fleet specific elements including a location decision for microdepots within its destroy and repair operators.

The structure of the paper is as follows. In Section 1.2, different delivery methods and mix of methods as well as the problem are described in detail. Section 1.3 presents a literature review on parcel delivery with trucks and drones. In Section 1.4, we present the MILP before describing the ALNS in Section 1.5. The numerical study is shown in Section 1.6. Lastly, Section 1.7 summarizes the main findings of the contribution and provides directions for future research.

1.2 Problem setting

To introduce the problem setting, we first elaborate relevant delivery methods with trucks and drones. In the second subsection we detail the decision problem based on these delivery methods.

1.2.1 Delivery system

A very common system for drone delivery in the literature is one where drones are launched from trucks (see, e.g., Murray and Chu 2015, Wang et al. 2016, Agatz et al. 2018, Sacramento et al. 2019). Other forms of drone delivery are conceivable, such as starting drones from the central distribution center (CDC) or microdepots, which are small, possibly mobile warehouses. Microdepots have the option of being placed in a more economically favorable location compared to the CDC for a certain period of time (Hemmelmayr et al. 2012). Additionally, these microdepots allow customers who are out of range of the CDC to be served via drones (Boysen et al. 2021). Since these microdepots are first supplied by trucks, they operate as transshipment points where drones are the second-tier transportation mode.

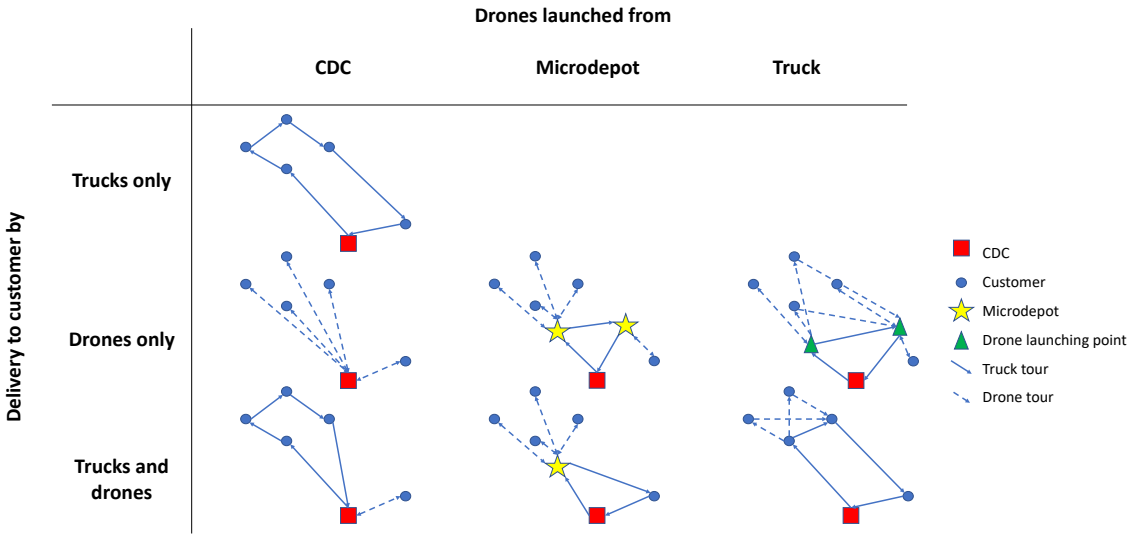

Figure 1.1: Drone and/or truck delivery methods

Figure 1.1 illustrates the different potential delivery methods of trucks and drones, depending on where the drone is launched from and how the customer is visited. The example in the first row of Figure 1.1 assumes that only trucks are used. In that case no variation of the delivery method exists and the problem can be formulated as a classical vehicle routing problem (VRP) (Toth and Vigo 2014). The examples in the second row assume that deliveries are performed exclusively by drones. In these cases, drones can be launched either from the CDC, from microdepots, or from trucks. Note that the microdepots have to be supplied by trucks but trucks do not deliver to customers. Instead, they only serve as launching platforms for drones. Launching drones from trucks instead of microdepots offers the advantage that the launch and return location can be flexibly selected and changed (Luo et al. 2017). Examples two and three can be modeled as a facility location problem

(FLP) (e.g., Kim et al. 2017), two-echelon location routing problem (2E-LRP), or two-echelon vehicle routing problem (2E-VRP) depending on the assumptions made. Finally, the examples in the third row of Figure 1.1 assume that the deliveries are carried out by both trucks and drones. The delivery processes can be organized either independently of each other (first and second example) or synchronized with each other (third example). The truck that supplies microdepots can also deliver to customers before and after serving the microdepot (second example). The first example of the three cases considered in the third row of Figure 1.1 can be modeled as a heterogeneous VRP where drones are presented by a second type of vehicle. The second example can be modeled as 2E-LRP. The third example requires the synchronization of drone and truck deliveries that is denoted as a VRP with drones (VRPD) in the literature (e.g., Wang et al. 2016). .

In this paper, we consider all delivery methods shown in Figure 1.1 as well as all possible subsets, i.e., a mix of these methods by allowing a truck to serve both customers and microdepots as well as carrying drones, or the decision to set up microdepots or potentially handle deliveries without these transshipment points. Figure 1.2 shows a potential delivery configuration serving eleven customers. The configuration serves customers C_1, C_2, C_3, C_4, and C_5 by one drone launched from microdepot M_1, customer C_{11} directly by one drone launched from the CDC and customers C_6 and C_9 by a conventional delivery truck. Additionally, this truck launches two drones to serve customers C_7, C_8, and C_{10} and supplies the microdepot M_1, so drone deliveries to customers C_1, C_2, C_3, C_4, and C_5 have to start after that. The truck in this example is equipped with two drones. These drones launch from and return to the truck, while it is stationary. This is a typical restriction for the VRPD chosen in the literature (e.g., Wang et al. 2016, Otto et al. 2018, Agatz et al. 2018)

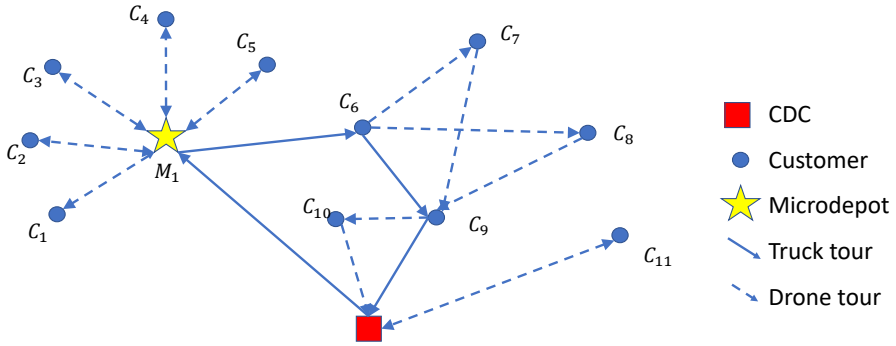

Figure 1.2: Example of mixed truck and drone delivery methods.

1.2.2 Decision problem

We consider a tactical truck and drone fleet planning problem including a microdepot location problem for a single logistics service provider that has to serve a given set of customers. Similar to other tactical planning problems in last-mile delivery (e.g., Fontaine et al. 2021) and drone delivery (e.g., Wankmüller et al. 2020), we assume a representative demand scenario as given input of the problem that is repeated throughout the planning horizon. Minor demand variations are then considered in the operational day-ahead planning problem.

As delivery options, we consider the truck and drone delivery methods presented (Figure 1.1) as well as the mix of these methods. We are interested in determining the cost-optimal number of trucks and drones as well as the locations of microdepots from where drones can be launched. This further implies the allocation of drones to microdepots, the CDC, and trucks. Note that we assume that the drones will need to return to their respective trucks, microdepots, or the CDC. We consider the following costs: variable costs per distance covered (including personnel costs), fixed costs per vehicle and microdepot, possible additional fixed costs, if a truck is equipped with a drone launching station, costs for the time serving a microdepot or customer, and waiting costs for trucks, as the problem setting requires the synchronization of trucks and drones that are launched from both trucks and microdepots. This implies that a truck has to wait at the landing node of the drone in case it arrives earlier. On the contrary, waiting times of drones do not occur since a drone can reduce its travel speed to arrive at the landing node on time. However, the flight time of the drone cannot be reduced arbitrarily since the drone needs a minimum flight speed because of aerodynamic reasons. In addition, the total flight time of a drone is limited by an endurance. A truck driver on the other hand would not and maybe even cannot simply reduce the travel speed on a highway. Additionally, we prohibit drones to return to a truck arc (e.g., Wang et al. 2016, Agatz et al. 2018). Trucks can send out all of their drones at a node. Trucks can thus also operate as "flexible microdepots". For drones launched from microdepots, the synchronization requires that a truck first has to deliver the parcels to the microdepots. The time until the microdepot is filled reduces the available time for satisfying customers from this microdepot.

Further, we take the following assumptions for customers (C), trucks (T), drones (D), and microdepots (M):

C1 All customers have to be served exactly once.

C2 Each customer has a deterministic demand of one parcel. There are no split deliveries.

C3 Some customers cannot be served by drones due to personal preferences or technical reasons. These customers must be served by trucks.

T1 Trucks have a maximum payload of parcels and a maximum delivery time.

T2 Trucks have a maximum payload of drones.

T3 If drones are launched from a truck, this truck needs an additional launching platform on top of it which adds additional costs, but does not reduce the truck's payload.

D1 Each drone can serve one customer per flight (e.g., Roberti and Ruthmair 2021).

D2 If a drone is launched from a truck, it may return to the same or any later node within this truck's tour

D3 We assume two types of drones: large drones for the CDC and microdepots and small drones for trucks which vary in fixed costs, speed and endurance.

M1 There is one predefined location for the CDC and multiple potential microdepot locations.

M2 Microdepots can at maximum be served once by a truck.

M3 Before a drone is launched from a microdepot, it has to be served by a truck.

M4 Microdepots have a maximum payload of drones.

The problem introduced belongs to the class of 2E-LRPs (Li et al. 2021). The first level considers all arcs used by trucks, the second level all arcs followed by drones. We denote the associated decision problem as 2E-LRP with drones (2E-LRPD). The 2E-LRPD extends the 2E-LRP and VRPD in several ways. The model does not only include the synchronized truck and drone delivery, but also drones launched from microdepots and/or the CDC. Therefore, the model represents the most comprehensive model in the literature so far. The model determines the best delivery method or mix of methods, the number of drones, trucks, and location of microdepots. In addition, the model also decides on the route planning of trucks and drones.

1.3 Literature review

Our literature review is divided in two main subsections. Subsection 1.3.1 presents the most relevant literature on route planning with trucks and drones. In this subsection, we also consider delivery planning problems with ground robots and trucks with detachable trailers, which show similarities to our problem. Subsection 1.3.2 then reviews the drone-relevant literature on facility location and vehicle fleet planning since we consider the problem of tactical fleet planning of trucks and drones, which also includes the decision on the locations of microdepots.

We recommend the paper of Otto et al. (2018) for an overview of drone-related topics in logistics including more possible applications than delivery, Boysen et al. (2021) for a more recent overview on drone delivery, and Li et al. (2021) for a specific overview of two-echelon routing problems with drones. For a review of fleet planning related literature, we refer to Baykasoğlu et al. (2019).

1.3.1 Route planning with drones and robots

Drones launched from a single truck The first combination of truck and drone delivery was conducted by Murray and Chu (2015), where a single truck equipped with a single drone serves customers with the objective of minimizing delivery time. The specialty about this delivery concept is the required synchronization between the truck and the drone, since drones typically return to the truck at a later node within the truck's route. However, taking synchronization into account increases the combinatorial complexity. So, the most successful exact solution method so far for this truck-and-drone concept is presented by Roberti and Ruthmair (2021) who develop a specialized branch-and-price approach in order to solve instances with up to 39 customers to optimality. Therefore, the literature mainly focuses on heuristic methods when solving instances with practically relevant customer sizes (e.g., Luo et al. 2017, Agatz et al. 2018, Sacramento et al. 2019).

Several authors vary or extend the truck-and-drone delivery problem originally developed by Murray and Chu (2015). For example, Ha et al. (2018) quantify waiting costs for trucks, if a truck arrives earlier at a node than the drone. Thus, their problem formulation minimizes variable delivery

costs. Agatz et al. (2018) also consider cost minimization, but in contrast to the model of Murray and Chu (2015) or Ha et al. (2018) the truck may visit customer nodes multiple times in order to pick up drones. Luo et al. (2017), on the other hand, allow drone deliveries to multiple customers per flight. Furthermore, all customers must be served by drone and not by truck. Wang et al. (2022) also assume a pure drone delivery mode. The truck is used only to launch drones at a favorable node of the delivery network. After serving one customer, each drone returns to the depot and can be picked up again by the truck in its next tour.

Drones launched from multiple trucks Another stream of literature deals with drone deliveries from multiple trucks, with each truck equipped with one or even multiple drones. Wang et al. (2016), for example, derive and prove several upper and lower bounds for the objective of completion time minimization for different delivery settings with drones. Poikonen et al. (2017) extend the paper by presenting and proving upper and lower bounds to include more use cases. Similar to Luo et al. (2017), Kitjacharoenchai et al. (2020) assume multiple drone deliveries per drone flight, but the authors define the problem as 2E-VRP with multiple trucks and multiple drones per truck.

Sacramento et al. (2019) develop an ALNS to solve a VRPD with one drone per truck. A particular limitation of the problem they consider is that the drones must not return to the same node from which they were launched, but must return to a node that the truck visits later on its route. Euchi and Sadok (2021) derive an hybrid genetic algorithm for the same problem setting and find multiple best-known solutions for the instances from Sacramento et al. (2019).

Drones launched from dedicated drone stations Kim and Moon (2019), for example, assume a delivery system where customers are delivered by drones or by one single truck. The drones are located at a dedicated drone station that is close to the customer area. The single truck serves both the customers and the drone station with parcels delivered by drones. Thus, drone delivery cannot begin until the truck arrives at the drone station. However, if advantageous, the truck can also serve some customers first before delivering the drone station.

Drones launched from trucks and the CDC The combination of two drone delivery methods is considered by Wang et al. (2019). They extend the VRPD with one drone launched per truck by also launching several drones from the CDC. Murray and Raj (2020) also consider both the truck-and-drone-concept and drones launched from the CDC. In contrast to Wang et al. (2019), the authors only consider a single truck, but it is equipped with several drones. Drones launched from trucks and drones launched from the CDC differ in speed, payload, service times, and maximum flight time.

Ground robots Simoni et al. (2020) develop a truck-and-robot concept with a single truck and a single robot launched from the truck. Robots are slower, but can carry multiple packages more easily than drones and thus can serve more than a single customer per tour. Chen et al. (2021) develop a truck-and-robot concept, where robots are exclusively allowed to return to the same node

they have been launched from. The authors moreover take time-windows into account and derive a specialized ALNS to solve larger instances.

Due to the robot's low speed, some publications assume a delivery method where robots launch from a truck but return to the closest microdepot. The synchronization is missing due to an unbounded occurrence of robots per microdepot. This problem is first introduced by Boysen et al. (2018), who also assume that a single truck picks up robots at microdepots and releases them to serve customers but the truck cannot serve customers on its own. Ostermeier et al. (2022) and Heimfarth et al. (2022) follow up on this work by considering, among other things, fixed time windows for deliveries (Ostermeier et al. 2022) or, in addition, direct deliveries by trucks (Heimfarth et al. 2022).

Truck-and-trailer The truck-and-trailer routing problem (TTRP) is a related problem where trucks have a detachable trailer and need to serve customers. But, in contrast to delivery by drones, which can operate independently, the trailer's tour is totally dependent on the truck (Agatz et al. 2018). The pecularity of the TTRP is that some customers cannot be reached with the trailer but always by the truck. So the trailer is decoupled and temporarily parked at customers while the truck travels a subtour. This results in synchronization efforts between the trucks and their trailer (e.g. Lin et al. 2009). While typically in TTRP the trailer can be parked at any customer it can reach, Accorsi and Vigo (2020) consider a variant of this problem with only one truck and additional parking spots that are not customer locations. They also assume that only a subset of all customers have parking spots.

1.3.2 Facility location and fleet planning

Vehicle fleet planning in combination with microdepot location for delivery with drones is hardly represented in the literature, because the focus on this research question requires the combination of different delivery methods, which is not done yet. Thus, most publications on this topic focus on location problems for microdepots (e.g., Chauhan et al. 2019, Wankmüller et al. 2020) or refuel stations (e.g., Shavarani et al. 2019) or the determination of drone and battery amounts (e.g., Troudi et al. 2018). For this, Chauhan et al. (2019) and Troudi et al. (2018) put a special focus on energy consumption whereas Troudi et al. (2018) consider time-windows and different methods of drone charging as well. Wankmüller et al. (2020) focus on the supply of defibrillators via drones. The authors investigate an allocation problem of drones to base stations in mountainous regions under minimization of the number of drones used or the average travel time for drones.

To summarize the previous literature review, Table 1.1 provides an overview of the drone and robot delivery methods and problem settings. Integrated vehicle fleet planning with trucks and drones including a microdepot location decisions has not yet been covered in the literature. Particularly, none of the above publications on truck and drone delivery combine both drones launched from trucks as well as drones launched from microdepots and the CDC. We address this gap in literature and derive a vehicle fleet planning and microdepot location problem that involves a mix of trucks and drones launched from trucks, microdepots, and the CDC, as well as deciding which microdepots to open.

	Trucks		Drones/Robots		Launched from			Problem setting		
Paper	Single	Multiple	Single	Multiple	CDC	Truck	Microdepot	Routing	Facility location	Vehicle fleet
Lin et al. (2009)		✓						✓		
Murray and Chu (2015)	✓		✓			✓		✓		
Wang et al. (2016)		✓		✓		✓		✓		
Poikonen et al. (2017)		✓		✓		✓		✓		
Luo et al. (2017)	✓*		✓			✓		✓		
Ha et al. (2018)	✓		✓			✓		✓		
Agatz et al. (2018)	✓		✓			✓		✓		
Troudi et al. (2018)				✓	✓					✓**
Boysen et al. (2018)	✓			✓		✓		✓		
Sacramento et al. (2019)		✓	✓			✓		✓		
Kim and Moon (2019)	✓			✓			✓	✓		
Wang et al. (2019)		✓	✓[h] ***		✓	✓		✓		
Chauhan et al. (2019)				✓			✓		✓	✓**
Shavarani et al. (2019)				✓			✓		✓	✓**
Accorsi and Vigo (2020)	✓							✓		
Kitjacharoenchai et al. (2020)		✓		✓		✓		✓		
Simoni et al. (2020)	✓		✓			✓		✓		
Murray and Raj (2020)	✓			✓[h]	✓	✓		✓		
Wankmüller et al. (2020)				✓[h]			✓		✓	✓**
Roberti and Ruthmair (2021)	✓		✓			✓		✓		
Euchi and Sadok (2021)		✓	✓			✓		✓		
Chen et al. (2021)		✓		✓		✓		✓		
Wang et al. (2022)	✓			✓		✓		✓		
Ostermeier et al. (2022)	✓			✓		✓		✓		
Heimfarth et al. (2022)	✓			✓		✓		✓		✓**
Our paper		✓		✓[h]	✓	✓	✓	✓	✓	✓

Table 1.1: Overview of relevant problem settings with drones or robots in the literature.
[h] Heterogeneous trucks/drones are considered * Truck does not serve customers
** Only the number of drones/robots per CDC/microdepot are determined *** Single drone per truck, multiple drones per CDC.

In summary, our work contributes to the literature as follows. (1) We decide on the cost-optimal fleet mix and microdepot locations considering different truck-and-drone delivery methods that are relevant in practice. (2) We formulate a MILP in form of a specialized 2E-LRPD and (3) we present a problem-specific ALNS for solving large instances. (4) To generate managerial insights, we conduct an extensive numerical study that analyzes a variety of demand distributions in differently

structured delivery areas.

1.4 Mathematical formulation

In this section, we introduce the mathematical model for the 2E-LRPD. First we discuss the general problem structure, including notation and modeling assumptions. Section 1.4.2 presents the MILP formulation of the problem.

Variables and parameters associated with drones, trucks, and microdepots are superscripted $(.)^D$, $(.)^T$, and $(.)^M$, respectively, for ease of reading. Sets that include the CDC are denoted by $(.)_0$. As we assume two types of drones, variables and parameters that affect both types of drones are marked with a superscripted $(.)^{D_1}$, if drones belong to the CDC or microdepots, and with $(.)^{D_2}$, if drones belong to trucks.

1.4.1 Modeling assumptions, sets, parameters, and variables

The 2E-LRPD is defined on a directed graph $G(\mathcal{N}_0, \mathcal{A}_0)$ with node set $\mathcal{N}_0$ and arc set $\mathcal{A}_0 = \{(i,j)|i,j \in \mathcal{N}_0\}$. $\mathcal{N}_0$ consists both of the customer set $\mathcal{N}^C$ as well as the microdepot set $\mathcal{N}^M$ and the CDC 0. Thus, $\mathcal{N}_0$ is defined as $\mathcal{N}_0 = \mathcal{N}^C \cup \mathcal{N}^M \cup \{0\}$. $\mathcal{N}_D^C \subseteq \mathcal{N}^C$ denotes the set of customers that can be served by drones.

General problem structure The problem is a set partitioning problem since all customers considered have to be served by the available fleet of trucks $\mathcal{T}$ or drones $\mathcal{D}$.

Decision variables The main decision variables determine the vehicle fleet, i.e., whether truck $t \in \mathcal{T}$ is used ($y_t^T \in \{0,1\}$), whether it is equipped with a launching platform for drones ($y_t^{T_{mod}} \in \{0,1\}$) and the number of its drones ($z_t^{D_2} \in \mathbb{N}$). Further, $y_j^M \in \{0,1\}$ define whether microdepot $j \in \mathcal{N}^M$ is opened and $y_d^{D_1} \in \{0,1\}$ whether drone $d \in \mathcal{D}$ is in use. $y_d^{D_1}$ moreover determines if a location is used.

Aligned variables determine the routing of each vehicle. $u_{i,j,t}$ equals 1 if truck t travels on arc (i,j) and 0 otherwise. The binary decision $w_{i,c,t}$ indicates whether a drone is launched from a truck t at node i to serve customer c. Similarly, $x_{c,j,t} \in \{0,1\}$ denotes the flight back from a customer c to a node j. Finally, $v_{i,c,d}$ equals 1 if customer c is served by drone d launched from the CDC or a microdepot i and 0 otherwise. Note that drones launched from trucks have a binary decision each for their traveled arcs in their outbound flight and return flight, since the variables are affected by different restrictions.

Parameters The variable costs for trucks, $c_{i,j}^T$ and drones, $c_{i,j}^{D_1}$ and $c_{i,j}^{D_2}$ depend on the distance traveled for an arc $(i,j) \in \mathcal{A}_0$, while fixed costs for trucks, c_{fix}^T, drones, $c_{fix}^{D_1}$ and $c_{fix}^{D_2}$, and microdepots, c_{fix}^M depend on the number of vehicles or microdepots used. $c_{fix}^{T_{mod}}$ are additional fixed costs, if a truck is equipped with a drone launching station. c_{wait} are waiting costs for trucks that are dependent on their waiting time at each node. Last, service costs depend on each customer and microdepots served by trucks, c_{serv}^T and for each customer served by drones, $c_{serv}^{D_1}$ and $c_{serv}^{D_2}$.

Index sets	
$\mathcal{N}^C$, $\mathcal{N}_0^C$	Node set for customers (and the CDC)
$\mathcal{N}_D^C$	Node set for customers that can be served by drones
$\mathcal{N}^M$, $\mathcal{N}_0^M$	Node set for microdepots (and the CDC)
$\mathcal{N}$, $\mathcal{N}_0$	Node set for customers and microdepots (and the CDC)
$\mathcal{A}$, $\mathcal{A}_0$	Arc set between customers and microdepots (and the CDC)
$\mathcal{T}$	Index set for trucks
$\mathcal{D}$	Index set for drones launched from microdepots and the CDC
Parameters	
a^T, a^{D_1}, a^{D_2}	Speed of trucks/drones in distance unit per time unit
$c_{i,j}^T$, $c_{i,j}^{D_1}$, $c_{i,j}^{D_2}$	Variable costs for traveling arc $(i,j) \in \mathcal{A}_0$ for trucks/drones
c_{wait}	Waiting costs for trucks per time unit
c_{serv}^T, $c_{serv}^{D_1}$, $c_{serv}^{D_2}$	Service costs for trucks/drones per customer and microdepot
c_{fix}^T, $c_{fix}^{D_1}$, $c_{fix}^{D_2}$, c_{fix}^M	Fixed costs per truck/drone/microdepot
$c_{fix}^{T_{mod}}$	Additional fixed costs per truck, if the truck is equipped with drones
$d_{i,j}$	Distance between customers, microdepots and CDC
e^{D_1}, e^{D_2}	Maximum endurance time traveled of drones per flight
K_t^T	Maximum number of drones per truck $t \in \mathcal{T}$
K_i^M	Maximum number of drones per microdepot $i \in \mathcal{N}^M$
M_l^{big}	big M for $l = 1, 2, 3, 4$
Q	Payload of trucks in number of customers
Q_{time}^T, Q_{time}^D	Maximum time for each truck/drone within the planning period considered
s_i^T	Service time for trucks at each node $i \in \mathcal{N}$
$s_c^{D_1}$,$s_c^{D_2}$	Service time for drones at each node $c \in \mathcal{N}_D^C$
Decision variables	
$u_{i,j,t}$	Binary variable*, indicating truck $t \in \mathcal{T}$ travels arc $(i,j) \in \mathcal{A}_0$
$v_{i,c,d}$	Binary variable*, indicating drone $d \in \mathcal{D}$ launched from $i \in \mathcal{N}_0^M$ serves customer $c \in \mathcal{N}_D^C$
$w_{i,c,t}$	Binary variable*, indicating drone launched from $i \in \mathcal{N}_0$ and truck $t \in \mathcal{T}$ serves customer $c \in \mathcal{N}_D^C$
$x_{c,j,t}$	Binary variable*, indicating drone returns from customer $c \in \mathcal{N}_D^C$ to $j \in \mathcal{N}_0$ and truck $t \in \mathcal{T}$
y_t^T, $y_t^{T_{mod}}$	Binary variable*, if truck $t \in \mathcal{T}$ is in use/equipped with a drone launching station
$y_d^{D_1}$, y_i^M	Binary variable*, if drone $d \in \mathcal{D}$ is in use/ microdepot $i \in \mathcal{N}^M$ is opened
$z_t^{D_2}$	Integer variable, indicating the number of drones per truck ($t \in \mathcal{T}$)
Auxiliary variables	
κ_i	Subtour elimination variable for node $i \in \mathcal{N}$ by Miller et al. (1960)
$\lambda_{i,t}$	Integer variable indicating the demand per microdepot $i \in \mathcal{N}^M$ served by truck $t \in \mathcal{T}$
$\xi_{i,d}$	Binary variable*, indicating if drone $d \in \mathcal{D}$ is allocated to microdepot or CDC $i \in \mathcal{N}_0^M$
$\pi_{i,j,t}$	Integer variable indicating the number of drones traveling arc $(i,j) \in \mathcal{A}_0$ on truck $t \in \mathcal{T}$
$\tau_{i,j,t}$	Real-value variable indicating the accumulated travel time of truck $t \in \mathcal{T}$ traveling arc $(i,j) \in \mathcal{A}_0$ in its route taking into account waiting times for its drones

Continued on next page

Table 1.2 – *Continued from previous page*

$\phi^T_{i,j,t}$	Real-value variable to determine waiting times of truck $t \in \mathcal{T}$ at node $j \in \mathcal{N}_0$ dependent on the time the truck travels arc $(i,j) \in \mathcal{A}_0$ if drones are launched from a previous node $(i \neq j)$ and if drones perform commuting tours j $(i = j)$. The nodes i and j may but do not have to be visited subsequently.
$\phi^D_{c,j,t}$	Real-value variable quantifying the extended flight time of a drone launched from truck $t \in \mathcal{T}$ to serve customer $c \in \mathcal{N}^C_D$ so that the drone does not arrive at the return node $j \in \mathcal{N}_0$ before its associated truck.
$\chi_{i,t}$	Binary variable*, indicating node $i \in \mathcal{N}$ gets visited by truck $t \in \mathcal{T}$
ψ_c	Binary variable*, indicating customer $c \in \mathcal{N}^C$ gets served by drone from a CDC or microdepot
$\omega_{c,t}$	Binary variable*, indicating customer $c \in \mathcal{N}^C$ gets served by drone launched from truck $t \in \mathcal{T}$

Table 1.2: Index sets, parameters, decision variables, and auxiliary variables.
* binary variables have a value of 1, if they are true, and 0 otherwise.

For the synchronization of trucks and drones we consider the distance per arc $d_{i,j}$, the truck speeds a^T, the drone speeds a^{D_1} and a^{D_2}, the service times s^T_i for trucks per customer or microdepot $i \in \mathcal{N}$, and the service times $s^{D_1}_c$ and $s^{D_2}_c$ for drones per customer.

The truck tours are restricted through a maximum time limit Q^T_{time} and to the number of customers that can be served by a payload of Q. For trucks equipped with drones this payload includes the customers served by a drone from this truck. The maximum available travel time for drones within the planning period is denoted as Q^D_{time}. This maximum time is reduced by the amount of time the respective truck needs to serve the microdepot assigned to it. The later a truck arrives at the microdepot, the less time the drones stationed at that microdepot have to serve customers. The total time Q^D_{time} is not to be confused with the endurance of a drone (e^{D_1} and e^{D_2}) which limits each flight's duration per flight. The minimum of the two time spans (time remaining within the planning period and endurance of a drone) defines for each drone launched from a microdepot whether a potential customer can be served. The same applies to drones launched from trucks, but then the total available travel time for drones is considered within the maximum time limit for truck tours, Q^T_{time}. Furthermore, each microdepot $i \in \mathcal{N}^M$ and each truck $t \in \mathcal{T}$ has a limited capacity of at most K^M_i and K^T_t drones, respectively.

1.4.2 MILP formulation

In the following, we first introduce the objective function and then the constraints. The constraints are split into five parts: first, the assignment of customers to one of the delivery options. Second, the contraints regarding truck tours including the service of microdepots are presented. Third, we show constraints regarding drones launched from microdepots or the CDC including the synchronization between trucks and microdepots. Fourth, constraints regarding drones launched from trucks, and fifth constraints regarding the synchronization of trucks and drones are introduced.

1.4.2.1 Objective function

$$\begin{aligned}\min \sum_{t\in\mathcal{T}}\Big(c^T_{fix}\cdot y^T_t + c^{T_{mod}}_{fix}\cdot y^{T_{mod}}_t + c^{D_2}_{fix}\cdot z^{D_2}_t\Big) + \sum_{d\in\mathcal{D}} c^{D_1}_{fix}\cdot y^{D_1}_d + \sum_{i\in\mathcal{N}^M} c^M_{fix}\cdot y^M_i \\ + \sum_{(i,j)\in\mathcal{A}_0,\, t\in\mathcal{T}} c^T_{i,j}\cdot u_{i,j,t} + \sum_{i\in\mathcal{N}^M_0,\, c\in\mathcal{N}^C_D,\, d\in\mathcal{D}} 2\cdot c^{D_1}_{i,c}\cdot v_{i,c,d} + \sum_{i\in\mathcal{N}^M_0,\, c\in\mathcal{N}^C_D,\, t\in\mathcal{T}} c^{D_2}_{i,c}\cdot(w_{i,c,t}+x_{c,i,t}) \\ + \sum_{i,j\in\mathcal{N},\, t\in\mathcal{T}} c_{wait}\cdot\phi^T_{i,j,t} + \sum_{j\in\mathcal{N},\, t\in\mathcal{T}} c^T_{serv}\cdot\chi_{j,t} + \sum_{c\in\mathcal{N}^C_D} c^{D_1}_{serv}\cdot\psi_c + \sum_{c\in\mathcal{N}^C_D,\, t\in\mathcal{T}} c^{D_2}_{serv}\cdot\omega_{c,t} \qquad (1.1)\end{aligned}$$

The objective function minimizes the fixed, variable, synchronization and service costs. The first row describes all fixed costs including costs for each truck, each drone launching station per truck, each drone, and each microdepot. The second row defines all variable costs for trucks and drones traveling an arc. The third row indicates possible waiting costs if trucks are waiting for drones to return, and service costs for all customers and microdepots served by trucks and customers served by drones.

1.4.2.2 Constraints

$$\sum_{t\in\mathcal{T}}\chi_{c,t} + \left\{\begin{array}{ll}\sum\limits_{t\in\mathcal{T}}\omega_{c,t}+\psi_c & ,c\in\mathcal{N}^C_D \\ 0 & ,else\end{array}\right\} = 1 \qquad \forall c\in\mathcal{N}^C \qquad (1.2)$$

$$\sum_{t\in\mathcal{T}}\chi_{c,t}\le 1 \qquad \forall c\in\mathcal{N}^M \qquad (1.3)$$

$$\chi_{i,t},\ \omega_{k,t},\ \psi_k\in\{0,1\} \qquad \forall i\in\mathcal{N},\ c\in\mathcal{N}^C,\ k\in\mathcal{N}^C_D,\ t\in\mathcal{T} \qquad (1.4)$$

Constraints (1.2) ensure that each customer $c\in\mathcal{N}^C$ is visited exactly once by one delivery option while Constraints (1.3) guarantee that each microdepot might be served at maximum of once by a truck. Next, we will introduce the constraints for each of these options.

Trucks

$$\sum_{i\in\mathcal{N}_0} u_{j,i,t} - \sum_{i\in\mathcal{N}_0} u_{i,j,t} = 0 \qquad \forall j\in\mathcal{N}_0,\ t\in\mathcal{T} \quad (1.5)$$

$$\sum_{i\in\mathcal{N}_0} u_{i,c,t} = \chi_{c,t} \qquad \forall c\in\mathcal{N}, t\in\mathcal{T} \quad (1.6)$$

$$\kappa_i + \left\{\begin{array}{ll}\sum\limits_{k\in\mathcal{N}^M}\lambda_{k,t} & ,i\le|\mathcal{N}^M| \\ 1 & ,else\end{array}\right\} + \sum_{c\in\mathcal{N}^C_D} w_{i,c,t}\le\kappa_j + Q\cdot(1-u_{i,j,t}) \qquad \forall(i,j)\in\mathcal{A},\ t\in\mathcal{T} \quad (1.7)$$

$$\sum_{j\in\mathcal{N}_0} u_{0,j,t}\le y^T_t \qquad \forall t\in\mathcal{T} \quad (1.8)$$

$$u_{i,j,t}, y^T_t\in\{0,1\} \qquad \forall(i,j)\in\mathcal{A}_0,\ t\in\mathcal{T} \quad (1.9)$$

$$w_{i,c,t}\in\{0,1\} \qquad \forall i\in\mathcal{N}_0,\ c\in\mathcal{N}^C_D,\ t\in\mathcal{T} \quad (1.10)$$

$$\kappa_i\in\mathbb{R} \qquad \forall i\in\mathcal{N} \quad (1.11)$$

$$\lambda_{i,t} \in \mathbb{N} \qquad \forall i \in \mathcal{N}^M,\ t \in \mathcal{T} \quad (1.12)$$

Constraints (1.5) to (1.8) are VRP-related restrictions for the truck. Constraints (1.5) and (1.6) conserve flow. Constraints (1.7) are the subtour elimination constraints by Miller et al. (1960), including both the set of microdepots and customers, since trucks may deliver both in one route. The constraints also consider the maximum payload Q of each truck $t \in \mathcal{T}$ by taking into account the demand of one unit per customer, the demand $\lambda_{k,t}$ per microdepot $k \in \mathcal{N}^M$ served per truck $t \in \mathcal{T}$, and the total service of all drones launched from that truck. The variable $\lambda_{k,t}$ is restricted in Constraints (1.21), since the service of microdepots is taken into account. Constraints (1.8) ensure both that there is a maximum of one tour per truck $t \in \mathcal{T}$ and whether truck $t \in \mathcal{T}$ is used or not. Lastly, the domains of the decision variables are defined.

Drones launched from the CDC or microdepots

$$v_{i,c,d} \leq y_i^M \qquad \forall i \in \mathcal{N}^M,\ c \in \mathcal{N}_D^C,\ d \in \mathcal{D} \quad (1.13)$$

$$\sum_{i \in \mathcal{N}_0^M, d \in \mathcal{D}} v_{i,c,d} = \psi_c \qquad \forall c \in \mathcal{N}_D^C \quad (1.14)$$

$$\sum_{c \in \mathcal{N}_D^C} \left(\frac{2 \cdot d_{i,c}}{a^{D_1}} + s_c^{D_1} \right) \cdot v_{i,c,d} \leq Q_{time}^D \cdot \xi_{i,d} - \sum_{j \in \mathcal{N}_0,\, t \in \mathcal{T}} \tau_{j,i,t} \qquad \forall i \in \mathcal{N}^M,\ d \in \mathcal{D} \quad (1.15)$$

$$\sum_{c \in \mathcal{N}_D^C} \left(\frac{2 \cdot d_{i,c}}{a^{D_1}} + s_c^{D_1} \right) \cdot v_{i,c,d} \leq Q_{time}^D \cdot \xi_{i,d} \qquad \forall i \in \{0\},\ d \in \mathcal{D} \quad (1.16)$$

$$\xi_{i,d} \leq y_d^{D_1} \qquad \forall i \in \mathcal{N}_0^M,\ d \in \mathcal{D} \quad (1.17)$$

$$\sum_{d \in D} \xi_{i,d} \leq K_i^M \qquad \forall i \in \mathcal{N}^M \quad (1.18)$$

$$2 \cdot \frac{d_{i,c}}{a^{D_1}} \cdot v_{i,c,d} + s_c^{D_1} \cdot \psi_c \leq e^{D_1} \qquad \forall i \in \mathcal{N}_0^M,\ c \in \mathcal{N}_D^C,\ d \in \mathcal{D} \quad (1.19)$$

$$v_{i,c,d} \leq \xi_{i,d} \qquad \forall i \in \mathcal{N}_0^M,\ c \in \mathcal{N}_D^C,\ d \in \mathcal{D} \quad (1.20)$$

$$\lambda_{i,t} \geq \sum_{c \in \mathcal{N}_D^C,\, d \in \mathcal{D}} v_{i,c,d} - M_1^{big} \cdot \left(1 - \sum_{j \in \mathcal{N}_0} u_{j,i,t} \right) \qquad \forall i \in \mathcal{N}^M,\ t \in \mathcal{T} \quad (1.21)$$

$$\sum_{i \in \mathcal{N}_0,\, t \in \mathcal{T}} u_{i,j,t} = y_j^M \qquad \forall j \in \mathcal{N}^M \quad (1.22)$$

$$v_{i,c,d},\ y_i^M,\ y_d^{D_1},\ \xi_{i,d} \in \{0,1\} \qquad \forall i \in \mathcal{N}_0^M,\ c \in \mathcal{N}_D^C,\ d \in \mathcal{D} \quad (1.23)$$

$$\tau_{i,j,t} \in \mathbb{R}^+ \qquad \forall (i,j) \in \mathcal{A}_0,\ t \in \mathcal{T} \quad (1.24)$$

Constraints (1.13) to (1.22) are restrictions related to drones launched from the CDC or microdepots. Constraints (1.13) ensure that drones can only launch and return from a microdepot if the microdepot has been opened and thus been supplied by a truck. Constraints (1.14) define whether a customer is served by a drone launched from the CDC or microdepots. Constraints (1.15) and (1.16) ensure that each drone $d \in \mathcal{D}$ may not exceed its total maximum service time Q_{time}^D per time period. This time is reduced by the accumulated travel time $\tau_{j,i,t}$ of the supply truck until the truck arrives at the microdepot. Auxiliary variables $\tau_{j,i,t}$, $(j,i) \in \mathcal{A}_0$, $t \in \mathcal{T}$ are defined in

Constraints (1.38) and (1.39) since waiting times for drones launched from trucks are taken into account (Note, $\tau_{j,i,t}$ is adapted from the load-based subtour elimination constraint). The later the truck arrives at the microdepot the less total time drones have left to serve customers. If drones are launched from the CDC there is no decrease of a drone's maximum service time since the CDC does not need to be served first (Constraints (1.16)). Constraints (1.17) determine, if drone $d \in \mathcal{D}$ can be launched from a microdepot. Constraints (1.18) ensure that there is a maximum number of K_i^M drones per microdepot $i \in \mathcal{N}^M$ and Constraints (1.19) guarantee that only customers in range are served by drones. Constraints (1.20) ensure that each drone $d \in \mathcal{D}$ can only serve customers if it is assigned to microdepot or CDC $i \in \mathcal{N}_0^M$. The demand $\lambda_{i,t}$ of microdepot $i \in \mathcal{N}^M$ to serve all its customers is determined by Constraints (1.21). Truck $t \in \mathcal{T}$ must transport this quantity to the microdepot. M_1^{big} can be set as the truck payload Q. Constraints (1.22) define, if drone $d \in \mathcal{D}$ is used and microdepot $j \in \mathcal{N}^M$ is opened. Lastly, decision variables and auxiliary variables are defined.

Drones launched from trucks For all trucks $t \in \mathcal{T}$, the following constraints restrict drones launched from trucks:

$$\pi_{i,j,t} \leq \sum_{k \in \mathcal{N}_0:\, k \neq i} \pi_{k,i,t} + \sum_{c \in \mathcal{N}_D^C} \Big(x_{c,i,t} - w_{i,c,t} \Big) \qquad \forall (i,j) \in \mathcal{A}_0 :\ i \neq j \qquad (1.25)$$

$$\pi_{i,j,t} \leq K_t^T \cdot u_{i,j,t} \qquad \forall (i,j) \in \mathcal{A}_0 \qquad (1.26)$$

$$\sum_{i \in \mathcal{N}} \pi_{0,i,t} + \sum_{c \in \mathcal{N}_D^C} w_{0,c,t} = z_t^{D_2} \qquad (1.27)$$

$$\pi_{i,j,t} + \sum_{c \in \mathcal{N}_D^C} \Big(w_{i,c,t} - x_{c,i,t} \Big) \leq z_t^{D_2} \qquad \forall (i,j) \in \mathcal{A}_0 :\ i \neq 0 \qquad (1.28)$$

$$\sum_{c \in \mathcal{N}_D^C} w_{i,c,t} \leq z_t^{D_2} \leq K_t^T \qquad \forall i \in \mathcal{N}_0 \qquad (1.29)$$

$$w_{j,c,t} + x_{c,j,t} \leq 2 \cdot \sum_{i \in \mathcal{N}_0} u_{i,j,t} \qquad \forall c \in \mathcal{N}_D^C,\ j \in \mathcal{N} \qquad (1.30)$$

$$\Big(\sum_{f \in \mathcal{N}_0} \tau_{f,j,t} - \tau_{f,i,t} \Big) \cdot M_2^{big} \geq w_{i,c,t} + x_{c,j,t} - M_3^{big} \cdot (2 - w_{i,c,t} - x_{c,j,t}) \qquad \forall (i,j) \in \mathcal{A}_0, i \neq j, c \in \mathcal{N}_D^C \qquad (1.31)$$

$$\sum_{j \in \mathcal{N}_0} x_{c,j,t} = \sum_{i \in \mathcal{N}_0} w_{i,c,t} = \omega_{c,t} \qquad \forall c \in \mathcal{N}_D^C \qquad (1.32)$$

$$\frac{1}{a^{D_2}} \cdot \Big(d_{i,c} \cdot w_{i,c,t} + d_{c,j} \cdot x_{c,j,t} \Big) + \phi_{c,j,t}^D + s_c^{D_2} \cdot \omega_{c,t} \leq e^{D_2} \qquad \forall (i,j) \in \mathcal{A}_0, c \in \mathcal{N}_D^C \qquad (1.33)$$

$$w_{i,c,t} \leq y_t^{T_{mod}} \qquad \forall i \in \mathcal{N}_0,\ c \in \mathcal{N}_D^C \qquad (1.34)$$

$$x_{c,i,t},\ y_t^{T_{mod}} \in \{0,1\}, \phi_{c,i,t}^D \in \mathbb{R}^+ \qquad \forall i \in \mathcal{N}_0,\ c \in \mathcal{N}_D^C \qquad (1.35)$$

$$z_t^{D_2},\ \pi_{i,j,t} \in \mathbb{N} \qquad \forall (i,j) \in \mathcal{A}_0,\ c \in \mathcal{N}_D^C \qquad (1.36)$$

Constraints (1.25) determine the number of drones on each truck traveling an arc. This number is less than or equal to the number of drones that have been carried by the truck on its previous arc

plus returning minus leaving drones at the node it visited. There may only be drones on a truck, if the arc has been traveled by a truck (Constraints (1.26)). Moreover there are a maximum of K_t^T drones traveling the arc from truck $t \in \mathcal{T}$. Constraints (1.27) to (1.29) ensure that there is always a sufficient number of drones on truck $t \in \mathcal{T}$. The number of drones when leaving the CDC is defined in Constraints (1.27), which is reduced by the number of drones released from the truck at the CDC. During each trucks' tour additionally returning drones are considered (Constraints (1.28)). The number of drones that can be launched at each node is limited in Constraints (1.29) to the number of drones the truck carries at that node. Moreover, the number of drones per node is limited to a maximum of K_t^T drones (Constraints (1.29)).

Constraints (1.30) ensure that each drone can only launch from or return to a node that the associated truck $t \in \mathcal{T}$ also visits on its tour. The cumulative truck travel time is included in Constraints (1.31) to ensure that the drones return to the same or any later truck position than the drone was initially launched. M_2^{big} can be set as reciprocal of the closest two customers' delivery time by truck. To ensure that the inequality also applies to arcs that are not traveled by the truck, the right side of the inequality is reduced by M_3^{big} in these cases, which can be set as the maximum travel time. Constraints (1.32) are flow conservation constraints for drones launched from trucks. Constraints (1.33) ensure that the flight time of a drone tour does not exceed the drone-specific endurance. The flight time of a drone includes the regular times for covering the arcs (i, c) and (c, j), the service time at the customer's site, $s_c^{D_2}$ and a potentially extended flight time $\phi_{c,j,t}^D$ realized by speed reduction so that the drone does not arrive at the return node j before its associated truck. Note that the speed can only be reduced up to a certain minimum speed for aerodynamic reasons. Constraints (1.33) also reflect this fact. Constraints (1.40) set the potentially extended flight times $\phi_{c,j,t}^D$.

Constraints (1.34) define whether a truck needs to be equipped with a drone launching station. Finally, decision variables and auxiliary variables are defined.

Synchronization of trucks and drones For all trucks $t \in \mathcal{T}$, the following constraints ensure the synchronization of trucks, microdepots, and drones launched from trucks:

$$\phi_{i,j,t}^T \geq \frac{1}{a^{D_2}} \cdot \left(d_{i,c} \cdot w_{i,c,t} + d_{c,j} \cdot x_{c,j,t}\right) + s_c^{D_2} \cdot \omega_{c,t} - M_4^{big} \cdot (2 - w_{i,c,t} - x_{c,j,t}) - \begin{cases} \sum_{h \in \mathcal{N}_0} (\tau_{h,j,t} - \tau_{h,i,t}) & , i \neq j \\ 0 & , else \end{cases} \quad \forall (i,j) \in \mathcal{A}_0 :\ j \neq 0,\ c \in \mathcal{N}_D^C \quad (1.37)$$

$$\tau_{i,j,t} \geq \left(\frac{d_{i,j}}{a^T} + s_j^T\right) \cdot u_{i,j,t} + \begin{cases} \sum_{k \in \mathcal{N}_0} \left(\tau_{k,i,t} + \phi_{k,i,t}^T\right) - M_4^{big} \cdot (1 - u_{i,j,t}) & , i \neq 0 \\ 0 & , else \end{cases} \quad \forall (i,j) \in \mathcal{A}_0 \quad (1.38)$$

$$\tau_{i,j,t} \leq Q_{time}^T \cdot u_{i,j,t} \quad \forall (i,j) \in \mathcal{A}_0 \quad (1.39)$$

$$\phi^D_{c,j,t} \geq \sum_{h \in \mathcal{N}_0} (\tau_{h,j,t} - \tau_{h,i,t}) - \frac{1}{a^{D_2}} \cdot \Big(d_{i,c} \cdot w_{i,c,t} + d_{c,j} \cdot x_{c,j,t} \Big) - s_c^{D_2} \cdot \omega_{c,t} - (2 - w_{i,c,t} - x_{c,j,t}) \cdot M_4^{big} \qquad \forall (i,j) \in \mathcal{A}_0 :\ j \neq 0,\ c \in \mathcal{N}_D^C \quad (1.40)$$

$$\phi^T_{i,j,t} \in \mathbb{R}^+ \qquad \forall (i,j) \in \mathcal{A}_0 \quad (1.41)$$

Constraints (1.37) to (1.40) ensure the synchronization of trucks, microdepots, and drones launched from trucks by computing the waiting times in (1.37) and adding these times to the accumulated travel time in (1.38). Constraints (1.37) determine the possible waiting times for each truck after traveling an arc (i, j) and for each customer note c that can be supplied by drone, $c \in \mathcal{N}_D^C$. To compute the waiting times for an arc, the accumulated travel time $\tau_{i,j,t}$ for truck $t \in \mathcal{T}$ for traveling up to node $j \in \mathcal{N}_0$ is compared to the drone's travel and service time. A truck is waiting at a node $j \in \mathcal{N}_0$ if a drone that returns to j is launched at the same node j. In this case waiting times only arise, if the truck's service at node j needs less time than the drone tour to serve customer $c \in \mathcal{N}_D^C$.

Constraints (1.38) define $\tau_{i,j,t}$ during the tour. At the beginning of a truck's tour ($i = 0$) no previous travel and waiting times are taken into account, but the time traveling the first arc and a first service time are. Otherwise, previous travel times and waiting times are added to the accumulated travel time. M_4^{big} ensures that the accumulated travel time is not greater than zero if an arc is not traveled, and can be set as the truck's total travel time Q^T_{time}. Constraints (1.39) limit the maximum cumulative travel time of a truck on arc (i, j), $\tau_{i,j,t}$ by Q^T_{time} and set $\tau_{i,j,t}$ to 0 if a truck does not travel arc (i, j).

Constraints (1.40) quantifies the potentially extended flight time $\phi^D_{c,j,t}$ so that a drone does not arrive at the return node j before its associated truck. This is realized by speed reduction of the drone and satisfies the endurance constraint for each drone flight. Finally, the auxiliary variables $\phi^T_{i,j,t}$ are defined.

As a generalization of the 2E-LRP and the VRPD, the 2E-LRPD is $\mathcal{NP}$-hard (e.g., Sacramento et al. 2019) and only small instances can be solved optimally using the MILP. To solve larger instances, we introduce an ALNS in the following section.

1.5 Adaptive large neighborhood search

The ALNS was first introduced in Ropke and Pisinger (2006) and Pisinger and Ropke (2007) and has also been widely used for both truck and drone routing problems (Sacramento et al. 2019) as well as two-echelon routing problems (Mühlbauer and Fontaine 2021, Voigt et al. 2022). The basic concept of our ALNS approach is adapted from Ropke and Pisinger (2006) and Pisinger and Ropke (2007). However, we modify the operators significantly with respect to the specifics of our problem setting. They differ from classical truck operators (e.g., Ropke and Pisinger 2006, Pisinger and Ropke 2007), typical drone operators (e.g., Sacramento et al. 2019), and two-echelon operators (e.g., Hemmelmayr et al. 2012) suggested in literature in terms of three aspects. First, we consider more general assumptions regarding the vehicle fleet and drone flights. Second, our operators directly factor in the impact on the vehicle fleet. And, third, we have additional problem specific mixed operators, which assess the benefits of different delivery methods or mix of methods.

In the following we first describe the solution representation and then detail the ALNS in general. In the third subsection we introduce the destroy and repair operators used. In the fourth subsection the local search within the ALNS is explained in detail.

1.5.1 Solution representation and penalized costs

The 2E-LRPD is a set partitioning problem regarding customers. Thus, it allocates each customer exactly once to either a route of trucks, a route of drones launched from microdepots or the CDC, or a route of drones launched from trucks. Therefore, a solution R is represented by the following three subsets:

1) R^T: Truck routes that serve customers and microdepots directly.

2) $R^D_{M_0}$: Drone routes launched from microdepots or the CDC.

3) R^D_T: Drone routes launched from trucks including both the launch and return node of drones.

Each customer is assigned to exactly one route. Once a microdepot is included to serve customers via drones, it also becomes part of the set R^T and decreases the remaining payload of a truck in R^T accordingly. Thus, while a route $r \in R^D_{M_0}$ or R^D_T only contains the sequence of customers, a route $r \in R^T$ further includes visits at microdepots. Therefore, the three routes determine the vehicle fleet and the design of the distribution system. That is, which of the microdepots to open, the truck types used and their respective numbers, as well as the number and types of drones. For the example illustrated in Figure 1.2 the associated design setting is represented by the three sets R^T, $R^D_{M_0}$, and R^D_T as follows.

1) $R^T = \{CDC, M_1, C_6, C_9, CDC\}$. The order of the elements in the set defines the route schedule. The sequence "$CDC, \cdots, CDC$" is repeated when multiple trucks are used.

2) $R^D_{M_0} = \{C_1(M_1),\ C_2(M_1),\ C_3(M_1),\ C_4(M_1),\ C_5(M_1),\ C_{11}(CDC)\}$. The node identifier in the brackets provides information, on which microdepot or CDC the respective drone is assigned to.

3) $R^D_T = \{C_7(C_6, C_9),\ C_8(C_6, C_9),\ C_{10}(C_9, CDC)\}$. The node identifiers in the brackets provide information on the launch and return node of a drone.

Following the scheme of Vidal et al. (2013), we allow infeasible solutions and penalize the infeasibility by adding a penalty term to the objective function of the MILP. Infeasibility may occur in five different cases. First, the load of a truck exceeds its payload. Second, a truck route exceeds its total maximum delivery time. Third, the maximum number of drones per truck is violated. Fourth, a drone route exceeds its maximum endurance. Fifth, drones launched from microdepots or the CDC exceed their delivery day's total running time.

1.5.2 ALNS algorithm

Algorithm 1 presents the general outline of the ALNS. In the beginning, the best found solution R^{global}, the current solution R and the initial temperature Temp for the simulated annealing process are initialized. For a starting solution all customers that can be supplied by drones and are in range of the CDC are served by drones launched from the CDC. The remaining customers are allocated to truck routes in the greedy best way taking both variable and fixed costs for each truck used into account. The while-loop starts with randomly choosing one destroy and one repair operator based on weights (line 4). This destroy operator removes customers of one or possibly more routes (line 5) and inserts them in a RemovedCustomers set. The removed customers are reinserted by applying the chosen repair operator (line 6). At this stage, a drone insertion operator could potentially be selected. In this case, it is necessary to check whether customers to be reassigned are eligible for drone deliveries at all. If this is not the case, another repair operator must be chosen that inserts these customers to truck routes. The same holds true when a new microdepot is opened.

A local search is then executed (lines 7 - 9) if the new solution $\hat{R}$ has potential for a new global best solution, i.e., the costs of the new solution found $f(\hat{R})$ are lower than the costs of the global best solution $f(R^{global})$ adjusted by a factor μ.

Algorithm 1: ALNS framework for vehicle fleet planning

```
1  R, R^global ← Initial Solution;
2  Temp ← GetInitialTemp();
3  while Time < MaxTime do
4  |   ChooseOperator();
5  |   (R̂, RemovedCustomers) ← RemoveCustomers(R);
6  |   R̂ ← RepairCustomers(R̂, RemovedCustomers);
7  |   if f(R̂) < (1 + μ)· f(R^global) then
8  |   |   R̂ ← Local Search(R̂);
9  |   end
10 |   if f(R̂) < f(R^global) then
11 |   |   R, R^global ← R̂;
12 |   else if accept(f(R̂), f(R), Temp) then
13 |   |   R ← R̂;
14 |   Temp ← UpdateTemp(Temp);
15 |   UpdateWeights();
16 end
```

Lines 10 - 14 specify the simulated annealing process that updates both global and current solution depending on Temp and if a new global best solution is found. At the end of each iteration, the weights of the operators are updated based on the performance of the chosen operator. The weight $\eta_{i,j}$ for operator i at iteration j is updated analogous to Sacramento et al. (2019): $\eta_{i,j+1} = \zeta\eta_{i,j} + \theta(1-\zeta)$, where ζ is the reaction factor for the learning curve and θ are values dependent of the performance of the operator. The algorithm runs until a maximum time is reached (line 3).

1.5.3 Operators

The destroy and repair operators base on the operators suggested by Ropke and Pisinger (2006), Hemmelmayr et al. (2012), and Sacramento et al. (2019). However, we modify these operators with respect to the specifics of our problem setting, as explained below. In general, we consider either inter-route or intra-route operators.

1.5.3.1 Destroy operators

We consider five destroy operators that remove α customers. The number of removed customers is randomly drawn from a descending exponential distribution that is further limited by an upper bound and therefore favors a small number of customers which reduces the computation time within each iteration of the ALNS. As suggested by Sacramento et al. (2019), the corresponding customers in R_T^D are removed only if a node in the truck routes R^T is removed from which drones launch or return. If the node removed in R^T is a microdepot, all its customers are removed from $R_{M_0}^D$. The operators applied possibly reduce the vehicle fleet of trucks and drones and/or close microdepots.

Random customer removal – The random customer removal operator removes α customers from one specific route.

Random microdepot removal – The random microdepot removal operator removes one random microdepot from the truck route and all its connected customers.

Closest customer removal – The closest customer removal operator removes a random customer from one route and $\alpha - 1$ closest customers from the same route. The closest operator is chosen since it generally generates good results within a short run time.

Random any removal – The random any removal operator selects one random customer and removes it from the one of the three routes that includes it.

Closest any removal – This operator works in a similar way as the closest removal operator, but removes the closest customers from any of the three routes.

1.5.3.2 Repair operators

We consider 15 repair operators that reinsert the removed customers in one of the three or multiple route types. Trucks or drones might be added to the vehicle fleet or a new microdepot might be opened by applying these operators. In the following, we cluster these operators according to the related route.

For the truck routes R^T, five operators are used:

Random customer to truck insertion - This operator adds customers one by one to a random place in R^T. It is checked first whether a customer might fit in a route.Otherwise a new route is created.

Closest customer to truck insertion - Customers are added to a truck's route one by one after their closest node. If the customer does not fit in a truck's route, the next closest node in a different route is chosen.

Greedy customer to truck insertion - The greedy truck insertion operator adds a customer to the truck's route in the greedy best place. For this it is for each node within a route checked,

which costs arise, if the customer is added after this node. For this fixed, variable, synchronization, and penalty costs for upcoming infeasibility are considered. Moreover, it is checked whether adding a truck to the fleet might be more cost effective.

Greedy customer to truck insertion - new route - All customers are added one by one to the greedy best place in one new route only. Thus, exactly one truck is added to the fleet, always.

Greedy customer to truck insertion - existing routes - This operator places all customers in a truck's route greedy best place. It is not checked, if the customer might fit better in a new tour. Thus, no trucks are added to the fleet.

For the drone routes that are launched from trucks R_T^D, three operators are used:

Random customer to drone launched from truck insertion - This operator chooses a random launching position for a drone from a truck route. The drone afterwards returns to the next truck's position. We expect that in most cases the drone returns to the next truck position, since the drone can be used frequently in this manner, but the truck only rarely has to wait. If a later return node would improve the solution, the local search implements the necessary changes.

Closest customer to drone launched from truck insertion - The closest operator works in a similar way to the previous random insertion operator, but it chooses the closest truck position for the launch node of the drone. The drone returns again to the next truck's position. Since fixed costs are neglected in this operator, this operator typically results in adding new drones to the fleet early in an iteration rather than trying to serve all customers with the existing number of drones.

Greedy customer to drone launched from truck insertion - It is checked which is the best launch and return node for the drone to serve the customer. Account is taken of variable, fixed, and penalty costs, as well as an estimate of synchronization costs.

For the drone routes that are launched from microdepots $R_{M_0}^D$, five operators are used.

Random customer to microdepots insertion - A random microdepot or the CDC in range of the customer is chosen and opened if it is not in use yet. The customer gets served by a drone launched from that microdepot.

Closest customer to microdepots insertion - This operator works in a similar way to the previous random insertion operator, but the closest microdepot or CDC is chosen.

Greedy customer to microdepots insertion - It is checked, which microdepot can serve as launching node for drones at lowest total costs. All microdepots and the CDC are taken into account.

Closest customer to open microdepots insertion - This operator works in a similar way to the closest customer to microdepot insertion operator, but only takes into account microdepots or the CDC that are already in use.

Greedy customer to open microdepots insertion - This operator works in a similar way as the greedy customer to microdepot insertion operator, but only takes into account microdepots or the CDC that are already in use.

Last, two operators combine all routes:

Greedy customer insertion - This operator combines the operators greedy customer to truck insertion, greedy customer to drone launched from truck insertion and greedy customer to microdepots insertion. One by one it is checked, where a customer can be added in any route best. This

operator might extend the vehicle fleet by trucks and drones launched from trucks, microdepots, or the CDC or open new microdepots.

Greedy customer insertion - existing trucks and microdepots - This operator works in a similar way as the previous operator, but the vehicle fleet might only be increased by drones and neither trucks are added to the fleet nor microdepots are opened.

1.5.4 Local search

We apply a local search procedure independently for each of the three route types if the current solution is within a threshold μ of the global best solution. The changes have no or only little impact on both other routes as these changes are only for route optimization and do not aim to optimize the drone location or vehicle fleet. Our destroy and repair operators, on the other hand, are developed to vary and optimize the drone location and the vehicle fleet. The local search for the three routes work as follows:

R^T The local search for the truck routes R^T is a two-opt that reconnects each two arcs within a tour, if drones are not launched from the affected nodes. This procedure results in swapping two nodes in R^T that are not microdepots or customers from which drones are launched since this would have a sufficient impact on $R^D_{M_0}$ and R^D_T.

$R^D_{M_0}$ For the drone routes $R^D_{M_0}$, a two-opt with no restrictions on the node is used. The local search swaps the microdepots or CDC, from which the corresponding drones launch and return for two customers. This swap has no impact on R^T as the same delivery volumes continue to be transported to the microdepots.

R^D_T The local search for R^D_T first identifies the cost-optimal starting node for each customer and secondly the landing position on the same truck. The number of drones per truck can be changed by this swap.

All local searches apply a first-improvement strategy and execute the change if an improvement in costs is achieved. Smaller dependencies between the three routes are still considered if a truck arrives at a microdepot or a return node for a drone at an earlier or later date. This is the case if the route of the truck or its waiting time at a previous node is adjusted before arrival at the microdepot or at the return node. These variation of arrival lead to an adjustment of remaining time for drones of the microdepots to serve customers or drone flight time for drones launched from trucks. Thus, the local searches may only vary penalty costs.

1.6 Numerical experiments

In this section we first introduce the numerical setup. We then evaluate the performance of the proposed ALNS before showing managerial insights. The MILP is implemented in OPL and solved using CPLEX v12.10. The ALNS is implemented in C++. All experiments are conducted on an AMD Ryzen 9 3950X with 32 GB RAM.

1.6.1 Instance generation

1.6.1.1 Network

We consider a network that states a rural area with random CDC location and five randomly located demand areas within a 60km × 60km map. In each demand area, there is a potential microdepot location at its center. This means that we assume five potential microdepots.

We generate demand settings with 50 to 200 customers. 70-100% of all customers are randomly placed in demand areas and the remaining customers across the entire map. Three (two) demand areas comprise 80% (20%) of the total demand allocated to all five demand areas. 25% of all customers cannot be served by drones on average.

1.6.1.2 Parameter settings

Table 1.3 presents truck, drone, and microdepot parameters that are specified for a period of one day. The column T represents parameter settings for trucks, T_{mod} additional parameter settings if a truck is equipped by a docking station for drones, D^T parameter settings for drones launched from trucks, D^{M_0} parameter settings for drones launched from microdepots or the CDC, and M parameter settings for microdepots (Campbell et al. 2017, Keeney 2015, Murray and Raj 2020). In the calculation of the drone variable costs, personnel costs for the flight control of drones by an external employee are already included, who can supervise an average of 10-12 drones in parallel (Keeney 2015).

We assume two different sizes of drones, small drones launched from trucks and large drones launched from microdepots and the CDC. Large drones have the advantage that they can travel faster and longer distances, but involve higher fixed costs than small drones. We correct the euclidean distances of trucks and drones by a vehicle-specific detour factor since drones can travel a more direct path than delivery trucks.

Parameter	T	T_{mod}	D^T	D^{M_0}	M
Q	100	-	1	1	100
Q_{time}	8	-	-	14	-
detour factors	1.2	-	1.1	1.1	-
a	35	-	50	100	-
e^D	-	-	0.49	0.66	-
K	-	4	-	-	4
s	0.05	-	0.01	0.01	-
c	0.70	-	0.03	0.03	-
c_{wait}	13.00	-	-	-	-
$c_{service}$	0.65	-	0.13	0.13	-
c_{fix}	23.00	3.00	3.61	5.37	14.07

Table 1.3: Parameter settings.

The ALNS parameters are based on pre-testing. A maximum of eight customers can be removed from a tour per iteration. The reaction factor ζ for the learning curve of the ALNS is set to 0.7. Starting with an initial weight $\eta_{i,0}$ of 100 per operator i, the weights are changed by $\theta = 330$ for a global best new solution, by $\theta = 130$ for a local best new solution, by $\theta = 90$ for a local worse new

solution but accepted in Simulated Annealing, and by $\theta = 0$ for a worse new solution. The local search parameter μ is set to 0.02. The initial temperature factor for the simulated annealing is set to 100 and cools down by a cool rate dependent on the remaining run time of the ALNS.

1.6.2 Performance evaluation

1.6.2.1 Small instances

The ALNS is compared to the solutions obtained using CPLEX for the MILP. The run time limit was set to 60 minutes and the ALNS was executed five times. Table 1.4 shows the results for 20 scenarios assuming a certain number of customers (9 to 15) and microdepots (1 to 3) within a 10km × 10km, 20km × 20km, 30km × 30km, or 60km × 60km map. Each Scenario is denoted in the form of [#customers].[#microdepots].[#non-eligible customers for drone delivery]. The column labeled Map indicates the size of the delivery area in km^2. C^{BKS} quantifies the costs for the best-known solution, i.e., the optimal solution or upper bound found by CPLEX. Column *Gap* shows the optimality gap reported by CPLEX in % in the event that optimality has not yet been proven. The columns C^{best}_{ALNS} and C^{avg}_{ALNS} describe the costs for the best and average solution out of five runs. Finally, the run time in seconds of both the average of five runs for the ALNS (t^{avg}_{ALNS}) and CPLEX (t^{opt}) are reported. The results show that CPLEX was not able to find or prove the optimal solution in four cases within the time limit of 60 minutes. On the contrary, the ALNS always found this solution with a maximum average run time of less than one second.

Scenario	**Map**	C^{BKS}	*Gap* [%]	C^{best}_{ALNS}	C^{avg}_{ALNS}	$t^{avg}_{ALNS}[s]$	$t^{opt}[s]$
10.01.04	10 x 10	46.3*	0	46.3	46.3	0.0024	386
10.03.02	10 x 10	38.3*	0	38.3	38.3	0.0000	70
11.02.05	10 x 10	52.3	14	52.3	52.3	0.0036	3600
13.02.03	10 x 10	50.2	37	50.2	50.2	0.0104	3600
13.03.02	10 x 10	53.4	48	53.4	53.4	0.0026	3600
09.01.03	20 x 20	59.3*	0	59.3	59.3	0.0008	47
10.03.01	20 x 20	56.3*	0	56.3	56.3	0.0022	19
11.01.03	20 x 20	65.3*	0	65.3	65.3	0.0010	3580
11.01.06	20 x 20	82.7*	0	82.7	82.7	0.2668	482
13.02.03	20 x 20	77.8	34	77.8	77.8	0.0098	3600
09.03.05	30 x 30	112.2*	0	112.2	112.2	0.0094	12
10.01.04	30 x 30	86.8*	0	86.8	86.8	0.0064	39
11.01.05	30 x 30	93.5*	0	93.5	93.5	0.0020	76
11.01.06	30 x 30	103.3*	0	103.3	103.3	0.0028	119
11.02.04	30 x 30	94.7*	0	94.7	94.7	0.0938	3296
11.01.03	60 x 60	155.3*	0	155.3	155.3	0.0182	7
12.02.05	60 x 60	150.1*	0	150.1	150.1	0.0312	23
13.03.06	60 x 60	169.4*	0	169.4	169.4	0.0126	9
14.03.06	60 x 60	190.0*	0	190.0	190.0	0.0988	568
15.02.07	60 x 60	200.0*	0	200.0	200.0	0.0628	382

Table 1.4: Results for small instances (* optimal solution).

1.6.2.2 VRPD benchmark

Next, we compare the performance of the ALNS introduced to the benchmark instances from Sacramento et al. (2019) for the VRPD, which have also been used by Euchi and Sadok (2021) to test the solution approach they developed. The VRPD instances consider a problem setting with one drone per truck. For this, our operators concerning drones launched from microdepots or the CDC are omitted and customers are supplied by trucks or drones launched from trucks. Additonally, as Sacramento et al. (2019) forbid drones to return to the same node, they have been launched, our operators have been modified in the same way.

The results for the ALNS are compared to those of the best solutions by Sacramento et al. (2019) and Euchi and Sadok (2021) for the same run time of five minutes and ten runs, Sacramento et al. (2019) used. For this purpose, the deviation $\bar{\sigma}$ of the best found $\bar{C}^{best}$ compared to the average found solution $\bar{C}^{avg}$ for the ALNS of Sacramento et al. (2019), the hybrid genetic algorithm of Euchi and Sadok (2021), and our ALNS and the percentage deviation of our best found solution to the existing global best-known-solution $\bar{\sigma}^{BKS}$ are computed. Table 1.5 shows the aggregated results for the 112 instances for different demand classes, i.e., the average results obtained for scenarios of the same demand class. Table A.2 in the appendix shows detailed results for all 112 instances.

Our ALNS has on average a lower σ and is more stable than both the heuristics developed by Sacramento et al. (2019) and Euchi and Sadok (2021). Moreover, we find best solutions for instances with 200 customers on average and our ALNS outperforms the approach by Sacramento et al. (2019) in 30 and the approach by Euchi and Sadok (2021) in 23 instances. In addition, we find 17 new best-known solutions. Sacramento et al. (2019) optimally solve small instances with up to 12 customers. Our ALNS approach also finds these optimal solutions. For larger instances with 20, 50, 100, and 150 customers our approach performance slightly worse than the approaches suggested by Sacramento et al. (2019) and Euchi and Sadok (2021). However, this can be explained by the short run time of five minutes and that our operators are designed for multiple drones per truck and a possible return to the same location from which the drone takes off. Nevertheless, the results confirm the quality of the procedure we have developed, also because our method is designed for tactical fleet and drone location planning and does not only consider route planning with trucks, each equipped with a single drone.

Demand	**Sacramento et al. (2019)**			**Euchi and Sadok (2021)**			**Own results**			
class	$\bar{C}^{best}$	$\bar{C}^{avg}$	$\bar{\sigma}$[%]	$\bar{C}^{best}$	$\bar{C}^{avg}$	$\bar{\sigma}$[%]	$\bar{C}^{best}$	$\bar{C}^{avg}$	$\bar{\sigma}$[%]	$\bar{\sigma}^{BKS}$[%]
6-12	2.8762	2.8762	0.00	2.8762	2.8762	0.00	2.8762	2.8766	0.01	0.00
20	4.1111	4.1152	0.09	3.8832	4.0331	5.46	4.0890	4.0905	0.02	7.47
50	13.4792	13.6293	1.03	13.2746	13.4606	1.46	13.4845	13.6678	1.54	2.21
100	18.3439	18.6604	1.59	18.0009	18.1871	1.24	18.4121	18.6450	1.29	3.79
150	21.7796	22.5680	3.36	21.5250	22.5542	4.39	21.8360	22.2623	1.83	2.15
200	26.3185	26.9347	2.29	25.9771	26.0861	0.51	25.9569	26.4741	1.60	0.40
Average			1.19			1.67			0.90	2.02

Table 1.5: Approach suggested by Sacramento et al. (2019) and Euchi and Sadok (2021) vs. our approach for VRPD instances from Sacramento et al. (2019).

1.6.2.3 Large instances

We further show the performance and the solution stability of the fleet mix and microdepot locations generated by the ALNS introduced for 30 different demand settings. Table 1.6 presents the aggregated results for different demand classes and gives information on the average of the best fleet mix (T, D^T, D^M, D^{CDC}) and the microdepots used within the demand class. Further, the average of the best costs ($\bar{C}^{best}$), and its deviation ($\bar{\sigma}$) from average costs ($\bar{C}^{avg}$) are reported. Table A.1 in the appendix shows detailed results for all scenarios tested. We limit the computational time per run to 60 minutes and perform five runs to solve a scenario.

Demand class	T	D^T	D^M	D^{CDC}	Microdepots used	$\bar{C}^{best}$	$\bar{C}^{avg}$	$\bar{\sigma}$[%]
$50-57$	1	2.5	0	0		216.14	216.33	0.09
$58-63$	1	2.5	1	0	M_3	229.35	230.87	0.66
$64-79$	1	1.5	2	0	M_2, M_5	244.71	245.96	0.51
$80-114$	1	0	2	1	M_2, M_5	286.06	286.17	0.04
$115-129$	1.3	0	3	1	M_2, M_3, M_5	308.49	309.05	0.16
$130-178$	2	0	4	0.1	M_1, M_2, M_3, M_5	383.38	383.98	0.15
$179-200$	2	0	4	1	M_1, M_2, M_3, M_5	433.20	434.80	0.36

Table 1.6: Results for large instances.

The results show that the ALNS finds solutions with an average deviation to the best found solution (σ) of less than 1% for all scenarios. The fleet mix found and the microdepots used are stable within each demand class, but varies with increasing demands in this network. Moreover, the table indicates that also both the fleet mix and the selected locations of the microdepots are stable. Microdepot 4 is never opened, for instance.

1.6.3 Sensitivity analysis

1.6.3.1 Experiments with varying network structure

In this subsection, we analyze the potential cost savings of different fleet mix modeling approaches relative to sole truck deliveries assuming a classical VRP context. The analysis varies the size and overall structure of the delivery area, i.e., the number of demand areas (four, six, eight, and ten), the location of the CDC, i.e., a remote (A) and a more central (B) location within the delivery area and the num

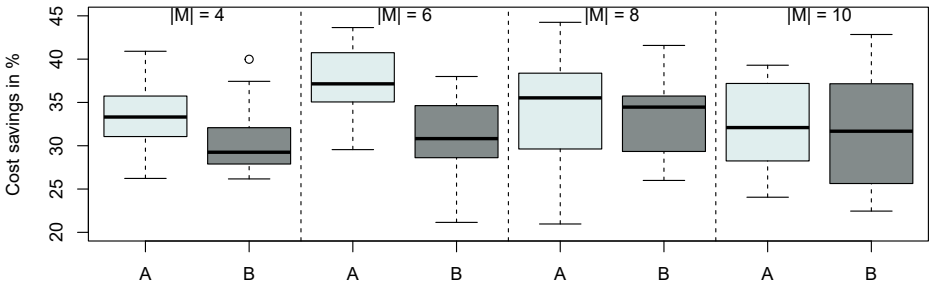

Figure 1.3: Cost savings of our fleet mix modeling approach (2E-LRPD) compared to a sole truck delivery for different networks, if the CDC is remote (A) or more central located (B).

Figure 1.3 shows the cost savings of our fleet mix and microdepot location modeling approach (2E-LRPD) compared to the sole truck delivery approach (note, we aggregate 160 different demand classes in this study). The results lead to the following observations. Average cost savings of 2E-LRPD decrease if the CDC is remotely located. A centrally located CDC allows the deployment of more drones than a CDC that is located at a greater distance to potential customers. This saves trucks and travel distances for trucks and drones. The differences in cost savings between a centrally and remotely located CDC diminish assuming more demand areas (eight and ten). In these cases the CDC has less relevance as a potential drone location.

Next we consider different fleet mix modeling approaches and analyze the respective cost savings in comparison to sole truck delivery. In this analysis, we distinguish different demand classes (50 to 100, 101 to 150, and 151-200 customers) but aggregate the results for both CDC locations and for the respective number of demand areas. The different fleet mix modeling approaches considered are as follows. The VRPD approach assumes a vehicle mix that consists of trucks and drones launched from trucks. The 2E-LRP approach assumes a vehicle mix that consists of trucks and drones, but drones are only launched from microdepots and the CDC. It also decides on the number and the location of microdepots. Finally, our 2E-LRPD approach allows the selection of the best fleet mix from the two previously mentioned approaches or a combination of both modeling approaches. Figure 1.4 s

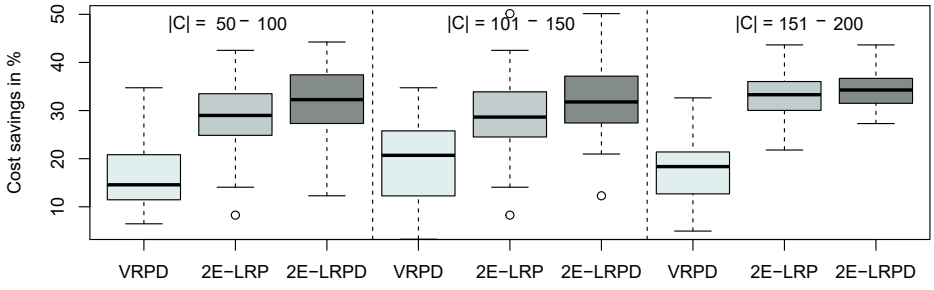

Figure 1.4: Cost savings of drone delivery compared to sole truck delivery for three demand classes considering different delivery methods.

Both the truck-drone concept (VRPD) and drones launched from microdepots (2E-LRP) lead to sufficient cost savings compared to truck-only deliveries in all scenarios for all demand classes. Moreover, we can observe, that the cost savings potential of drones is relatively constant for all demand classes and increases only slightly at higher demands for microdepots or the mix. The VRPD approach achieves average cost savings of 19.2% compared to sole truck delivery. These savings increase to 31.1% by following the 2E-LRP approach. The average cost savings can however be further increased by 14.1% and 2.2%, respectively, if the best delivery method or mix of methods is chosen (2E-LRPD approach). Note that in 58% of all scenarios a mix of drones launched from trucks (VRPD) and drones launched from the CDC or microdepots (2E-LRP) is best. This shows that it is insufficient to choose only the best solution from both approaches. An integrated modeling and solution approach is needed that also models and possibly selects the respective combinations.

Summary. The size and overall structure of the delivery area, especially the location of the CDC, has a significant influence on the vehicle fleet. Launching drones from microdepots instead

of trucks leads to higher cost savings compared to sole truck delivery. A mix of drone delivery methods may even increase these cost savings.

1.6.3.2 Experiments with varying deliverability of drones

In this subsection the impact of varying the deliverability by drones is analyzed. We perform a sensitivity analysis with a variation of the average customer share β that cannot be served by drones, but by trucks. Fewer customers may be served by drones, for example, if there is less acceptance of drones in a network or if packages tend to be particularly heavy or numerous. Drones may serve more customers, for example, if more smaller products are supplied due to increasing e-commerce (Keeney 2015).

Table 1.7 presents the development of the average number of deployed vehicles within the demand classes of 50 to 100 customers, 101 to 150 customers and 151 to 200 customers for varying β ceteris paribus.

	$\beta = 50\%$				$\beta = 25\%$				$\beta = 0\%$			
Demand class	T	D^T	D^M	D^{CDC}	T	D^T	D^M	D^{CDC}	T	D^T	D^M	D^{CDC}
50-100	1.8	2	1.1	0.2	1	1.3	1.4	0.4	1	0.1	2.4	0.9
101-150	2	2.8	1.5	0.6	1.5	0	3.2	0.6	1	0	2.8	1.5
151-200	2.7	2.3	2.2	0.7	2	0	4	0.4	1.4	0	3.4	1.6

Table 1.7: Average vehicle fleet, depending on the respective share of their eligibility for drone delivery β for three different demand classes.

As drone deliverability increases, stationary drones become more profitable compared to a truck-drone concept. Moreover, we can observe that stationary drones reduce the number of trucks used. Up to three trucks are still necessary if only every second customer can be supplied by drones. With increasing deliverability, a maximum of only two trucks is necessary. The strongest limitation for trucks is no longer the delivery time but the maximum payload. Due to increased deliveries by drones, the CDC is more frequent equipped with more than one drone from medium demand onwards, on average.

Summary. The vehicle fleet mix is sensitive to drone deliverability. In cases with low eligibility of customers for drone delivery, it is more profitable to launch drones from both delivery trucks and stationary depots, even if demand is high. On the other hand, the concept of stationary drone delivery becomes relevant when more customers agree to receive their deliveries by drone.

1.6.3.3 Experiments with drone properties.

Lastly, the impact of drone property changes is analyzed. Due to technological progress, drones are expected to travel faster and with a greater endurance (Wingcopter GmbH 2020). Thus, two linearly increased speeds and endurance of drones by a factor γ are considered ceteris paribus. Table 1.8 presents the development of the average number of vehicles for the demand classes of 50 to 100 customers, 101 to 150 customers and 151 to 200 customers for improved drone properties.

					$\gamma = 25\%$				$\gamma = 50\%$			
Demand class	T	D^T	D^M	D^{CDC}	T	D^T	D^M	D^{CDC}	T	D^T	D^M	D^{CDC}
50-100	1	1.3	1.4	0.4	1	2.5	0.3	0	1	3.4	0.1	0
101-150	1.5	0	3.2	0.6	1	1.9	1.5	1	1	2.7	1.2	1
151-200	2	0	4	0.4	1.7	1.6	2.6	0.9	1.7	4.6	1	0.8

Table 1.8: Average vehicle fleet, depending on improved speed a and endurance e by factor γ.

With increasing drone properties, drones launched from trucks become more advantageous towards drones launched from stationary depots, especially for low and high demands proportionally more drones are launched from trucks than from microdepots or CDC. As distances increase, drones launched from trucks become more and more capable of delivering to individual dispersed customers. This leads to substantial cost savings compared to the truck or stationary drone delivering to these customers instead since synchronization efforts reduce with increasing speed and drones launched from microdepots are already technologically mature in the numerical setup.

Summary. The synchronized truck-and-drone delivery method is more restricted by the drone properties flight distance and speed than the microdepot method. Improving drone properties thus leads to greater competition of the two delivery methods, resulting in a mix of mobile and stationary drones becoming even more cost effective.

1.7 Conclusion

This paper considers tactical vehicle fleet and microdepots planning for commercial parcel delivery using different delivery methods and mixes of methods with trucks and aerial drones. We introduced the two-echelon location routing problem with drones denoted as 2E-LRPD that defines the cost-optimal fleet mix of trucks and drones as well as the number and locations of microdepots. We developed a problem-specific ALNS that generates near-optimal solutions.

The numerical study shows that a combination of trucks and drones in delivery always leads to significant cost savings compared to sole truck delivery. We further demonstrate that the best fleet mix often combines all the different delivery methods, so that customers in the delivery area can be served by drones launched from the CDC, microdepots, and trucks as well as by direct truck delivery. While we observed that it is mostly profitable to launch drones from stationary depots (microdepots and/or CDC) instead from trucks, drones launched from trucks are increasingly preferred as the drone range increases or customer eligibility for drone deliveries decreases. The study also shows that under certain circumstances only a subset of all possible delivery methods is cost-optimal. Nevertheless, it is insufficient to choose only the best solution from the VRPD and the 2E-LRP approach. A combination of both approaches turns out to be best in 58% of all cases analyzed. This result justifies the increased effort involved in fleet mix, microdepot and delivery planning using the integrated modeling and solution approach (2E-LRPD) proposed in this paper.

Future research possibilities could include the impact of weather information on the vehicle fleet since drones are more vulnerable to weather, especially precipitation and wind, compared to delivery trucks. In addition, some assumptions could be extended, such as the possibility that drones can

transport multiple packages instead of only one. It can also be considered that drones return to a different stationary depot than the one they started from, or different demand distributions can be assumed in each period of a planning horizon (e.g., each day of a week). However, the latter two extended assumptions lead to a multi-period problem that makes the problem even more difficult to solve.

Acknowledgments

The authors would like to thank the anonymous reviewers and the editors for their valuable recommendations, which have significantly improved the paper.

Contribution 2 - Two-indexed formulation of the traveling salesman problem with multiple drones performing sidekicks and loops

2 Two-indexed formulation of the traveling salesman problem with multiple drones performing sidekicks and loops

Alexander Rave

Abstract Aerial drone delivery has great potential to improve delivery time in package delivery, as drones can fly autonomously over obstacles at a possibly higher speed than trucks. The benefits of drones in delivery can even be increased in a truck-and-drone tandem where a truck carries one or multiple drones and releases them at advantageous places. This problem is known as the traveling salesman problem with multiple drones (TSPmD). We focus on a variant of this problem, where the drones have two options after serving the customer: they can return to a node the truck visits at a later stage (sidekick) or return to the same node they were launched from (loop).

While several variants of the TSPmD have been studied, considering sidekicks and loops in combination with minimizing the makespan is not represented so far. We fill this gap and introduce an efficient two-indexed mixed-integer linear program (MILP) formulation that provides new optimal solutions for instances with up to 28 nodes for benchmark purposes. Our MILP formulation outperforms two state-of-the-art MILP formulations from the literature considering one drone. In a case study, we analyze the impact on the minimization of the makespan when allowing drones to perform loops. Loops mainly become relevant when drones travel faster than trucks resulting in average makespan savings of up to 2.7%.

URL (working paper): `http://dx.doi.org/10.2139/ssrn.4431738`

(a) Performed sidekick by a drone.

(b) Performed loop by a drone.

Figure 2.1: Illustration of drone routes.

2.1 Introduction

Parcel delivery via aerial drones is much considered in academia (e.g., Murray and Chu 2015) and also in practice (e.g., Gartner 2016). One known delivery option is the interaction of one or more drones with a delivery truck. The routing of both a truck and one drone is known in the literature as traveling salesman problem with drone (TSPD). In the case of multiple drones, the problem is called traveling salesman problem with multiple drones (TSPmD) (e.g., Seifried 2019). Initially introduced by Murray and Chu (2015), many publications on the truck-and-drone tandem only consider drones performing sidekicks, which means that they return to a node the trucks visits at any later stage in its tour (see Figure 2.1a). However, only a few publications consider additionally drones performing loops, meaning drones return to the same node they are launched from (see Figure 2.1b). Thereby, (Schermer et al. 2019) already found that drones perform loops in the final found routing if these are allowed.

Considering multiple drones that can perform both sidekicks and loops while minimizing the makespan is not represented in the literature, and thus, the literature also lacks suitable benchmark instances. We fill this gap and introduce a compact two-indexed mixed-integer linear program (MILP) formulation of this TSPmD. This MILP formulation is easily implemented and outperforms MILP formulations for the single drone case from the literature for larger instances, i.e., it finds the optimal solution faster.

This paper contributes to the literature as follows: First, we introduce the TSPmD with drones performing both sidekicks and loops while minimizing the makespan. Second, we formulate the problem as MILP with only two-indexed variables that outperforms MILP formulations from the literature for the single drone case. Third, we present new optimal solutions for the instances of Murray and Chu (2015) and Bouman et al. (2018) for up to 28 nodes for benchmark purposes. Fourth, in a numerical study, we analyze the impact of allowing drone loops for different numbers of drones on minimizing the makespan and the runtime of a MILP solver and present managerial insights.

The structure of this paper is as follows. In Section 2.2, we describe the decisions and assumptions in detail. In Section 2.3, we present the relevant literature and delimit our paper to this literature. Next, we introduce the MILP in Section 2.4. In Section 2.5, we describe the instances for which we present benchmark results, analyze the runtime, and give managerial insights on allowing drone loops. Last, in Section 2.6, we summarize the results and give a brief outlook.

2.2 Problem setting

We decide on the routing of one truck and its equipped multiple drones that need to visit certain nodes, i.e., customers. Additionally, we also decide if a customer is served by a truck or else by drone. For this, we minimize the makespan, i.e., the time until the last vehicle has returned to the depot, starting with the first release at time zero. The peculiarity of the considered problem setting is that we consider multiple drones and these can both perform sidekicks and loops. Additionally, we make the following assumptions:

- Traveling times of the truck and the drones generally differ and thus, different speeds and distance metrics can be considered.
- Drones have an endurance limit, i.e., maximum flight time per flight.
- Assumptions regarding customers:
  - All customers must be served once by truck or by drone.
  - Some customers cannot be served by drones, but all by truck (e.g., Murray and Chu 2015).
  - The truck has a sufficient high payload to serve all customers in one tour.
  - A drone can serve one customer per trip and has to return to the truck afterwards.
- Assumptions regarding synchronization:
  - If drones return to a node, the truck continues its tour at this node as soon as all returning drones have landed.
  - Drones do not wait for the truck but reduce their speed instead to a certain extent (e.g., Murray and Chu 2015, Rave et al. 2023b). This allows to avoid unrealistic routes where the drone has to wait for almost the complete truck's tour at a node, for example, at the end of the tour.
  - Drones only return to the truck at a node the truck visits. This node must be the same node they are launched from (loop) or a node the truck visits later in its tour (sidekick).
  - Drones can perform loops at the depot, but these are only allowed at the end of the truck's tour, which results in waiting times at the end of the tour (e.g., Dell'Amico et al. 2021a).
  - Each drone can only perform at maximum one loop at a node.
- There are no service, preparation, or rendezvous times for trucks and drones.
- There are no loading or battery change times for drones.

Exemplary routing plan For a better understanding of the problem setting, Figure 2.2 presents an example routing of the truck equipped with two drones serving ten customers. Customers (C_1,...,C_{10}) are numbered in the order of serving. Starting at the depot, C_1 is served by the truck

first, where one drone is launched to perform a sidekick to serve C_2. The truck and the drone meet again at C_3, where a second drone performs a loop and serves C_4. Note that the truck continues its tour as soon as both drones have returned from serving C_2 and C_4. Next, the truck serves customer C_5 and launches a drone to perform a sidekick to serve C_7. Note that the drone can return to any node, the truck visits at a later stage as long as the flight time is within the endurance limit. At C_6, the second drone is launched to perform a sidekick to serve C_8. Both drones return to the truck at C_9. The truck and its drones return to the depot afterwards, where again, one drone is launched to serve C_{10} in a loop. The tour is finished as soon as this drone returns. Thus, the truck waits at the depot for the drone to return.

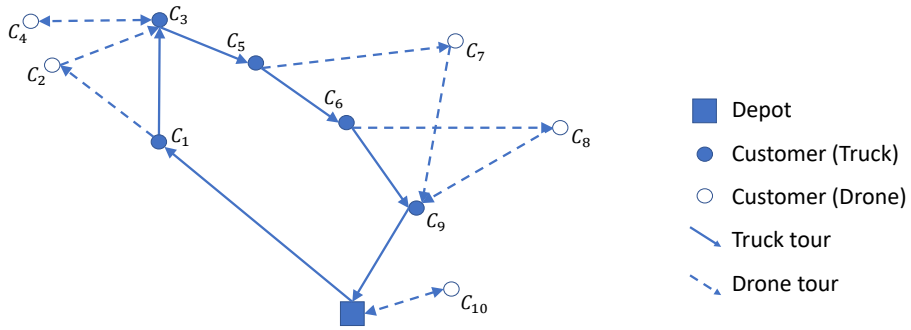

Figure 2.2: Exemplary routing plan for ten customers served by one truck equipped with two drones.

2.3 Related literature

In this section, we differentiate this paper to the relevant literature regarding truck-and-drone tandems, where one or multiple trucks are equipped with at least one drone. Especially, we only focus on literature that includes a MILP formulation without special assumptions like, e.g., battery consumption or a sole supply of drones where the truck only has auxiliary means to launch drones at advantageous locations. First, we present the literature where drones only perform sidekicks, and second, we present the literature where drones can perform both sidekicks and loops. We recommend the paper of Otto et al. (2018) for an extensive review of drone operations and Boysen et al. (2021) for a more recent literature review.

Sidekicks The truck-and-drone tandem is initially introduced by Murray and Chu (2015) who present a three-indexed MILP formulation with makespan minimization, which has difficulties to be solved to optimality, if instances with eleven nodes are considered. As a result, Dell'Amico et al. (2021b) and Freitas et al. (2023) published new and improved modelling approaches, which accelerate a standard solver. Further, multiple publications consider close problem settings with either a different objective or extensions like an increased number of trucks or drones. So Seifried (2019) and Cavani et al. (2021) consider multiple drones and Murray and Raj (2020) and Tamke and Buscher (2021) additionally multiple trucks. Cost minimization is considered by Ha et al. (2018) (single truck) and Sacramento et al. (2019) (multiple trucks) who present heuristic solution

approaches.

Sidekicks and loops Drone loops are rarely represented in the literature, however, Schermer et al. (2019) show that the final found routing might include drone loops as well. The authors analyze – among other things – the number of loops and sidekicks performed in a truck-and-drone tandem with multiple trucks and drones. Drones' speed was found to be a significant influencing factor on performed loops. Tiniç et al. (2023) propose two MILP formulations and analyze – among other things – the impact of loops on the objective of cost minimization, if the truck is equipped with an unlimited number of drones. The authors find that allowing drones to perform loops can significantly reduce routing costs. However, an analysis of the impact on minimizing the makespan when permitting loops and for different numbers of drones is missing. Kitjacharoenchai et al. (2019) present a multiple TSPD problem where the assumption that a drone might only return to the same truck is relaxed and thus drones can return to a different truck. The authors consider loops but only if performed at the depot. Dell'Amico et al. (2021a) derive several benchmark results for the instances of Murray and Chu (2015) for different drone settings including loops, however, multiple drones are missing. Roberti and Ruthmair (2021) and El-Adle et al. (2021) present a two-indexed formulation of a TSPD. While Roberti and Ruthmair (2021) additionally introduce an exact branch-and-price approach, El-Adle et al. (2021) accelerate the solver by adding upper and lower bounds by, e.g., starting with an initial solution that is generated by a greedy insertion heuristic, and additionally assess the data in a pre-processing step to reduce the number of possible drone arcs. Considering multiple drone delivery options, Rave et al. (2023b) present both a MILP formulation and heuristics solution approach for a problem setting where drones may launch from trucks and additionally from the depot or microdepots.

Differentiation to the literature Table 2.1 summarizes the major assumptions, the objective, the largest number of variables' indices in the MILP formulation, and the largest instance size (including the depot once) solved to optimality with the MILP formulation. While there are three two-indexed formulations for the TSPD (El-Adle et al. 2021, Dell'Amico et al. 2021b, Roberti and Ruthmair 2021), there is one publication with a two-indexed formulation for the TSPmD (Seifried 2019). However, among other things, the author does not consider loops for drone delivery.

	Assumptions			Objective			
	# Trucks	# Drones (per truck)	Loops	Costs	Make-span	# Variables' indices	Instance size
Murray and Chu (2015)	1	1			✓	3	-
Ha et al. (2018)	1	1		✓		3	11
Dell'Amico et al. (2021b)	1	1			✓	2	14
Freitas et al. (2023)	1	1			✓	5	11
Sacramento et al. (2019)	n	1		✓		3	13

Continued on next page

Continued from previous page

Seifried (2019)	1	m			✓	2	14
Cavani et al. (2021)	1	m			✓	3	25
Murray and Raj (2020)	n	m			✓	4	9
Tamke and Buscher (2021)	n	m			✓	5	9
El-Adle et al. (2021)	1	1	✓		✓	2	32*
Dell'Amico et al. (2021a)	1	1	✓		✓	3	11
Roberti and Ruthmair (2021)	1	1	✓		✓	2	10
Tiniç et al. (2023)	1	m	✓	✓		3	20
Schermer et al. (2019)	n	m	✓		✓	3	11
Kitjacharoenchai et al. (2019)	n	m	✓**		✓	3	10
Rave et al. (2023b)	n	m	✓	✓		3	15
This paper	1	m	✓		✓	2	28

Table 2.1: Comparison of the relevant literature on truck-and-drone tandems. Note that each publication considers drones performing sidekicks.
* The authors added lower and upper bounds and a pre-processing step before running the MILP, ** drone loops only allowed at the depot.

The truck-and-drone tandem presented in this paper extends the one of Rave et al. (2023b). In contrast to their paper, we minimize the makespan, have additional assumptions (e.g., the return time of drones to the depot is sufficient), and an enhanced modelling version of some constraints accelerating the runtime of the solver.

To sum up, this paper introduces the first TSPmD considering both loops and sidekicks while minimizing the makespan. Moreover, we present a two-indexed MILP formulation that can solve instances with more nodes.

2.4 Two-indexed TSPmD formulation

In this section, we present the MILP formulation for the TSPmD. First, in Section 2.4.1, we describe the proceeding of creating the two-indexed formulation. Second, in Section 2.4.2, the used index sets, parameters, and variables are introduced. Third, in Section 2.4.3, the MILP formulation is presented, and last, in Section 2.4.4, the adjustment for preventing loops is described, as this is needed in the numerical study to show the impact of loops.

2.4.1 Proceeding of the two-indexed formulation

A full flight of a drone can be interpreted as a three-node sortie (i, c, j) including the launch node i, the served customer c, and the landing node j (Murray and Chu 2015), and thus consisting of the outbound flight to the customer and the return flight to the truck. To formulate a TSPD using only

two-indexed variables, the drone's flights are split up into two variables instead of one: one for the outbound $\overrightarrow{y}_{i,c}$ and one for the return flights $\overleftarrow{y}_{c,j}$ and these flights are matched in the constraints (e.g., Dell'Amico et al. 2021b).

Considering multiple drones per truck, each vehicle is typically represented in an index set for vehicles (e.g., Murray and Raj 2020), which is, however, not necessary, i.e., the TSPmD can be formulated without the index set for vehicles. Each drone flight can be defined over the same variables $\overrightarrow{y}_{i,c}$ and $\overleftarrow{y}_{c,j}$ with a flow formulation (Seifried 2019). For this, an auxiliary variable ($\pi_{i,j}$) is introduced to monitor the number of drones on the truck traveling from i to j.

To also include loops in the MILP, which only affect the truck's waiting time, a variable for the truck's waiting time $\phi_{i,j}$ is defined with two indices. $\phi_{i,j}$ determine the truck's waiting time at node j for each node i where a drone is launched, and thus the variable includes sidekicks ($i \neq j$) and loops ($i = j$). The truck's waiting time at node j results from the variable $\phi_{i,j}$ for each i. Thus, in contrast to the literature for the TSPD (e.g., El-Adle et al. 2021, Roberti and Ruthmair 2021), there is no need for variables that track drones traveling an arc while staying on the truck, i.e., the drone is not flying.

2.4.2 Decisions and relevant parameters

We consider the index set for customers $\mathcal{I}$, customers including the depot $\mathcal{I}_0$, and customers that can be served by both the truck and drones $\mathcal{I}_D$. In contrast to, e.g., Dell'Amico et al. (2021a), we include the depot only once in the index set $\mathcal{I}_0$. Therefore, constraints regarding a launch or return at the depot are handled differently.

The decisions taken are the routing of the truck ($x_{i,j}$) and the routing of the drones ($\overrightarrow{y}_{i,c}$, $\overleftarrow{y}_{c,j}$). Additionally, the model decides on the customers served by truck (z_c^T) and drones (z_c^D).

The truck is equipped with m drones, each with an endurance e per flight. Similar to, e.g., Dell'Amico et al. (2021a), the different speeds or distance metrics of the truck and drones are also considered in $t_{i,j}^T$, and $t_{i,j}^D$, respectively.

Index sets	
$\mathcal{I}$, $\mathcal{I}_0$, $\mathcal{I}_D$	Node sets for customers, customers and the depot, and customers that can be served by drones.
Parameters	
e	Endurance time for each drone flight.
m	Number of drones on the truck.
M_l^{big}	Big M for $l = 1, 2, 3, 4$.
$t_{i,j}^T$, $t_{i,j}^D$	Truck's (drones') traveling time from node $i \in \mathcal{I}_0$ to node $j \in \mathcal{I}_0$.
Decision variables	
$x_{i,j}$	Binary variable indicating if the truck travels from node i to j ($i, j \in \mathcal{I}_0$).
$\overrightarrow{y}_{i,c}$	Binary variable indicating if a drone is launched at node $i \in \mathcal{I}_0$ to serve customer $c \in \mathcal{I}_D$.
$\overleftarrow{y}_{c,j}$	Binary variable indicating if a drone returns from customer $c \in \mathcal{I}_D$ to node $j \in \mathcal{I}_0$.

Continued on next page

Continued from previous page

z_c^T, z_k^D	Binary variable indicating if customer $c \in \mathcal{I}$ ($k \in \mathcal{I}_D$) gets served by truck (drone).
Auxiliary variables	
u_c	Real-value variable for subtour elimination by Miller et al. (1960) ($c \in \mathcal{I}$).
$\lambda_{i,c}$	Binary variable indicating if customer $c \in \mathcal{I}_D$ is served in a drone loop launched at node $i \in \mathcal{I}_0$.
$\pi_{i,j}$	Positive integer variable monitoring the number of drones that travel on the truck from node i to j ($i, j \in \mathcal{I}_0$) and thus do not serve a customer at that time.
$\tau_{i,j}$	Positive real-value variable indicating the accumulated travel time of the truck traveling from node i to j including the waiting times for drones at node $j \in \mathcal{I}$. Note that waiting times at the depot are excluded and must be considered separately in the objective function.
τ^*	Positive real-value variable indicating the makespan.
$\phi_{i,j}$	Positive real-value variable indicating the waiting times of the truck on the last returning drone at node j, if the drone performs a sidekick ($i \neq j$) or a loop ($i = j$).

Table 2.2: Index sets, parameters, and decision and auxiliary variables.
Note that binary variables have a value of 1, if they are true, and 0 otherwise.

Table 2.2 describes index sets, parameters, and decision and auxiliary variables in detail.

2.4.3 MILP

Objective function The objective is to minimize the makespan.

$$\min \quad \tau^* \tag{2.1}$$

Definition of the makespan τ^* is defined in Constraint (2.2) as the truck's accumulated travel time $\tau_{i,0}$ when arriving at the depot plus the truck's waiting time for returning drones at the depot, as these are not included in $\tau_{i,0}$ when returning to the depot. This objective function results in runtime issues, as a solver has a severe problem finding a lower bound (Seifried 2019). To overcome this issue, we add another definition of the makespan, which helps to find strong lower bounds, particularly in initial iterations (Constraint (2.3)). Note that either Constraint (2.2) or Constraint (2.3) can be chosen. The solver has the best runtime if both constraints are chosen.

$$\tau^* = \sum_{i \in \mathcal{I}_0} \left(\tau_{i,0} + \phi_{i,0}\right) \tag{2.2}$$

$$\tau^* = \sum_{i,j \in \mathcal{I}_0} \left(t_{i,j}^T \cdot x_{i,j} + \phi_{i,j}\right) \tag{2.3}$$

Set partitioning problem Constraints (2.4) ensure that the problem is a set partitioning problem. Constraints (2.5) determine the customers that are served by truck and Constraints (2.6) the customers that are served by drones.

$$z_i^T + \left\{ \begin{array}{ll} z_i^D & , i \in \mathcal{I}_D \\ 0 & , else \end{array} \right\} = 1 \qquad \forall i \in \mathcal{I} \tag{2.4}$$

$$\sum_{i \in \mathcal{I}_0} x_{i,j} = z_j^T \qquad \forall j \in \mathcal{I} \tag{2.5}$$

$$\sum_{i \in \mathcal{I}_0} \overrightarrow{y}_{i,c} = \sum_{j \in \mathcal{I}_0} \overleftarrow{y}_{c,j} = z_c^D \qquad \forall c \in \mathcal{I}_D \tag{2.6}$$

Truck related constraints Constraints (2.7) conserve the truck's flow. Subtours are eliminated by Constraints (2.8) (Miller et al. 1960). M_1^{big} can be set as the number of nodes $|\mathcal{I}_0|$. The truck is launched at maximum once from the depot (Constraint (2.9)). Note that a solution might be that all customers are served by drones that perform a loop at the depot and thus the truck does not leave the depot. Constraints (2.10) ensure that the truck only travels to a different node.

$$\sum_{i \in \mathcal{I}_0} x_{j,i} - \sum_{i \in \mathcal{I}_0} x_{i,j} = 0 \qquad \forall j \in \mathcal{I}_0 \tag{2.7}$$

$$u_i + 1 \leq u_j + M_1^{big} \cdot (1 - x_{i,j}) \quad \forall i, j \in \mathcal{I} \tag{2.8}$$

$$\sum_{j \in \mathcal{I}_0} x_{0,j} \leq 1 \tag{2.9}$$

$$\sum_{i \in \mathcal{I}_0} x_{i,i} = 0 \tag{2.10}$$

Drone related constraints Constraint (2.11) defines the number of drones the truck carries starting from the depot. Constraints (2.12) are balance constraints during the tour to ensure that the number of drones on the truck that leaves a node is equal to the number of drones that were previously on the truck minus launching plus landing drones. The number of drones carried by truck in its complete tour is limited in Constraints (2.13).

Drones may only launch and land on nodes, the truck has visited (Constraints (2.14)). Drone flights must not exceed an endurance (Constraints (2.15)). Additionally, the truck must pick up the drone within the considered endurance limit (Constraints (2.16), if launched at node $i \in \mathcal{I}$ and Constraints (2.17), if launched at the depot). M_2^{big} can be set as the truck's maximum possible tour length.

$$\sum_{j \in \mathcal{I}} \pi_{0,j} + \sum_{c \in \mathcal{I}_D} (\overrightarrow{y}_{0,c} - \lambda_{0,c}) = m \tag{2.11}$$

$$\sum_{j \in \mathcal{I}_0 : i \neq j} \pi_{i,j} = \sum_{k \in \mathcal{I}_0 : k \neq i} \pi_{k,i} + \sum_{c \in \mathcal{I}_D} \left(\overleftarrow{y}_{c,i} - \overrightarrow{y}_{i,c} \right) \qquad \forall i \in \mathcal{I} \tag{2.12}$$

$$\pi_{i,j} \leq m \cdot x_{i,j} \qquad \forall i, j \in \mathcal{I}_0 : i \neq j \tag{2.13}$$

$$\overrightarrow{y}_{j,c} + \overleftarrow{y}_{c,j} \leq 2 \cdot \sum_{i \in \mathcal{I}_0} x_{i,j} \qquad \forall c \in \mathcal{I}_D, j \in \mathcal{I} \tag{2.14}$$

$$t_{i,c}^D \cdot \overrightarrow{y}_{i,c} + t_{c,j}^D \cdot \overleftarrow{y}_{c,j} \leq e \qquad \forall i, j \in \mathcal{I}_0, c \in \mathcal{I}_D \tag{2.15}$$

$$\sum_{f \in \mathcal{I}_0} (\tau_{f,j} - \tau_{f,i}) - M_2^{big} \cdot (2 - \overrightarrow{y}_{i,c} - \overleftarrow{y}_{c,j}) \leq e \quad \forall i \in \mathcal{I}, j \in \mathcal{I}_0, c \in \mathcal{I}_D \tag{2.16}$$

$$\sum_{f \in \mathcal{I}_0} \tau_{f,j} - M_2^{big} \cdot (2 - \overrightarrow{y}_{0,c} - \overleftarrow{y}_{c,j}) \leq e \quad \forall j \in \mathcal{I}_0, c \in \mathcal{I}_D \tag{2.17}$$

Setting up the truck's travel time The truck's accumulated travel times at the beginning of the tour are defined in Constraints (2.18). Constraints (2.19) defines the lower and Constraints (2.20) the upper bound for the accumulated travel times during the truck's tour. These are equal if the truck travels from node i to node j. The accumulated travel time is zero, if the truck does not travel from i to j (Constraints (2.21)).

$$\tau_{0,j} = t_{0,j}^T \cdot x_{0,j} \quad \forall j \in \mathcal{I} \tag{2.18}$$

$$\tau_{i,j} \geq t_{i,j}^T \cdot x_{i,j} + \sum_{f \in \mathcal{I}_0} \left(\tau_{f,i} + \phi_{f,i}\right) - M_2^{big} \cdot (1 - x_{i,j}) \quad \forall i \in \mathcal{I}, j \in \mathcal{I}_0 \tag{2.19}$$

$$\tau_{i,j} \leq t_{i,j}^T \cdot x_{i,j} + \sum_{f \in \mathcal{I}_0} \left(\tau_{f,i} + \phi_{f,i}\right) + M_2^{big} \cdot (1 - x_{i,j}) \quad \forall i \in \mathcal{I}, j \in \mathcal{I}_0 \tag{2.20}$$

$$\tau_{i,j} \leq M_2^{big} \cdot x_{i,j} \quad \forall i, j \in \mathcal{I}_0 \tag{2.21}$$

Sidekicks Constraints (2.22) (at the beginning of the tour) and Constraints (2.23) (during the tour) ensure that drones do not return to a node that was visited by the truck previously on its tour. M_3^{big} can be set as twice the reciprocal value of the truck's shortest travel time $t_{i,j}^T$ between two nodes. M_4^{big} is dependent on the values of M_2^{big} and M_3^{big} and has to be at least $M_2^{big} \cdot M_3^{big}$. There are at maximum m sidekicks per node (Constraints (2.24)). The lower bound of the truck's waiting time arriving at node j is presented in Constraints (2.25) at the beginning of the tour and in Constraints (2.26) during the tour. The inequality exists since the truck waits at a node until the last drone has returned.

$$\begin{aligned} &\overrightarrow{y}_{0,c} + \overleftarrow{y}_{c,j} \leq M_3^{big} \cdot \sum_{f \in \mathcal{I}_0} \tau_{f,j} \\ &\quad + M_4^{big} \cdot (2 - \overrightarrow{y}_{0,c} - \overleftarrow{y}_{c,j}) \quad \forall j \in \mathcal{I}, c \in \mathcal{I}_D \end{aligned} \tag{2.22}$$

$$\begin{aligned} &\overrightarrow{y}_{i,c} + \overleftarrow{y}_{c,j} \leq M_3^{big} \cdot \sum_{f \in \mathcal{I}_0} \left(\tau_{f,j} - \tau_{f,i}\right) \\ &\quad + M_4^{big} \cdot (2 - \overrightarrow{y}_{i,c} - \overleftarrow{y}_{c,j}) \quad \forall i \in \mathcal{I}, j \in \mathcal{I}_0, i \neq j, c \in \mathcal{I}_D \end{aligned} \tag{2.23}$$

$$\sum_{c \in \mathcal{I}_D} (\overrightarrow{y}_{i,c} - \lambda_{i,c}) \leq m \quad \forall i \in \mathcal{I}_0 \tag{2.24}$$

$$\begin{aligned} &\phi_{0,j} \geq t_{0,c}^D \cdot \overrightarrow{y}_{0,c} + t_{c,j}^D \cdot \overleftarrow{y}_{c,j} \\ &\quad - \sum_{f \in \mathcal{I}_0} \tau_{f,j} - M_2^{big} \cdot (2 - \overrightarrow{y}_{0,c} - \overleftarrow{y}_{c,j}) \quad \forall j \in \mathcal{I}, c \in \mathcal{I}_D \end{aligned} \tag{2.25}$$

$$\phi_{i,j} \geq t_{i,c}^D \cdot \overrightarrow{y}_{i,c} + t_{c,j}^D \cdot \overleftarrow{y}_{c,j}$$

$$- \sum_{f \in \mathcal{I}_0} (\tau_{f,j} - \tau_{f,i} - \phi_{f,i})$$
$$- M_2^{big} \cdot (2 - \overrightarrow{y}_{i,c} - \overleftarrow{y}_{c,j}) \qquad \forall i \in \mathcal{I}, j \in \mathcal{I}_0, c \in \mathcal{I}_D : i \neq j \tag{2.26}$$

Loops The truck waits at node i until all drones planned to return have returned to node i (Constraints (2.27)). Constraints (2.28) ensure that drones are only launched to perform loops if there is a sufficient number of drones on the truck at node j. Constraints (2.29) set up $\lambda_{i,c}$, if a customer is supplied in a loop. If a drone starts from node i to serve customer c and returns to node i, $\lambda_{i,c}$ must be set to 1 (left side). If $\lambda_{i,c}$ is set to 1, a drone must start from and return to node i (right side).

$$\phi_{i,i} \geq 2 \cdot t_{i,c}^D \cdot \lambda_{i,c} \qquad \forall i \in \mathcal{I}_0, c \in \mathcal{I}_D \tag{2.27}$$
$$\sum_{i \in \mathcal{I}_0} \pi_{i,j} + \sum_{c \in \mathcal{I}_D} (\overleftarrow{y}_{c,j} - 2 \cdot \lambda_{j,c}) \geq 0 \qquad \forall j \in \mathcal{I}_0 \tag{2.28}$$
$$\frac{\overrightarrow{y}_{i,c} + \overleftarrow{y}_{c,i}}{2} \geq \lambda_{i,c} \geq \overrightarrow{y}_{i,c} + \overleftarrow{y}_{c,i} - 1 \quad \forall i \in \mathcal{I}_0, c \in \mathcal{I}_D \tag{2.29}$$

Definition of variables Last, decision and auxiliary variables are defined.

$$x_{i,j}, \overrightarrow{y}_{i,c}, \overleftarrow{y}_{c,j}, \lambda_{i,c} \in \{0,1\}, \pi_{i,j} \in \mathbb{N}, \phi_{i,j}, \tau_{i,j}, \tau^* \in \mathbb{R}^+ \quad \forall i,j \in \mathcal{I}_0, c \in \mathcal{I}_D \tag{2.30}$$
$$z_i^T, z_c^D \in \{0,1\}, u_i \in \mathbb{R} \qquad \forall i \in \mathcal{I}, c \in \mathcal{I}_D \tag{2.31}$$

2.4.4 Adjustment for preventing drone loops

Variable structures are generally chosen such that drones might perform loops. Thus, to prevent drone loops the variable $\lambda_{i,c}$ needs to be removed from the Constraints (2.11), (2.24), and (2.30), and the Constraints (2.32) need to replace Constraints (2.27), (2.28), and (2.29). These constraints prevent drones to launch and return to the same node.

$$\overrightarrow{y}_{i,c} + \overleftarrow{y}_{c,i} \leq 1 \quad \forall i \in \mathcal{I}_0, c \in \mathcal{I}_D \tag{2.32}$$

2.5 Numerical experiments

In this section, we describe the instances for which we present new benchmark solutions (Section 2.5.1). Next, we analyze the runtime solving the MILP and compare the runtime of our MILP to MILPs for the TSPD from the literature (Section 2.5.2). Last, we show the impact of considering drone loops on minimizing the makespan and the solver's runtime for different drone speeds and endurance limits (Section 2.5.3).

The MILP is implemented in OPL, solved using CPLEX v12.10., and executed on an AMD Ryzen 9 3950X with 32 GB of RAM (single thread). Each instance has a runtime limit of 3600 seconds.

2.5.1 Benchmark instances

In the following, we describe two published instance sets. Detailed solutions of each individual instance for benchmark purposes can be found in Appendix B.1 for the instances of Murray and Chu (2015) and in Appendix B.2 for the instances of Bouman et al. (2018). We present results for these instances, if one ($m = 1$), three ($m = 3$), and a theoretically unlimited number of drones ($m = \infty$) are considered.

Instances of Murray and Chu (2015) Murray and Chu (2015) published twelve instances with eleven nodes (ten customers and the depot) whose locations are uniformly distributed in an 8×8 mile region. The authors consider two endurance limits of 20 and 40 minutes and three different drone-to-truck speed ratios $\alpha \in \{0.6, 1.0, 1.4\}$. Thus, there are 72 instances for which we present results for benchmark purposes. Within the instances, the truck follows a Manhattan distance, while the drone flies the Euclidean path. 80 - 90% of all customers can be served via drones.

Instances of Bouman et al. (2018) Bouman et al. (2018) published instances with 20 and 50 customers that are uniformly distributed with coordinates from 0 to 100. From these instances, we consider 16, 20, 24, 28, and 32 nodes as in El-Adle et al. (2021). These are drawn by taking the first 16, 20, 24, 28, and 32 nodes from the instance with the next-largest number of nodes, i.e., 16 and 20 nodes from instances with 20 nodes, and 24, 28, and 32 nodes from instances with 50 nodes. The endurance limit is set to 30, and drones have the same speed as the truck. Both drones and the truck travel the Euclidean path. All customers can be served by drones.

2.5.2 Runtime analysis

For the runtime analysis, the instances are aggregated by the number of nodes $|\mathcal{I}_0|$ and the endurance e. Table 2.3 presents for each number of drones ($m = 1$, $m = 3$, and $m = \infty$) the number of instances solved to optimality, the average runtime needed in seconds and the average optimality gap, if the solver could not find the optimal solution within 3600 seconds.

Findings: For the instances of Murray and Chu (2015), we could find all optimal solutions except three if one drone is considered. In particular, it is noticeable for all these instances that the optimal solution is found much faster when multiple drones are considered.

			$m = 1$			$m = 3$			$m = \infty$		
	$\|\mathcal{I}_0\|$	e	Opt	CPU [s]	Gap	Opt	CPU [s]	Gap	Opt	CPU [s]	Gap
Murray	11	20	36/36	104	0%	36/36	6	0%	36/36	4	0%
and Chu	11	40	33/36	880	1%	36/36	16	0%	36/36	4	0%
(2015)	Summary		69/72	492		72/72	11		72/72	4	
	16	30	10/10	11	0%	10/10	6	0%	10/10	11	0%
Bouman	20	30	10/10	247	0%	10/10	299	0%	10/10	319	0%
et al.	24	30	8/10	1327	1%	8/10	1319	1%	8/10	1387	1%

Continued on next page

Continued from previous page

(2018)	28	30	1/10	3294	4%	1/10	3305	4%	2/10	3237	4%
	32	30	0/10	3600	12%	0/10	3600	10%	0/10	3600	11%
	Summary		29/50	1696		29/50	1706		30/50	1711	

Table 2.3: Aggregated results for instances of Murray and Chu (2015) and Bouman et al. (2018).

For the instances of Bouman et al. (2018), we could find all optimal solutions for instances with 16 and 20 nodes, eight of ten optimal solutions for instances with 24 nodes, and up to two optimal solutions for instances with 28 nodes when considering one, three, and an infinite number of drones. In contrast to the instances of Murray and Chu (2015), there is no significant change in runtime if multiple drones are considered.

Runtime comparison to the literature The two-indexed MILP formulation of the TSPmD presented in this paper can solve instances with more nodes than the literature (see also Table 2.1). So, Murray and Chu (2015) could not solve one of the 72 instances with eleven nodes to optimality. Considering the instances of Bouman et al. (2018), El-Adle et al. (2021) could find optimal solutions for up to two out of the ten instances with 24 nodes.

			MILP of Roberti and Ruthmair (2021)			MILP of El-Adle et al. (2021)			This paper		
	$\lvert\mathcal{I}_0\rvert$	e	Opt	CPU [s]	Gap	Opt	CPU [s]	Gap	Opt	CPU [s]	Gap
Murray	11	20	24/24	238	0%	24/24	93	0%	24/24	148	0%
and Chu	11	40	24/24	76	0%	23/24	399	1%	21/24	870	2%
(2015)	Summary		48/48	157		47/48	246		45/48	509	
	16	30	0/10	3600	19%	10/10	27	0%	10/10	11	0%
Bouman	20	30	0/10	3600	28%	10/10	576	0%	10/10	247	0%
et al.	24	30	0/10	3600	30%	5/10	2165	4%	8/10	1327	1%
(2018)	28	30	0/10	3600	36%	0/10	3600	9%	1/10	3294	4%
	32	30	0/10	3600	42%	0/10	3600	17%	0/10	3600	12%
	Summary		0/50	3600		25/50	1994		29/50	1696	

Table 2.4: Aggregated results running the MILPs of Roberti and Ruthmair (2021), El-Adle et al. (2021), and from this paper for the instances of Murray and Chu (2015) and Bouman et al. (2018). All MILP formulations represent a TSPD (single drone) with the same objective and assumptions.

However, it is difficult to compare the MILPs based on results in the literature, as they have slightly different assumptions, a different solver (or version of solver) is used, and they were run on a computer with different RAM. Thus, to show the efficiency of our MILP formulation in comparison to the literature, we implemented the MILPs of Roberti and Ruthmair (2021) and El-Adle et al. (2021) in OPL. Roberti and Ruthmair (2021) have an arc-based formulation and El-Adle et al. (2021) a node-based formulation of the TSPD, where additional variables track the drone's tour,

even if it is carried on the truck. Both MILP formulations are chosen for comparison, as they are efficient two-indexed MILP formulations for the TSPD and include loops while minimizing the makespan.

We tested both MILP formulations for the instances of Murray and Chu (2015) and Bouman et al. (2018). However, only a subset of the instances of Murray and Chu (2015) is suitable, because both MILP formulations require a drone speed that is at least the same as the truck's speed. Thus, only 48 of the 72 instances, but all of Bouman et al. (2018) are considered. The MILP of El-Adle et al. (2021) is additionally adjusted by endurance constraints that limit the waiting times of drones (similar to Constraints (2.16) and (2.17)). This is already considered by Roberti and Ruthmair (2021). Note that for implementing the MILPs, we also consider the enhanced modelling assumptions to accelerate the MILP solver presented in the papers (similar to Constraints (2.3)), but no lower or upper bounds or any pre-processing steps as in El-Adle et al. (2021). Table 2.4 presents the aggregated results solving the three MILPs. The column gap shows the gap to the own lower bound of the respective model. Note that all MILP formulations represent the same problem setting of the TSPD with one drone that can perform both sidekicks and loops.

Findings: The MILP of Roberti and Ruthmair (2021) works best for the instances of Murray and Chu (2015), as all 48 instances could be solved optimally with the lowest runtime on average, but, on the other hand, not one instance with 16 or more nodes could be solved. Running the MILP of El-Adle et al. (2021), optimal solutions for all ten instances with 16 and 20 nodes and five out of ten instances with 24 nodes could be found. In contrast, our MILP formulation could additionally be solved to optimality for three more instances with 24 nodes and one instance with 28 nodes. Moreover, the average runtime and the optimality gap are significantly lower. Thus, the MILP presented in this paper outperforms the literature for larger instances. Additionally, it should be noted that our MILP formulation is a more general formulation as drones might have lower speeds than trucks and multiple drones can be considered without any increase in runtime.

2.5.3 Impact of drone loops

Drone loops as an additional routing option for drones might reduce the makespan τ^*, but on the other hand, considering loops might increase the solver's runtime on average, which in turn can be problematic, as truck-and-drone tandems are difficult to solve even for heuristic solution approaches (e.g., Sacramento et al. 2019). So, Schermer et al. (2019) already found that drones perform loops in the solutions, and Tiniç et al. (2023) found that loops might reduce total routing costs. However, in the solutions presented by Dell'Amico et al. (2021a) drones do not perform a single loop. Thus, in the following, we give detailed insights on the makespan reduction and the runtime increase when allowing loops compared to prohibiting loops for the instances of Murray and Chu (2015) and Bouman et al. (2018) with a varying number of drones m, endurance limits e, and truck-to-drone speed ratios α. For this, we only compare instances solved optimally for the case with and without drone loops.

Instances of Murray and Chu (2015) Table 2.5 presents the reduction of the makespan τ^* and the increase in runtime of the MILP solver in percent if drones can perform loops. For this, the

makespan considering loops is compared to the makespan, if loops are forbidden. We generate results for three different numbers of drones ($m = 1$, $m = 3$, $m = \infty$), two endurance limits ($e = 20$, $e = 40$), and five speed factors ($\alpha = 0.6$, $\alpha = 1.0$, $\alpha = 1.4$, $\alpha = 2.0$, $\alpha = 2.8$). These are two additional speed factors ($\alpha = 2.0$, $\alpha = 2.8$) compared to the data considered in Murray and Chu (2015) as the speed has a significant impact on the number of performed loops (Schermer et al. 2019). Each entry presents the average τ^* reduction or runtime increase of up to twelve instances. Note that there might be less than twelve instances considered if they are not solved to optimality. A negative entry in column "Runtime increase [%]" means there is a decrease in runtime.

Findings. Considering instances of Murray and Chu (2015) with eleven nodes, loops can reduce the makespan τ^* by up to 1.9% on average. For these instances it can be stated that there are only improvements in the objective considering loops if drones travel faster than trucks ($\alpha > 1$). Note that in these instances, the drone follows a Euclidean path contrary to the truck that travels the Manhattan distance. The improvements considering loops occur especially when few drones are considered. However, slow-traveling drones are more likely to perform loops when the truck is equipped with multiple drones. If the truck is equipped with an unlimited number of drones, there are nearly no reductions of τ^*. Moreover, endurance does not have an impact on performed loops. The runtime, on the other hand, increases significantly by up to 113%, considering loops as an additional routing option. The runtime increase is significantly higher if the truck is equipped with only one drone.

			$m = 1$		$m = 3$		$m = \infty$	
$\lvert\mathcal{I}_0\rvert$	e	α	τ^* reduction [%]	Runtime increase [%]	τ^* reduction [%]	Runtime increase [%]	τ^* reduction [%]	Runtime increase [%]
11	20	0.6	-	62.2	-	-2.2	-	7.3
		1.0	-	23.4	-	33.5	-	-11.7
		1.4	-	-4.8	0.1	16.5	0.6	18.8
		2.0	0.6	79.1	0.1	9.4	-	3.8
		2.8	1.7	57.4	0.5	4.5	-	5.9
	40	0.6	-	48.7	-	34.4	-	37.8
		1.0	-	23.2	-	14.4	-	10.7
		1.4	-	29.1	0.3	-6.0	-	7.2
		2.0	0.6	113.3	0.1	46.2	-	-0.4
		2.8	1.9	5.0	0.5	32.0	-	1.6
Average			0.5	43.7	0.2	18.3	0.1	8.1

Table 2.5: Makespan reduction and the solver's runtime increase, if drones can perform loops, for the instances of Murray and Chu (2015).

Instances of Bouman et al. (2018) Similar to the previous table, Table 2.6 presents the results for 16 considered nodes for two different endurance limits ($e = 30$, $e = 60$) and three speed factors ($\alpha = 1$, $\alpha = 2$, $\alpha = 3$). The additional endurance limit and speed factors are similar as in El-Adle

et al. (2021). An analysis of instances with 20 or more nodes is not meaningful, as there are only a few instances solved to optimality for both the consideration and the ban of loops. Each entry presents the average τ^* reduction or runtime increase of up to 10 instances.

Findings Both the makespan reduction and runtime increase are on average larger for these instances compared to the instances of Murray and Chu (2015). So, allowing drones to perform loops may reduce τ^* by up to 2.7%. Again, the endurance e has no significant impact on τ^*, but a larger drone-to-truck speed ratio α has. Contrary to the results for the instances of Murray and Chu (2015), a larger number of drones now results in a larger reduction of τ^*. Additionally, if drones and trucks have the same speed ($\alpha = 1$), there is even an instance where one loop is performed in the optimal solution resulting in slight reductions of τ^*. Note that drones and trucks follow both the Euclidean path. The runtime increases significantly by up to 194.4% and is especially high if one drone is considered. However, considering an infinite number of drones, there is no significant runtime increase, but the impact on τ^* is high.

			$m = 1$		$m = 3$		$m = \infty$	
$\lvert\mathcal{I}_0\rvert$	e	α	τ^* reduction [%]	Runtime increase [%]	τ^* reduction [%]	Runtime increase [%]	τ^* reduction [%]	Runtime increase [%]
16	30	1	-	57.8	0.1	41.9	0.1	44.5
		2	1.0	63.8	1.5	-14.4	2.0	-24.6
		3	0.3	194.4	1.7	6.3	1.3	-11.4
	60	1	-	99.1	-	44.3	-	26.1
		2	./.	./.	-	19.2	1.7	9.5
		3	./.	./.	-	-2.7	2.7	-33.0
Average			0.3	103.8	0.6	15.8	1.3	1.9

Table 2.6: Makespan reduction and the solver's runtime increase, if drones can perform loops, for the instances of Bouman et al. (2018). Entry ./. indicates that no instance was solved to optimality for both the consideration and the ban of loops.

2.6 Conclusion

This paper considers the TSPmD with drones performing sidekicks and loops while minimizing the makespan. We introduce the problem as a two-indexed MILP formulation that outperforms MILP formulations for the single drone case from the literature. We present new benchmark solutions for instances of Murray and Chu (2015) and Bouman et al. (2018), which we could solve to optimality for up to 28 nodes. Additionally, we generate managerial insights on the impact of allowing drone loops on makespan minimization.

We can find that makespan savings of up to 2.7% can be achieved by allowing drones to perform loops. The savings are essentially dependent on the drone-to-truck speed ratio, but not on the endurance. It follows that there are no drone loops if the drones' speeds are too slow. On the other

hand, drone loops make the problem significantly harder to solve, even if in the optimal solution drones do not perform loops. Therefore, for the TSPmD with any number of drones, drone loops should only be considered if drones have at least the truck's speed.

Compact and efficient MILP formulations for truck-and-drone tandems are good competitors to exact algorithms. However, an efficient optimal solution approach is still required for the TSPmD that can solve instances with more than 28 nodes to optimality.

Contribution 3 - Cyclic stochastic inventory routing with reorder points and recourse decision for an application in medical supply

3 Cyclic stochastic inventory routing with reorder points and recourse decision for an application in medical supply

Alexander Rave, Pirmin Fontaine, Heinrich Kuhn

Abstract The drug availability in clinics is essential for patient services, whose demand for medication, on the other hand, is uncertain. Thus, clinics must have a variety of drugs available, leading to high inventory holding costs. In Germany, it is common for a larger central clinic to take over the procurement of drugs and distribute them to smaller surrounding clinics, which results in a two-echelon network structure. The clinics, however, operate according to their own inventory policy as they plan independently of each other. Additionally, these inventory policies include instant replenishment orders to avoid shortages. As these instant replenishment orders only include a few medications, they can be performed by various vehicle types, including vans, cabs, and aerial drones.

We present a two-stage stochastic program for a multi-product two-echelon inventory routing problem with stochastic demands under consideration of inventory policies. We decide on the cost-optimal cyclic delivery patterns and reorder points for the clinics with instant replenishment orders performed by drones as recourse decision in case of shortages. Due to the problem's complexity caused by the interdependencies of inventory policies in the two echelons, we develop a specialized adaptive large neighborhood search that includes an algorithm for determining local optimal reorder points for the routing in each iteration. We present a case study at a large German clinic, which is responsible for supplying surrounding clinics and plans to integrate drone instead of van deliveries as an emergency resupply decision. Our integrated approach not only leads to cost savings of 58.4% for the surrounding clinics but also 15.9% for the central clinic. Using drone delivery compared to van delivery, the average stock of medication at surrounding clinics can be reduced by 1.7% to 100% for expensive and rarely needed medication, resulting in a total cost decrease of 29.8% while maintaining medication availability.

URL (working paper): `http://dx.doi.org/10.2139/ssrn.4421477`

3.1 Introduction

Clinics are obligated to care for patients. To guarantee this treatment, each clinic has a pharmacy that is appropriately equipped with medication. The pharmacy is under pressure to operate cost-effectively while providing full medical care to patients. This is particularly important since a clinic spends about 10 to 18% of its total expenses on medications (Nicholson et al. 2004, Volland et al. 2017). A way to reduce inventory costs is to make use of pooling effects. This means that inventory is stored more centrally to exploit the stochastic balancing effect between the independent demands in the individual clinics. As a consequence, however, additional transports are necessary. An aerial drone is an option to perform these transports since the drone has the particular advantage that it can carry a few medications to clinics faster and at lower costs than vans (Otto et al. 2018). In Ghana, for example, medicine is pooled in a central warehouse and then transported by drones to increase the overall availability of medication (Asadi et al. 2022). A similar situation exists in Germany, a larger central clinic is typically responsible for procuring medications and then distributing them to surrounding small clinics in a cycling repeating manner (Quantum Systems 2020).

For the latter example, two key questions arise. How many medications should be delivered to which clinic at what period, and what tours for delivery should be taken? This simultaneous inventory and supply optimization is known in the literature as the Inventory Routing Problem (IRP) (e.g., Archetti and Ljubić 2022). The delivery amount for the supply of clinics, however, depends on the inventory policy, which is planned individually by each clinic. The clinics make use of inventory policies as inventory can thus be planned over a longer planning horizon. In particular, clinics have economic advantages when choosing cyclic delivery patterns, e.g., they can improve the organization of their own clinic's supply chains. To avoid shortages, the additional supply of clinics is ensured via emergency deliveries. The standard deliveries include a high transport volume and thus are usually made with vans. The emergency deliveries, however, only include a few medications and can be performed by various vehicle types, for example, by drones (Quantum Systems 2020). So far, the use of drones has not occurred in practice. Hence this paper aims to assess the impact of drones as a new transportation option for instant replenishment orders.

Motivated by the previously introduced healthcare application, we develop a two-stage stochastic program for a cyclic multi-product two-echelon IRP with stochastic demand and inventory policies (2E-SIRP) that determines cost-optimal reorder points for both the central and the surrounding clinics. In addition, it determines the delivery periods and routes for supplying the surrounding clinics. While these are decisions on the tactical plan of the first stage, in the second stage, instant replenishment orders performed by drones occur if the demand exceeds the inventory. Within this two-stage stochastic program, we take decisions that minimize the transport, expected inventory, and expected emergency delivery costs. To solve larger instances with a greater variety of products and scenarios, we develop a specialized adaptive large neighborhood search (ALNS). In each iteration of the ALNS, the locally optimal reorder points are determined for the routing that is modified by removal or insertion operators. We benchmark the performance of the ALNS with optimally solved instances for the two-stage stochastic program and with instances of Archetti et al. (2007).

Further, we generate managerial insights for a novel case study based on a large clinic in Germany. We present both the benefits of our integrated planning approach as well as the influence of drones as new vehicle types for emergency deliveries on the inventory levels of different products and total cost reduction. Moreover, we show the value of a multi-product optimization and the impact of a limited vehicle fleet on the resulting routing and reorder points.

We contribute to the literature as follows: First, our paper is the first that combines two different inventory policies with routing decisions. Second, we formulate this problem setting as a two-stage stochastic program. Third, we derive an ALNS that determines local optimal reorder points in each iteration after taking changes on the routing to clinics. Fourth, we present a novel case study based on a large clinic in Germany.

In the following, we describe the problem setting in detail (Section 3.2) and give a short literature review on inventory and routing planning (Section 3.3). We present the decision problem as a two-stage stochastic program in Section 3.4 and describe the ALNS in Section 3.5. In Section 3.6, we benchmark the performance of the ALNS and present the case study and managerial insights. Last, in Section 3.7, we summarize the results.

3.2 Problem setting

In this section, we first introduce the network structure of clinics in detail. In the second subsection, we present the inventory policy of clinics, and last, we describe the decision problem.

3.2.1 Network structure

The central clinic - which has its own need for medications - procures all kinds of medical goods like medicines, antibiotics, infusions, etc., from the central distributor of these products, who is assumed to have sufficient inventory at all times. The demand for these medical goods for each clinic is independent of each other and uncertain but can be assumed to follow a known distribution (e.g., Johansson et al. 2020). Thus, shortages may arise if the inventory at the central clinic is too low. Due to the characteristics of the treatment of patients, these have to be satisfied through emergency deliveries ordered from and supplied by a wholesaler. Note that emergency deliveries only have the purpose of satisfying urgent demand and do not additionally replenish inventories since standard deliveries are ordered from the central distributor. Standard deliveries from the distributor and emergency deliveries from the wholesaler are performed in commuting tours. Within these deliveries, different products are consolidated if they are ordered on the same day.

The central clinic supplies several surrounding clinics with the medical goods they need. The clinics are supplied by multiple homogeneous vans on predefined days within a recurring supply period. The vans are considered to have a limited capacity, and the supply is performed by a third-party logistics service provider. Therefore, it is not necessary to balance the workload of drivers between each day. Determining the respective delivery pattern for each clinic is part of the planning problem under consideration. In addition, the central clinic sets up an emergency delivery if shortages occur in the surrounding clinics. These deliveries are performed by vehicles specialized for fast deliveries. In our case, the fast deliveries are performed by drones (Quantum Systems 2020).

These drones are less expensive than delivery trucks in terms of a single delivery trip, but they can only carry a few medications per flight due to limited capacity (Otto et al. 2018) - which is, however, mostly the case in emergency deliveries.

The standard delivery for all clinics is only allowed during weekdays since a clinic's pharmacy is only staffed for emergency operations at the weekend. Contrary, emergency deliveries can be conducted every day but are costlier at the weekend. Note that these are case-related assumptions, which can be easily relaxed and do not change our introduced algorithm.

We assume an unlimited fleet of vans and drones. The vans and drones which visit the surrounding clinics have a limited capacity. On the other hand, the vans of the central distributor that supply the central clinic are assumed to have an unlimited capacity. If a surrounding clinic's demand exceeds the capacity in emergency delivery, the drone might visit the same clinic multiple times within a period. In a variation of the problem, we further consider a limitation of the vehicle fleet, i.e., we limit the maximum number of routes in standard delivery and the maximum number of emergency deliveries per day.

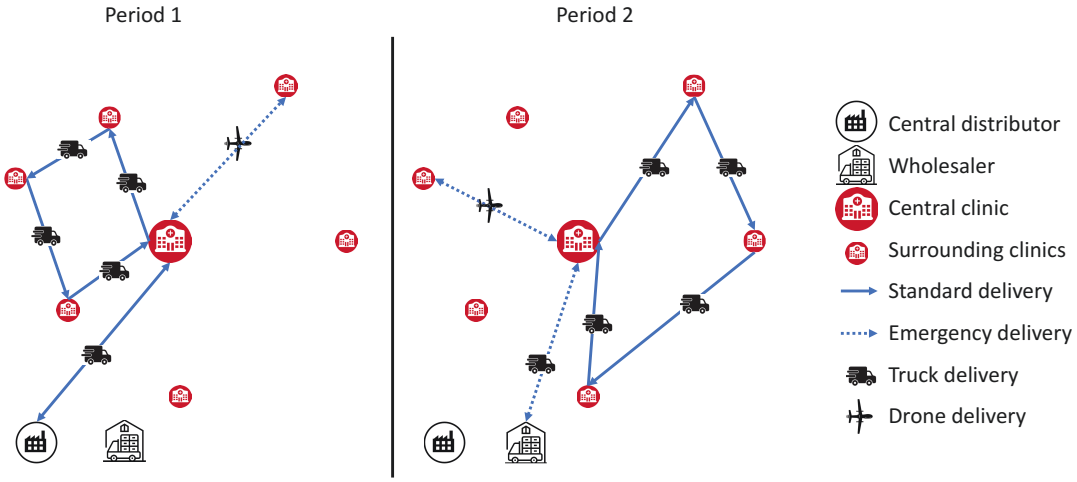

Figure 3.1: Delivery system of medicine.

Figure 3.1 presents an example network structure where the central clinic is fully responsible for delivering medication to six surrounding clinics. Three clinics are supplied in period 1 and the other three clinics in period 2 in standard delivery. Moreover, two emergency deliveries are carried out via drone due to shortages. The central clinic itself is supplied in period 1 via standard delivery by the central distributor and in period 2 via emergency delivery from the wholesaler.

3.2.2 Inventory policies

For each product $p \in \mathcal{P}$, the central clinic $\hat{c}$ operates an $(s_{p,\hat{c}}, Q_p)$ inventory policy with additional emergency resupply to avoid shortages. An order is placed at the central distributor for product $p \in \mathcal{P}$ with an amount of Q_p, if the inventory level is below the reorder point $s_{p,\hat{c}}$.

The replenishment quantity Q_p is assumed to be given. This quantity is typically based on long-term contracts between the central clinic and distributor, including total demand forecasts,

minimum order quantities, quantity discounts, and ordering and delivery costs. If the demand exceeds the current inventory level, additional emergency delivery costs arise as fast delivery is conducted. In this case, the delivery quantity equals the resulting shortages, i.e., only the missing quantity.

Surrounding small clinics $c \in \mathcal{C}$ operate an $(\mathcal{T}_c, s_{p,c}, n_{p,c} \cdot q_p)$ inventory policy with additional emergency resupply to prevent shortages. In periods $\mathcal{T}_c$ in a cyclic repeating pattern, the inventory is refilled by an order of $n_{p,c}$ packages á q_p consumer units, e.g., pills, if the inventory is below the reorder point $s_{p,c}$. The inventory is then replenished so that the inventory exceeds the reorder points $s_{p,c}$ if no additional demand occurs between ordering and delivery. Note that all subsets $\mathcal{T}_c$ of periods of $\mathcal{T}$ can be selected (e.g., delivery on Monday and Thursday). If there is not enough medication in stock, this demand is satisfied by an emergency delivery. This is a special case of back-ordering (Coelho et al. 2014) because the corresponding demand is served directly and not at a later stage. Note that the $(\mathcal{T}_c, s_{p,c}, n_{p,c} \cdot q_p)$ inventory policy with emergency resupply includes the case of $s_{p,c} = 0$, where nothing is stored in general and delivered in standard delivery and all demand is fulfilled via emergency deliveries. A characteristic of this problem with the focus on clinics is that the products are extremely varied, i.e., both daily and rarely needed (e.g., once every six months) drugs.

The demand for medication is any portion of a complete package, i.e., consumer units, but in a standard replenishment process, only complete packages are delivered. The emergency delivery, however, transports any package share since an emergency delivery is executed when the exact shortage is already known. In contrast, the target reorder points $s_{p,c}$ are quantified in complete packing units for practicability reasons.

Sequence of events for the replenishment cycle - central clinic At the beginning of each period, the inventory position equals the inventory on hand. In the first step, the demand of the surrounding clinics and the central clinic are known, which changes the inventory position. If the inventory position falls below the reorder point $s_{p,\hat{c}}$ during weekdays (Monday to Friday), an order of Q_p is triggered in the second step, which includes whole packing units. The inventory position is adjusted accordingly. If this results in a negative inventory position, the third step is to additionally place an emergency order to prevent a negative inventory on hand. Then, in the fourth step, the regular order quantity Q_p and emergency orders, if triggered, arrive in the central clinic. Next, in the fifth step, the surrounding and central clinics' demands are physically fulfilled. Inventory position and inventory on hand are then equivalent again and denote the inventory level at the end of the period, which is then used to quantify the inventory holding cost in the central clinic. The described disposition, supply, and delivery scheme of the central clinic allows for fulfilling the demand of the surrounding clinics and the central clinic itself in all periods considering a situation-related delivery time.

Sequence of events for the replenishment cycle - surrounding clinics Inventory on hand and inventory position are identical at the beginning of each period. Subsequently, the surrounding clinics' disposition and supply (delivery) are differentiated according to whether a standard delivery

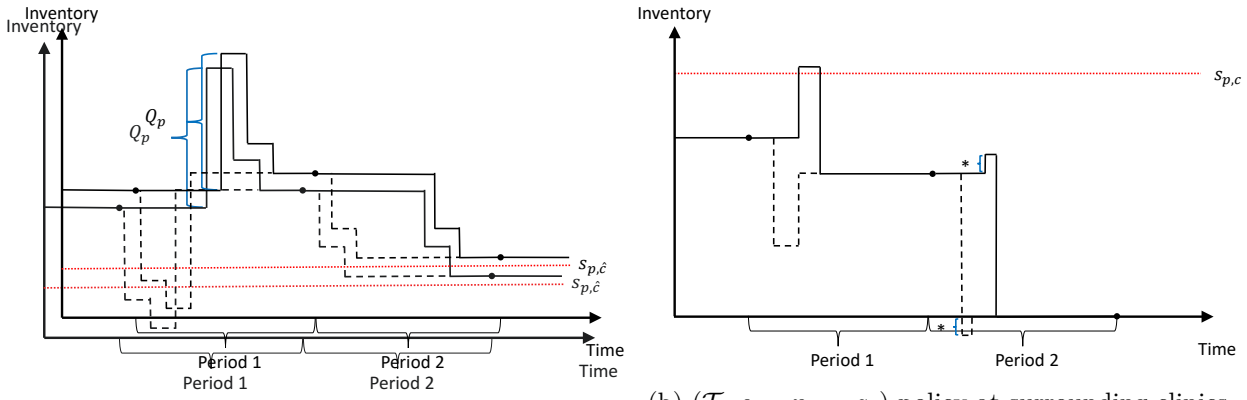

(a) $(s_{p,\hat{c}}, Q_p)$ policy at the central clinic.

(b) $(\mathcal{T}_c, s_{p,c}, n_{p,c} \cdot q_p)$ policy at surrounding clinics.
* emergency resupply

Figure 3.2: Replenishment policies of clinics.
The solid line represents the inventory on hand and the dashed line the inventory position.

is planned in the period. Note that the routing of the standard delivery affects the inventory policy, and therefore the routing sets $\mathcal{T}_c$. Thus, reordering only takes place if routing is planned and a clinic gets visited in a period. It first checks whether the inventory position is below the reorder point $s_{p,c}$. If so, an order is placed for this product that includes whole packaging units and increases the inventory position at least to the level $s_{p,c}$. The further events are then identical for all periods. The clinic's demand becomes known, and the inventory position is adjusted. If this results in a negative inventory position, an emergency order is placed (additionally to a standard delivery, if necessary), which balances the inventory position to zero. Subsequently, any triggered deliveries (standard and emergency) arrive at the considered clinic. Next, the clinic's demand is fulfilled. Inventory position and inventory on hand are equal again. The resulting inventory level is used to quantify the clinic's inventory holding costs. The described scheduling and supply scheme of the clinics enables them to completely fulfill the respective demands of each clinic in all periods. Note that an efficient routing also affects the inventory policies by reducing the transportation costs when the inventory is replenished, and, thus, reorder points and routing must be optimized simultaneously.

Example inventory level Figure 3.2 presents an example inventory level of a drug for the central clinic (Figure 3.2a) and one surrounding clinic (Figure 3.2b) for two periods. For the central clinic, orders are set as soon as the inventory position is below the reorder point $s_{p,\hat{c}}$, which is the case in period 1. The inventory on hand is then increased by the delivery quantity Q_p and reduced by both the demand of clinics and the central clinic's own demand. In period 2, the inventory position and the inventory on hand are decreased, but no order is placed, as the remaining inventory position is above the reorder point. The large points on the lines mark the time when inventory is assessed for the subsequent period.

For the surrounding clinics, standard delivery replenishes the inventory in period 1 by the missing inventory on hand at the end of the previous period compared to $s_{p,c}$ in complete packages. Afterwards, the inventory on hand is reduced by the demand. In period 2 there is no standard de-

livery, but demand exceeds the inventory position, and thus an emergency order is placed (∗). The emergency delivery only contains the missing inventory to fulfill the demand. Thus, the inventory on hand equals 0 afterwards. Note that an emergency delivery might occur in the same delivery period a standard delivery is conducted.

3.2.3 Decision problem

We determine cost-optimal reorder points $s_{p,\hat{c}}$ for the inventory policy of the central clinic and reorder points $s_{p,c}$, delivery days $\mathcal{T}_c$, and the corresponding routing for the inventory policy of the surrounding clinics. Then, emergency deliveries result from routing and reorder point decisions to prevent unmet demand at one of the clinics. The inventory and supply of the central and surrounding clinics are optimized simultaneously as the inventory decisions of surrounding clinics affect the inventory of the central clinic.

We minimize routing costs as well as expected inventory and emergency delivery costs. Due to stochastic demand, this methodically leads to a static stochastic program with a recourse decision in the form of emergency deliveries, which we formulate dependent on the scenario. We present a two-stage stochastic program that combines a two-echelon IRP with a $(\mathcal{T}_c, s_{p,c}, n_{p,c} \cdot q_p)$ inventory policy for surrounding clinics and a $(s_{p,\hat{c}}, Q_p)$ inventory policy for the central clinic.

The planning decision is made once for cyclic planning periods (in our case: one week) and then carried out over a longer planning horizon, e.g., three months, as long as there are no structural changes. Therefore, the cyclic inventory policy offers the advantage for clinics that the problem only has to be solved once, as long as no parameter values change structurally (e.g., seasonal fluctuations in demand). This is particularly advantageous for the smaller clinics, as there is a lack of personnel for extensive planning of, e.g., inventory. It follows that the considered problem setting is on a tactical level but includes operational aspects as well. This is common for tactical planning problems (e.g., Arslan 2021, Malicki and Minner 2021, Rave et al. 2023b).

We consider multiple products, as delivery patterns differ significantly from one another due to their differences in demand and holding costs. Moreover, different products are consolidated in standard and emergency delivery for both the surrounding and the central clinic and, thus, reduce the capacity of the respective vehicle. It follows that the simultaneous consideration of multiple products leads to a different solution than the consideration of each product separately. In Section 3.6.3.2, we show the impact of considering multiple products instead of each product separately. We neglect the limited shelf life of the products, as the inventory range of the given order quantity is well below the shelf life horizon of about two years. In addition, a strict first-in, first-out policy is followed in the clinics for inventory removal. The initial inventory of each product has a significant influence on the decisions to take in the cyclic planning and is thus dependent on the last delivery for surrounding clinics (e.g., Malicki and Minner 2021). Since the central clinic has no cyclical supply patterns, the initial stock is estimated as the average inventory level.

3.3 Literature review

Originally introduced by Bell et al. (1983), there is a variety of publications on the IRP. For an extensive review on inventory routing, we recommend the paper of Coelho et al. (2014) and Roldán et al. (2017), and for an overview on inventory management in hospitals, the paper of Volland et al. (2017).

The problem considered also belongs to the class of periodic vehicle routing problems (PVRP). A wide range of publications are available concerning the PVRP (Campbell and Wilson 2014). However, in our case, the clinics define clinic-specific delivery patterns (DP), and the central clinic cyclically supplies clinics with their requirements for medical goods. The DPs constitute a defined combination of weekdays on which the individual clinics are supplied. Defining the DPs also means determining the delivery frequency. The delivery frequency, however, impacts the volume per clinic delivery, affecting the associated cycle and safety stock in the central clinic and the surrounding clinics. Some recent publications quantify optimal delivery patterns in the area of grocery retailing. These approaches consider the supply of stores from a distribution center taking inventory holding costs and joint delivery costs into account (e.g., Frank et al. 2021). However, these approaches neglect the two-echelon structure and only implicitly model stochastic demand. Taube and Minner (2018) also quantifies DPs in the area of grocery retailing. They consider a classical joint replenishment problem with stochastic demand. In the following, we concentrate our literature review on contributions to inventory routing that focus in particular, on problems with stochastic demand and also consider time-based shipment consolidation.

Stochastic inventory routing - single product When considering stochastic demands, there are either lost sales or back-ordering, which state that unfulfilled demand can be met in a later period (Coelho et al. 2014). In our problem setting, additional emergency deliveries in the form of back-ordering occur. The difference between this emergency back-ordering and lost sales is that shortages from one clinic lead to inventory changes in the central clinic since the latter releases an emergency delivery in this case. Additionally, lost sales lead to penalty costs per patient and back-ordering to penalty costs per delivery.

IRPs with stochastic demands (SIRP) are considered by Campbell et al. (1998) and Campbell and Savelsbergh (2004). The authors focus on a heuristic solution method and decompose the decisions in two phases: first, the delivery period and quantities are determined, and second, an insertion heuristic creates routes. Nolz et al. (2014) consider stochasticity in their SIRP through recourse decisions and propose an ALNS and two versions of an LNS for a bi-objective IRP. Cui et al. (2023) choose a robust optimization approach for a SIRP that is modelled with demand scenarios.

Yadollahi et al. (2017) and Malicki and Minner (2021) choose a representation with chance constraints considering certain service levels for safety stock calculation. To solve the problem, Malicki and Minner (2021) present a multi-start adaptive local search heuristic that runs multiple instances of an adaptive local search simultaneously and an ALNS for a cyclic IRP with stochastic demands. They show that setting the initial inventory endogenously in cyclic IRPs is sufficient. Raa

and Aouam (2023) also consider a cyclic IRP with lost sales, but the delivery quantity depends on a base-stock unless the capacity is insufficient (shortfall). The authors develop a metaheuristic based on a first routing, second scheduling heuristic. Zheng et al. (2019) propose an exact algorithm based on the generalized benders decomposition for a SIRP, including an (T, S) inventory policy at the depot. Every cycles T, the inventory of the one considered product is replenished to an amount of S.

Stochastic inventory routing - multiple products Niakan and Rahimi (2015) and Rahimi et al. (2017) propose a formulation with fuzzy variables for the stochastic IRP in healthcare applications. Another healthcare application is considered by Jafarkhan and Yaghoubi (2018), who consider a SIRP for distributing blood cells, which are not in stock but can be substituted by other products. The authors propose a metaheuristic that makes use of two local searches in each iteration.

Time-based consolidation of customers Time-based consolidation of customers, which means that orders are collected in a vehicle first until it departures, is considered first by Higginson and Bookbinder (1995). The vehicle departs if it is fully loaded, but it may leave earlier for cost reasons. This problem setting does not include a routing decision. (Çetinkaya and Bookbinder 2003) extend this problem setting by deriving both a time-based and quantity-based consolidation policy. Stenius et al. (2016) derive an optimal solution framework for determining shipment intervals and reorder points for the time-based consolidation. Johansson et al. (2020) extend the article of Stenius et al. (2016) by deriving two approximation heuristics for large scale instances.

Table 3.1 differentiates our assumptions, decisions, and methodology chronologically from the publications described before. Our paper adds to the available literature, particularly with respect to the following issues.

1. Presenting a 2E-SIRP with the novel configuration of assumptions and decisions, especially:
   a) Combining both an $(\mathcal{T}_c, s_{p,c}, n_{p,c} \cdot q_p)$ and an $(s_{p,\hat{c}}, Q_p)$ inventory policy in a two-echelon IRP.
   b) Depot has its own demand.
   c) Instant replenishment orders as recourse decision.
2. Formulating a two-stage stochastic program and developing a specialized ALNS for solving larger instances.
3. Presenting a novel and real-life case study of a large German clinic.

3.4 Two-stage stochastic program

In this section, we introduce the mathematical model as a two-stage stochastic program for the 2E-SIRP. In Section 3.4.1, we describe the general problem setting, including notation and relevant sets, parameters, and variables, and in Section 3.4.2, we present the mathematical model.

	assumptions		inventory decisions				methodology			
Paper	multiple products	cyclic	limited inventory at depot	lost sales	back-orders	substitution by different products	MILP	Markov chain	exact solution method	heuristics
Higginson and Bookbinder (1995)								✓		
Campbell et al. (1998), Campbell and Savelsbergh (2004)				✓						✓
Çetinkaya and Bookbinder (2003)					✓				✓	
Nolz et al. (2014)				✓			✓			✓[A]
Niakan and Rahimi (2015)	✓			✓			✓*			✓
Stenius et al. (2016)	✓		✓		✓				✓	
Yadollahi et al. (2017)		✓		✓			✓			
Rahimi et al. (2017)	✓				✓		✓*			✓
Jafarkhan and Yaghoubi (2018)	✓		✓			✓	✓			✓
Rohmer et al. (2019)			✓				✓			✓[A]
Zheng et al. (2019)			✓				✓		✓	
Johansson et al. (2020)	✓		✓		✓					✓
Malicki and Minner (2021)		✓		✓			✓			✓[A]
Raa and Aouam (2023)		✓		✓			✓			✓
Cui et al. (2023)					✓		✓		✓	
Our paper	✓	✓	✓**		✓***		✓			✓[A]

Table 3.1: Overview of inventory optimization literature.
[A] ALNS, * MILNP with additional linearization, ** depot has own stochastic demand, *** unmet demand is served via emergency delivery.

3.4.1 Sets, parameters, and decision variables

We consider a set of $|\hat{\mathcal{C}}|$ nodes consisting both of the central clinic $\hat{c}$ as well as the set of surrounding clinics $\mathcal{C}$ with $\hat{\mathcal{C}} = \{\hat{c}\} \cup \mathcal{C}$. Moreover, we assume $|\mathcal{P}|$ products. $\mathcal{T}_0 = 0...T$ is the index set for the periods, including the initialization period 0. The standard delivery is permitted for all clinics in periods $\bar{\mathcal{T}} \subseteq \mathcal{T}$. Set Ω defines the demand scenarios.

General problem structure We present the mathematical model in the form of a two-stage stochastic program. In the first stage, tactical decisions are taken on routing and reorder points. In the second stage, emergency deliveries as recourse decisions are executed for each scenario, individually. The emergency deliveries result from the tactical decisions in the first stage and are only executed to prevent a clinic from running out of stock.

Parameters The total costs are composed out of travel costs $k^S_{i,j}$ per arc for standard delivery visiting the surrounding clinics, $\hat{k}^S$ for visiting the central clinic, $k^{em.}_{c,t}$ for emergency delivery as well as inventory holding costs k^I_p per period and product $p \in \mathcal{P}$.

For supply of surrounding clinics, each van has a capacity of K^S and each drone of $K^{em.}$. For this, the volume v_p for each product is considered. Q_p equals the fixed delivery quantity for product $p \in P$ at the central clinic. Clinics $c \in \hat{\mathcal{C}}$ have a demand of $d_{p,c,t,\omega}$ for each product $p \in \mathcal{P}$, in period $t \in \mathcal{T}$, and scenario $\omega \in \Omega$.

Index sets	
$\mathcal{C}$, $\hat{\mathcal{C}}$	Index set for clinics (including the central clinic $\hat{c}$)
$\mathcal{P}$	Index set for products
$\mathcal{T}$, $\mathcal{T}_0$	Index set for considered time periods (including period 0)
$\bar{\mathcal{T}}$	Index set for time periods in which standard delivery is permitted
Ω	Index set for scenarios
Parameters	
$k^S_{i,j}$	Costs traveling from clinic $i \in \hat{\mathcal{C}}$ to $j \in \hat{\mathcal{C}}$ in standard delivery
$\hat{k}^S$	Costs visiting the central clinic in standard delivery
$k^{em.}_{c,t}$	emergency delivery costs visiting clinic $c \in \mathcal{C}$ at time $t \in \mathcal{T}$
k^I_p	Inventory holding costs for product $p \in \mathcal{P}$ per time period
$d_{p,c,t,\omega}$	Demand of product $p \in \mathcal{P}$ in clinic $c \in \hat{\mathcal{C}}$ at time $t \in \mathcal{T}$ and scenario $\omega \in \Omega$
ε	sufficient small number
K^S	Maximum capacity for supply of surrounding clinics in standard delivery in volume equivalents
$K^{em.}$	Maximum capacity for supply of surrounding clinics in emergency delivery in volume equivalents
M_l	Big M for $l = 1, ..., 9$
n^S, $n^{em.}$	Number of routes per day that are allowed for standard and emergency delivery
Q_p	Delivery quantity of product $p \in P$ for the central clinic in the standard delivery, quantified in entire packaging units

Continued on next page

Continued from previous page

v_p	Volume of a package of product $p \in \mathcal{P}$
First stage decision variables	
$s_{p,c}$	Integer variable, indicating the reorder point (entire packaging units) of each product $p \in P$ at clinic $c \in \hat{\mathcal{C}}$
$y_{i,j,t}$	Binary variable*, indicating, if a van travels from clinic $i \in \hat{\mathcal{C}}$ to clinic $j \in \hat{\mathcal{C}}$ for resupply at time $t \in \mathcal{T}$
First stage auxiliary variables	
$u_{i,t}$	Subtour-elimination variable for node $i \in \mathcal{C}$ at time $t \in \bar{\mathcal{T}}$ by Miller et al. (1960)
$I_{p,c}^{Init}$	Initial inventory of product $p \in \mathcal{P}$ at clinic $c \in \hat{\mathcal{C}}$
$\eta_{p,c,t}$, $\theta_{p,c,t}$, $\zeta_{p,c,t}$	Binary*, binary*, and real-value variables to ensure cyclic planning
Second stage auxiliary variables	
$I_{p,c,t,\omega}$	Positive real-value variable, indicating the inventory level of product $p \in \mathcal{P}$ for clinic $c \in \hat{\mathcal{C}}$ at the end of period $t \in \mathcal{T}_0$ and scenario $\omega \in \Omega$
$q_{p,c,t,\omega}^{S}$	Integer variable, indicating transported amount of packages of product $p \in \mathcal{P}$ to clinic $c \in \mathcal{C}$ at time $t \in \bar{\mathcal{T}}$ and scenario $\omega \in \Omega$ in a standard delivery
$\phi_{i,j,t,\omega}^{S}$	Positive real-value variable, indicating accumulated transport volume from clinic $i \in \hat{\mathcal{C}}$ to clinic $j \in \hat{\mathcal{C}}$ at time $t \in \bar{\mathcal{T}}$ and scenario $\omega \in \Omega$ in a standard delivery
$q_{p,c,t,\omega}^{em.}$	Positive real-value variable, indicating transported amount of product $p \in \mathcal{P}$ to clinic $c \in \hat{\mathcal{C}}$ at time $t \in \mathcal{T}$ and scenario $\omega \in \Omega$ via emergency delivery
$r_{t,\omega}$	Binary variable*, indicating, if there is a standard resupply of the central clinic at time $t \in \bar{\mathcal{T}}$ and scenario $\omega \in \Omega$
$w_{c,t,\omega}$	Integer variable, indicating the number of emergency resupplies for a clinic $c \in \hat{\mathcal{C}}$ at time $t \in \mathcal{T}$ and scenario $\omega \in \Omega$
$x_{p,c,t,\omega}$	Binary variable*, indicating, if there are emergency resupplies for product $p \in \mathcal{P}$ at clinic $c \in \hat{\mathcal{C}}$ at time $t \in \mathcal{T}$ and scenario $\omega \in \Omega$
$z_{p,t,\omega}$	Binary variable*, indicating, if there is a standard resupply of the central clinic at time $t \in \bar{\mathcal{T}}$ for product $p \in \mathcal{P}$ and scenario $\omega \in \Omega$
$\xi_{p,c,t,\omega}$, $\kappa_{p,c,t,\omega}$, $\iota_{p,c,t,\omega}$	Binary*, real-value, and real-value variable for soft constraints

Table 3.2: Index sets, parameters, first stage decision variables, and first and second stage auxiliary variables.
* binary variables have a value of 1, if they are true, 0 else

Decision variables The following decisions are taken for all demand scenarios consolidated and thus are first stage decisions. The main decision variables determine the reorder points $s_{p,c}$ for product $p \in \mathcal{P}$ and clinic $c \in \hat{\mathcal{C}}$ and the routing $y_{i,j,t}$, i.e., if a van travels from clinic $i \in \hat{\mathcal{C}}$ to clinic $j \in \hat{\mathcal{C}}$ in period $t \in \bar{\mathcal{T}}$. Thus, $y_{i,j,t}$ gives information on the delivery days a clinic $j \in \mathcal{C}$ is visited.

The second stage defines the following directly related variables. For period $t \in \mathcal{T}$ and scenario $\omega \in \Omega$, $I_{p,c,t,\omega}$ defines the inventory levels for each product $p \in \mathcal{P}$ in clinic $c \in \hat{\mathcal{C}}$, $q_{i,j,t,\omega}^{S}$ the delivery amount by standard delivery, $w_{c,t,\omega}$ the number of emergency deliveries, and $q_{p,c,t,\omega}^{em.}$ the transported

amount in emergency deliveries. Moreover, $z_{p,t,\omega}$ determines if the central clinic is supplied in period $t \in \bar{\mathcal{T}}$ with product $p \in \mathcal{P}$, as the delivery days of the central clinic are not fixed and dependent on the reorder points.

3.4.2 Mathematical model

In this subsection, we present our two-stage stochastic program for the 2E-SIRP as a mixed-integer linear program. We decomposed the two-stage stochastic program into the objective function and different constraints for better reading.

Objective function

$$\begin{aligned}\min Z^{total} = & \sum_{i,j \in \hat{\mathcal{C}}, t \in \bar{\mathcal{T}}} k^S_{i,j} \cdot y_{i,j,t} \\ & + \mathbb{E}_{\omega \in \Omega} \left\{ \sum_{t \in \bar{\mathcal{T}}} \hat{k}^S \cdot r_{t,\omega} + \sum_{c \in \hat{\mathcal{C}}, t \in \mathcal{T}} k^{em.}_{c,t} \cdot w_{c,t,\omega} + \sum_{p \in \mathcal{P}, c \in \hat{\mathcal{C}}, t \in \mathcal{T}} k^I_p \cdot I_{p,c,t,\omega} \right\} \end{aligned} \tag{3.1}$$

The objective function (3.1) minimizes the total expected logistics costs in the time periods considered. It contains two major cost terms. The first applies to all scenarios and quantifies the delivery costs for standard deliveries in the first stage. The second term approximates expected costs, which are the average of additional delivery and inventory costs for all scenarios evaluated, i.e., standard delivery costs in the first echelon and emergency delivery costs in the second echelon, and inventory holding costs for all clinics.

Routing constraints

$$\sum_{i \in \hat{\mathcal{C}}} y_{j,i,t} = \sum_{i \in \hat{\mathcal{C}}} y_{i,j,t} \qquad \forall j \in \hat{\mathcal{C}}, t \in \bar{\mathcal{T}} \tag{3.2}$$

$$\sum_{i,j \in \hat{\mathcal{C}}} y_{i,j,t} \leq M_1 \cdot \sum_{j \in \mathcal{C}} y_{\hat{c},j,t} \qquad \forall t \in \bar{\mathcal{T}} \tag{3.3}$$

$$\sum_{i \in \hat{\mathcal{C}}} y_{i,j,t} \leq 1 \qquad \forall j \in \mathcal{C}, t \in \bar{\mathcal{T}} \tag{3.4}$$

$$u_{i,t} + 1 \leq u_{j,t} + M_2 \cdot (1 - y_{i,j,t}) \qquad \forall i,j \in \mathcal{C}, t \in \bar{\mathcal{T}} \tag{3.5}$$

$$\sum_{j \in \hat{\mathcal{C}}} (\phi^S_{j,c,t,\omega} - \phi^S_{c,j,t,\omega}) = \sum_{p \in \mathcal{P}} v_p \cdot q^S_{p,c,t,\omega} \qquad \forall c \in \mathcal{C}, t \in \bar{\mathcal{T}}, \omega \in \Omega \tag{3.6}$$

$$\phi^S_{i,j,t,\omega} \leq K^S \cdot y_{i,j,t} \qquad \forall i,j \in \hat{\mathcal{C}}, t \in \bar{\mathcal{T}}, \omega \in \Omega \tag{3.7}$$

$$\sum_{i \in \hat{\mathcal{C}} t \in \bar{\mathcal{T}}} y_{i,j,t} \geq 1 \qquad \forall j \in \mathcal{C} \tag{3.8}$$

$$y_{i,j,t} \in \{0,1\} \qquad \forall i,j \in \hat{\mathcal{C}}, t \in \bar{\mathcal{T}} \tag{3.9}$$

$$\phi^S_{i,j,t,\omega} \in \mathbb{R}^+ \qquad \forall i,j \in \hat{\mathcal{C}}, t \in \bar{\mathcal{T}}, \omega \in \Omega \tag{3.10}$$

$$q^S_{p,c,t,\omega} \in \mathbb{N} \qquad \forall p \in \mathcal{P}, c \in \mathcal{C}, t \in \bar{\mathcal{T}}, \omega \in \Omega \tag{3.11}$$

$$u_{i,t} \in \mathbb{R} \qquad \forall i \in \mathcal{C}, t \in \bar{\mathcal{T}} \tag{3.12}$$

Constraints (3.2) to (3.12) restrict the routing of the standard delivery in each period $t \in \bar{\mathcal{T}}$. Constraints (3.2) conserve the flow, and Constraints (3.3) ensure that the van that visits the clinics in the second echelon always starts at the central clinic. M_1 can be set as $|\hat{\mathcal{C}}|$ since each clinic is visited maximum once per period (Constraints (3.4)). Subtours are eliminated by Constraints (3.5) (Miller et al. 1960). M_2 can be set as $|\hat{\mathcal{C}}|$. Constraints (3.6) define the accumulated transported volume of each van's tour. This accumulated transported volume must be less than the van's capacity (Constraints (3.7)). Constraints (3.8) ensure that each surrounding clinic is visited at least once in the considered periods. Last, variables are defined.

Reorder point constraints for the central clinic

$$I_{p,\hat{c},t,\omega} - Q_p \cdot z_{p,t,\omega} \geq 0 \qquad \forall p \in \mathcal{P}, t \in \bar{\mathcal{T}}, \omega \in \Omega \tag{3.13}$$

$$I_{p,\hat{c},t,\omega} - Q_p \leq s_{p,\hat{c}} \leq I_{p,\hat{c},t,\omega} - \varepsilon \qquad \forall p \in \mathcal{P}, t \in \bar{\mathcal{T}}, \omega \in \Omega \tag{3.14}$$

$$\sum_{p \in \mathcal{P}} z_{p,t,\omega} \leq |\mathcal{P}| \cdot r_{t,\omega} \qquad \forall t \in \bar{\mathcal{T}}, \omega \in \Omega \tag{3.15}$$

$$r_{t,\omega} \in \{0,1\} \qquad \forall t \in \bar{\mathcal{T}}, \omega \in \Omega \tag{3.16}$$

$$s_{p,c} \in \mathbb{N} \qquad \forall p \in \mathcal{P}, c \in \hat{\mathcal{C}} \tag{3.17}$$

$$I_{p,c,t,\omega} \in \mathbb{R}^+ \qquad \forall p \in \mathcal{P}, c \in \hat{\mathcal{C}}, t \in \mathcal{T}_0, \omega \in \Omega \tag{3.18}$$

$$z_{p,t,\omega} \in \{0,1\} \qquad \forall p \in \mathcal{P}, t \in \bar{\mathcal{T}}, \omega \in \Omega \tag{3.19}$$

Constraints (3.13) to (3.19) define the reorder points for the central clinic. There are emergency deliveries only if the inventory at the end of the previous period is not sufficiently high to meet all demand (Constraints (3.13)). Constraints (3.14) (right side) ensure that there is only a delivery if inventory is below the reorder point. Standard delivery must be carried out if inventory is below the reorder point (left side of Constraints (3.14)). Constraints (3.15) ensure that the products are consolidated in delivery. Last, variables are defined.

Reorder point constraints for surrounding clinics

$$q^S_{p,c,t,\omega} \leq s_{p,c} - I_{p,c,t-1,\omega} + 1 - \varepsilon \qquad \forall p \in \mathcal{P}, c \in \mathcal{C}, t \in \bar{\mathcal{T}}, \omega \in \Omega \tag{3.20}$$

$$q^S_{p,c,t,\omega} \geq s_{p,c} - I_{p,c,t-1,\omega} - M_3 \cdot \left(1 - \sum_{i \in \hat{\mathcal{C}}} y_{i,c,t}\right) \qquad \forall p \in \mathcal{P}, c \in \mathcal{C}, t \in \bar{\mathcal{T}}, \omega \in \Omega \tag{3.21}$$

$$q^S_{p,c,t,\omega} \leq M_3 \cdot \sum_{i \in \hat{\mathcal{C}}} y_{i,c,t} \qquad \forall p \in \mathcal{P}, c \in \mathcal{C}, t \in \bar{\mathcal{T}}, \omega \in \Omega \tag{3.22}$$

Constraints (3.20) to (3.22) define the reorder points $s_{p,c}$ and the resulting delivery quantities $q^S_{p,c,t,\omega}$ for the surrounding clinics. Constraints (3.20) and (3.21) ensure that the delivery quantities - which have an integer value - fill up the inventory to the reorder point $s_{p,c}$. M_3 can be set as the fraction of the van's capacity and the smallest volume of any product, e.g., one pill. Medicine is only delivered in a period to a clinic if there is a standard delivery for this clinic in the considered period (Constraints (3.22)).

Emergency delivery constraints

$$\sum_{p\in\mathcal{P}} q^{em.}_{p,\hat{c},t,\omega} \leq M_4 \cdot w_{\hat{c},t,\omega} \qquad \forall t \in \mathcal{T}, \omega \in \Omega \tag{3.23}$$

$$q^{em.}_{p,c,t,\omega} \leq d_{p,c,t,\omega} - I_{p,c,t-1,\omega} + M_5 \cdot (1 - x_{p,c,t,\omega}) - \begin{cases} q^{S}_{p,c,t,\omega} & , t \in \bar{\mathcal{T}} \\ 0 & , else \end{cases} \qquad \forall p \in \mathcal{P}, c \in \mathcal{C}, t \in \mathcal{T}, \omega \in \Omega \tag{3.24}$$

$$q^{em.}_{p,\hat{c},t,\omega} \leq d_{p,\hat{c},t,\omega} - I_{p,\hat{c},t-1,\omega} + M_5 \cdot (1 - x_{p,\hat{c},t,\omega}) + \sum_{k\in\mathcal{C}} q^{em.}_{p,k,t,\omega} + \begin{cases} \sum_{k\in\mathcal{C}} q^{S}_{p,k,t,\omega} & , t \in \bar{\mathcal{T}} \\ 0 & , else \end{cases} \qquad \forall p \in \mathcal{P}, t \in \mathcal{T}, \omega \in \Omega \tag{3.25}$$

$$w_{c,t,\omega} \leq M_6 \cdot \sum_{p\in\mathcal{P}} x_{p,c,t,\omega} \qquad \forall c \in \hat{\mathcal{C}}, t \in \mathcal{T}, \omega \in \Omega \tag{3.26}$$

$$q^{em.}_{p,c,t,\omega} \leq M_6 \cdot x_{p,c,t,\omega} \qquad \forall p \in \mathcal{P}, c \in \hat{\mathcal{C}}, t \in \mathcal{T}, \omega \in \Omega \tag{3.27}$$

$$\sum_{p\in\mathcal{P}} v_p \cdot q^{em.}_{p,c,t,\omega} \leq K^{em.} \cdot w_{c,t,\omega} \qquad \forall c \in \mathcal{C}, t \in \mathcal{T}, \omega \in \Omega \tag{3.28}$$

$$w_{c,t,\omega} \in \mathbb{N} \qquad \forall c \in \hat{\mathcal{C}}, t \in \mathcal{T}, \omega \in \Omega \tag{3.29}$$

$$x_{p,c,t,\omega} \in \{0,1\}, q^{em.}_{p,c,t,\omega} \in \mathbb{R}^{+} \qquad \forall p \in \mathcal{P}, c \in \hat{\mathcal{C}}, t \in \mathcal{T}, \omega \in \Omega \tag{3.30}$$

Constraints (3.23) to (3.30) define the emergency delivery constraints for all clinics. Constraints (3.23) determine if there is an emergency delivery for the central clinic. M_4 must be set sufficiently high, as the capacity of the emergency delivery to the central clinic is unlimited. Constraints (3.24) and (3.25) restrict the delivery quantity to the unsatisfied demand of the current period to avoid emergency deliveries enabling stockpiling. M_5 needs to be greater than each clinic's possible maximum inventory capacities. Constraints (3.26) consolidate multiple products in one emergency delivery. Constraints (3.27) ensure that medicine is only delivered if there is an emergency delivery. M_6 can be set as a maximum reasonable amount of transported volume in emergency deliveries. Constraints (3.28) restrict the capacity of emergency deliveries for surrounding clinics. Last, auxiliary variables are defined.

Inventory constraints

$$I_{p,c,t,\omega} = I_{p,c,t-1,\omega} - d_{p,c,t,\omega} + q^{em.}_{p,c,t,\omega} + \begin{cases} q^{S}_{p,c,t,\omega} & , t \in \bar{\mathcal{T}} \\ 0 & , else \end{cases} \qquad \forall p \in \mathcal{P}, c \in \mathcal{C}, t \in \mathcal{T}, \omega \in \Omega \tag{3.31}$$

$$I_{p,\hat{c},t,\omega} = I_{p,\hat{c},t-1,\omega} - d_{p,\hat{c},t,\omega} + q^{em.}_{p,\hat{c},t,\omega} - \sum_{k\in\mathcal{C}} q^{em.}_{p,k,t,\omega} + \begin{cases} Q_p \cdot z_{p,t,\omega} - \sum_{k\in\mathcal{C}} q^{S}_{p,k,t,\omega} & , t \in \bar{\mathcal{T}} \\ 0 & , else \end{cases} \qquad \forall p \in \mathcal{P}, t \in \mathcal{T}, \omega \in \Omega \tag{3.32}$$

$$I^{Init}_{p,c} + \zeta_{p,c,\tau} = s_{p,c} + M_7 \cdot \sum_{t=\tau+1..|\bar{\mathcal{T}}|, i\in\hat{\mathcal{C}}} y_{i,c,t}$$

$$- \sum_{t=\tau..|\mathcal{T}|} \mathbb{E}_{\omega\in\Omega}\Big\{d_{p,c,t,\omega}\Big\} \qquad \forall p \in \mathcal{P}, c \in \mathcal{C}, \tau \in \mathcal{T} \qquad (3.33)$$

$$M_8 \cdot (\theta_{p,c,t} - 1) \leq \zeta_{p,c,t} \leq M_8 \cdot \eta_{p,c,t} \qquad \forall p \in \mathcal{P}, c \in \mathcal{C}, t \in \mathcal{T} \qquad (3.34)$$

$$\sum_{t\in\mathcal{T}} \eta_{p,c,t} = |\mathcal{T}| - 1 \qquad \forall p \in \mathcal{P}, c \in \mathcal{C} \qquad (3.35)$$

$$\zeta_{p,c,\tau} \geq s_{p,c} + M_7 \cdot \sum_{t=\tau+1..|\bar{\mathcal{T}}|, i\in\hat{\mathcal{C}}} y_{i,c,t} - \sum_{t=\tau..|\mathcal{T}|} \mathbb{E}_{\omega\in\Omega}\Big\{d_{p,c,t,\omega}\Big\} - M_9 \cdot \theta_{p,c,\tau} \qquad \forall p \in \mathcal{P}, c \in \mathcal{C}, \tau \in \mathcal{T} \qquad (3.36)$$

$$I^{Init}_{p,\hat{c}} = \frac{s_{p,\hat{c}} + Q_p}{2} \qquad \forall p \in \mathcal{P} \qquad (3.37)$$

$$I_{p,c,0,\omega} = I^{Init}_{p,c} \qquad \forall p \in \mathcal{P}, c \in \hat{\mathcal{C}}, \omega \in \Omega \qquad (3.38)$$

$$I^{Init}_{p,c} \in \mathbb{R}^+ \qquad \forall p \in \mathcal{P}, c \in \hat{\mathcal{C}} \qquad (3.39)$$

$$\eta_{p,c,t}, \theta_{p,c,t} \in \{0,1\}, \zeta_{p,c,t} \in \mathbb{R} \qquad \forall p \in \mathcal{P}, c \in \mathcal{C}, t \in \mathcal{T} \qquad (3.40)$$

Constraints (3.31) to (3.40) are inventory constraints for all clinics. Constraints (3.31) are the inventory balancing constraints for surrounding clinics for periods $t \in \mathcal{T}$ defining the inventory at the end of each period $t \in \mathcal{T}$ by reducing the inventory of the previous period by the demand and adding delivery quantities. The same is applied to the central clinic, but the inventory is additionally reduced by the total quantity delivered to clinics in the second echelon in standard and emergency deliveries (Constraints (3.32)). Constraints (3.33) are the cyclic formulations for the surrounding clinics. The initial inventory depends on the last replenishment in the cyclic planning periods, i.e., the reorder points are reduced by the expected demand from the last delivery on. M_7 can be set as the maximum reasonable inventory of a product. $\eta_{p,c,t}$ and $\zeta_{p,c,t}$ are auxiliary variables that ensure equality holds. Only for one period $\zeta_{p,c,t}$ is set to zero (Constraints (3.34) and (3.35)). M_8 can be set as the expected demand. Constraints (3.36) ensure that $\zeta_{p,c,t}$ might have negative values if the reorder points are lower than the expected demand. M_9 can be set as twice the maximum reasonable inventory of a product. Constraints (3.37) set the initial inventory for the central clinic as half of both the reorder point plus the order quantity. Constraints (3.38) define the inventory at period 0 for all scenarios. Last, auxiliary variables are defined.

Problem variant: limited number of vehicles We further consider a problem variant, where the number of vehicles for both standard and emergency delivery is limited. In accordance with Archetti et al. (2007), we model this by limiting the number of routes on a day to n^S (Constraints (3.41)) or $n^{em.}$ (Constraints (3.42)), respectively.

$$\sum_{j\in\hat{\mathcal{C}}} y_{0,j,t} \leq n^S \qquad \forall t \in \mathcal{T} \qquad (3.41)$$

$$\sum_{c\in\mathcal{C}} w_{c,t,\omega} \leq n^{em.} \quad \forall t \in \mathcal{T}, \omega \in \Omega \qquad (3.42)$$

These constraints are assumed in Section 3.6.2.2 for benchmark tests and in Section 3.6.3.4 to show the impact of a limited vehicle fleet.

3.5 Adaptive large neighborhood search

To solve the 2E-SIRP, we decompose the problem in its two echelons. We develop a problem-specific ALNS to generate routes and delivery days. Using this routing, we determine optimal reorder points in each iteration. Thus, this approach leads to a focus of the ALNS on the second echelon of the problem. The particularity of the presented ALNS is the inclusion of a reorder point algorithm as an additional step after executing operators that vary the routing. This simple and efficient separation of delivery quantities from routing allows any widely used ALNS for IRPs (e.g., Aksen et al. 2014) to be adapted for the problem at hand.

The structure of this section is as follows: First, we introduce the ALNS and describe the solution representation in Subsection 3.5.1, the pseudocode of our ALNS in Subsection 3.5.2, our routing-specific operators in Subsection 3.5.3, and the algorithm to find local optimal reorder points in Subsection 3.5.4.

3.5.1 Solution representation

The ALNS was first introduced in Ropke and Pisinger (2006) and Pisinger and Ropke (2007) for the class of vehicle routing problems and has been extended for inventory routing problems (e.g., Aksen et al. 2014). Our ALNS is specialized for the $(\mathcal{T}_c, s_{p,c}, n_{p,c} \cdot q_p)$ inventory policy of clinics on the second echelon and the $(s_{p,\hat{c}}, Q_p)$ inventory policy of the central clinic on the first echelon, which means that the delivery quantities are dependent on the inventory policies.

A solution is represented by the routing of the standard delivery (R), including information on delivery days within the cyclic planning horizon and the reorder points for the clinics ($s_{p,c}$). In each iteration, operators are chosen that take changes on just the routing R (see Section 3.5.3). Afterwards, the reorder points $s_{p,c}$ are optimized depending on the created routing R (see Section 3.5.4).

Within these changes, infeasible solutions are accepted but penalized in the objective function dependent on the degree of infeasibility (e.g., Vidal et al. 2013, Rave et al. 2023b). Infeasibility may occur in two different ways: first, a van may exceed its capacity in a scenario, and second, not all clinics are visited at least once. Additionally, when limiting the fleet size, violations of Constraints (3.41) and (3.42) are penalized, too.

3.5.2 ALNS algorithm

The general outline of the ALNS is presented in Algorithm 2. The algorithm begins with an initial solution (line 1) and a temperature $Temp$ for the simulated annealing process (line 2). The initial solution is generated by visiting all clinics once and only in the first period of the cyclic planning periods. The clinics are inserted one by one in the greedy best way in one tour. This initial solution is not necessarily feasible. The while-loop in line 3 stops after a maximum time. At the beginning of each iteration, operators and a delivery day T for the repair operator are chosen adaptively

(line 4). In line 5, operators modify the routing R. Local optimal reorder points $\bar{s}_{p,c}$ for this routing $\bar{R}$ are computed afterwards in our reorder point algorithm (lines 6), see Algorithm 3, and delivery quantities, inventories, and emergency deliveries are updated.

The simulated annealing process is described in lines 7 - 10. The costs f are based on changes made by operators and Algorithm 3. The solution is always accepted if it is better than the previous global solution (lines 7 - 8). Depending on the temperature $Temp$, the new solution ($\bar{R}$, $\bar{s}_{p,c}$) is accepted (lines 9 - 10) if it is worse than the global best solution. Last, the temperature and the weights of the operators and delivery days are updated, dependent on the performance of this iteration.

Algorithm 2: ALNS framework for the cyclic inventory and routing planning.

```
1  (R, R^global, s_{p,c}, s^global_{p,c}) ← Initial Solution;
2  Temp ← GetInitialTemp();
3  while Time < MaxTime do
4      Choose(Operator, T);
5      R̄ ← Operator(R);
6      s̄_{p,c} ← Optimize(s_{p,c});                    //see Algorithm 3
7      if f(R̄, s̄_{p,c}) < f(R^global, s^global_{p,c}) then
8          (R, R^global, s_{p,c}, s^global_{p,c}) ← (R̄, s̄_{p,c});
9      else if accept(f(R̄, s̄_{p,c}), f(R,s_{p,c}), Temp) then
10         (R,s_{p,c}) ← (R̄, s̄_{p,c});
11     Temp ← UpdateTemp(Temp);
12     UpdateWeights();
13 end
```

3.5.3 Operators

The used removal, selection, and insertion operators are extensions of the operators of Ropke and Pisinger (2006), Pisinger and Ropke (2007), Aksen et al. (2014), and Rave et al. (2023b). A selection operator only chooses clinics for insertion, in contrast to a removal operator that removes these clinics. In each iteration, operators are chosen in the following way, as the removal of customers decreases and the insertion of clinics increases the number of servings per clinic, which, however, is variable.

1. Remove clinic, insert clinic *(two operators chosen)*
2. Select clinic, insert clinic *(two operators chosen)*
3. Remove clinic *(one operator chosen)*
4. Shift delivery day of one route *(one operator chosen)*

We consider two operators that remove or select α clinics, three operators that insert these removed or selected clinics, and one operator that shifts the delivery day. α is randomly drawn (uniform) with a limited number of clinics.

Random removal/selection - The random removal/selection operator removes/selects α clinics from any route and delivery day.

Closest removal/selection - The closest removal/selection operator removes/selects a random clinic and at maximum $\alpha - 1$ closest clinics of all or one specific route/s within the same period.

Greedy insertion - This operator adds clinics one by one to existing van tours at day T in a greedy best way taking traveled distances into account. If there has not been a route on this day, a new route is created. Clinics might be inserted in any routes, as in the next step in the ALNS, the delivery quantity is adjusted.

Random insertion - This operator works in a similar way as the previous operator but adds clinics to a random place within the route.

Greedy insertion - new route - Similar to the previous operator, this operator inserts clinics always in one new route at the selected day T.

Delivery day shift - The delivery day of one route is shifted to the selected day T. If clinics have already been visited at that day, these clinics are removed from this shifted route.

3.5.4 Reorder point algorithm

Algorithm 3 describes the pseudo-code of the reorder point algorithm for calculating the reorder points $s_{p,c}$ and is executed for each clinic separately. For this, we use the integrality of $s_{p,c}$ to compute local optimal reorder points $s_{p,c}$ in each iteration of the ALNS. In the beginning, a reorder point $s_{p,c}^{new}$, the best reorder point $s_{p,c}$ found so far, and the considered routing R are initialized (line 1). As the initial reorder point, the reorder point of the routing before modification by operators is chosen. While there are still cost improvements (line 2) by adjusting $s_{p,c}^{new}$, $s_{p,c}$ is updated (line 3), and $s_{p,c}^{new}$ is either increased or decreased by one dependent on which change has a larger benefit (line 4).

Algorithm 3: Reorder point algorithm to determine $s_{p,c}$ on a given R.

```
1 Initialize (s^new_{p,c}, s_{p,c}, R);
2 while f(R, s^new_{p,c}) < f(R, s_{p,c}) do
3 |   s_{p,c} ← s^new_{p,c};
4 |   s^new_{p,c} ← adjust(s^new_{p,c});
5 end
```

The calculation of $s_{p,c}$ for a clinic and product requires a complex evaluation of the objective function and also has dependencies with the reorder points of both the central clinic and even other surrounding clinics because the capacity in standard delivery is limited. These dependencies are circumvented by randomly selecting the sequence of clinics and products the algorithm is applied to. Thus, the found reorder points are locally optimal and not necessarily globally optimal.

3.6 Numerical Study

In this section, we show the performance of our ALNS and present a case study based on the project MEDinTime (Quantum Systems 2020). First, in Section 3.6.1, we describe the numerical setup in detail. In Section 3.6.2, we show the performance of our ALNS compared to optimal results solving the two-stage stochastic program in CPLEX and to optimal solutions for IRP instances of Archetti et al. (2007). In Section 3.6.3, we present results for the case study and perform multiple sensitivity analysis. The mathematical model is implemented in OPL and solved using CPLEX v12.10. and the ALNS is implemented in C++. All experiments are conducted on an AMD Ryzen 9 3950X with 32 GB. The used instances are available at: https://github.com/FontainePirmin/2E-SIRP.

3.6.1 Numerical setup

Location and number of clinics The central clinic, Ingolstadt Hospital, supplies nine surrounding clinics located between 3 and 75 km (euclidean distance) from the central clinic. The surrounding clinics are supplied in a weekly repeating manner, and all clinics are in the range of drone delivery.

For a performance analysis (small instances), we also consider three random locations of clinics within a 100km × 100km map and the five locations as in Archetti et al. (2007) for 15 clinic locations, which are also conducted by, e.g., Cui et al. (2023). For the instances by Archetti et al. (2007), we assume similar demands as in Archetti et al. (2007) and Cui et al. (2023), i.e., daily demands with randomly chosen integer values between one and five for each clinic that are constant over time. For a performance analysis (large instances), we consider the 30 instances of Archetti et al. (2007) with up to 30 surrounding clinics and $|\mathcal{T}| = 6$ delivery days, clinic-dependent inventory holding costs of $k_c^I \in [0.1, 0.5]$ for clinic $c \in \mathcal{C}$, $k_0^I = 0.3$, and the constant demands of $d_{p,c,t,\omega} \in [10, 100]$.

Cost structure Various medications are needed for patient care, which we categorize by their sales price. The annual inventory holding costs k_p^I are approximated by 20% of the average sales price of the corresponding category.

Based on the information given in our case study, standard delivery costs k^S are assumed to be 1.4 € per km while drone delivery is 52% cheaper and thus equals 0.672 € per km. Each inventory replenishment at the central clinic is assumed to have delivery costs of 168 € for a standard delivery ($\hat{k}^S$) and twice as high for an emergency delivery ($\hat{k}^{em.}$). Due to weekend emergency staffing at all clinics, emergency delivery costs are always increased by a factor of three at this time.

A standard supply for surrounding clinics includes approximately 200 different products, for which the transportation costs are total. Thus, these costs are "fixed" costs and are reduced to the considered number of products, as we only consider a portion of the products. Considering only a share of these products leads to similar decisions but can save sufficient run time (e.g., Rahimi et al. 2017). This proportional cost adjustment is applied to all standard delivery and emergency delivery costs, as in each delivery, different products might be consolidated.

Demand The demand for medication is assumed to be gamma-distributed with varying mean and variance for each product and clinic as the demand is not negative and can be any share of a product. However, the demand is rounded to two decimal places as consumer units cannot be divided arbitrarily. The variance is assumed to be five times as high as the mean of the distribution (Johansson et al. 2020). Additionally, the demand for medications varies for each weekday, with its peak on Wednesday, and is especially lower at the weekend, as clinics have a 30% lower bed occupancy at the weekend. This is because patients in Germany are increasingly discharged at the weekend, and new patients mostly arrive at the beginning of the week.

Due to multiple products, the distribution of the scenarios is potentiated. Thus, to reduce this probability space, we use the latin hypercube sampling by McKay et al. (1979) to generate demands: the normal distribution for each product is divided into $|\Omega|$ intervals of equal size and then displayed in a hypercube. From this hypercube, $|\Omega|$ random demands are drawn for each product so that rows and columns do not overlap. This procedure is repeated for all hospitals and time periods.

Delivery quantities and capacities We assume that drugs that are high in demand are delivered in larger packages, which results in larger volume equivalents per package.

The van's capacity is based on the Mercedes Sprinter (Mercedes-Benz AG 2022) and reduced proportionally to the drugs under consideration so that the total average weekly demand of up to five clinics can be carried in each van's tour. This means that the van's capacity K^S depends on the considered drugs (e.g., $K^S = 138.7$ volume equivalents if one product of each category is considered). The considered drone has a capacity of 3.765 volume equivalents ($K^{em.}$).

Table 3.3 presents the parameter settings for the seven different products categorized by their price ranges, the resulting inventory holding costs per day k_p^I, the delivery quantity for the central clinic Q_p, their volume v_p, and their average mean and variance, which need to be adjusted based on the size, i.e., the bed number, for each clinic.

$p \in \mathcal{P}$	Price ranges [€]	k_p^I [€]	Q_p	v_p	Average mean of demand	Average variance of demand
1	< 12	0.0033	100	2	1.29	6.43
2	12 - 58	0.0193	30	2	0.21	1.07
3	59 - 129	0.0514	20	1	0.09	0.43
4	130 - 291	0.1153	15	1	0.06	0.32
5	292 - 778	0.2933	10	1	0.04	0.21
6	779 - 1758	0.6951	5	0.4	0.02	0.11
7	> 1759	2.4644	3	0.4	0.01	0.06

Table 3.3: Parameter values for product categories.

ALNS parameter The ALNS parameters are based on pre-testing. In each iteration, a randomly drawn number of one to all clinics is selected/removed if a selection/removal operator is chosen. The reaction factors for the learning curve and the weight adjustment are set similarly to Rave et al. (2023b). The initial temperature factor for the simulated annealing equals 1% of the costs

of the initial solution and cools down by a cool rate dependent on the remaining run time of the ALNS.

3.6.2 Performance analysis

In this section, we first benchmark our ALNS to solutions generated by CPLEX (Section 3.6.2.1), then to optimally solved IRP instances of Archetti et al. (2007) (Section 3.6.2.2), and last, we demonstrate the stability of the found solution (Section 3.6.2.3).

3.6.2.1 Small instances

The performance of the ALNS is compared to the solutions obtained using CPLEX for the two-stage stochastic program. The run time limit for the two-stage stochastic program was set to 60 minutes and for the ALNS to five minutes. The ALNS is executed five times. Table 3.4 presents aggregated results for 78 instances. Detailed results are provided in Table C.1 in Appendix C.1. Column $|\hat{\mathcal{C}}|$ describes the number of clinics, column $|\mathcal{P}|$ number of considered products, and column $|\Omega|$ the number of demand scenarios. The next four columns describe the best cost CPLEX found, the best cost the ALNS found, the average cost found, and the deviation between the best and average costs (σ). Columns eight and nine describe the number of optimal solutions found by CPLEX and the average gap of the not-to-optimality solved instances. Finally, the last two columns show the run time.

			Cost objective				CPLEX		Run time (s)	
$\|\hat{\mathcal{C}}\|$	$\|\mathcal{P}\|$	$\|\Omega\|$	CPLEX	ALNS best	ALNS avg	ALNS σ [%]	Opt	GAP [%]	CPLEX	ALNS
4	1	5	4.45	4.45	4.46	0.59	12 / 12	-	82	78
4	2	5	8.37	8.27	8.28	0.23	3 / 4	28	1465	183
4	3	5	16.70	16.50	16.51	0.12	1 / 4	21	2794	225
7	1	2	6.27	6.22	6.24	1.02	6 / 12	21	1940	207
7	2	2	14.47	12.49	12.51	0.12	0 / 4	42	3600	300
7	3	2	40.27	22.85	22.93	0.34	0 / 4	63	3600	300
10	1	1	13.51	13.46	13.49	1.01	17 / 28	24	1192	136
15	1	1	23.36	20.93	21.21	1.34	2 / 10	27	3083	278
Avg			13.59	12.24	12.30	0.38	43 / 78	23	1722	180

Table 3.4: Performance analysis for small instances.

Findings: The results show that CPLEX can only solve 43 out of the 78 small instances to optimality. For the other 35 instances, the gaps are rather large. The ALNS, on the other hand, finds for all clusters the same or better costs on average with up to 56% fewer costs by using only 10% of the run time. The results of the ALNS are stable as σ has a value of 0.38% on average for all instances.

3.6.2.2 Large instances

In this section, we benchmark the performance of our ALNS on the 30 instances of Archetti et al. (2007), which have also been considered by, e.g., Archetti et al. (2012). We consider these IRP instances because there is no similar problem setting in the literature so far, and for these instances,

the corresponding problem setting is closest to our problem setting. In comparison to our problem setting, Archetti et al. (2007) consider the following simplifications: The authors consider a single product whose demand is deterministic, constant, and known for the planning horizon of 6 periods, i.e., there is only a single scenario and no recourse decision. Moreover, the central clinic has no demand and its inventory is replenished in each period with a constant amount. All clinics' initial inventory is a given parameter; thus, no cycle is considered. The inventory is always replenished to an order-up-to-level, which is a parameter. In addition, there are no reduced quantities delivered if the van's capacity would exceed. Note that there is only a single vehicle. Last, the inventory holding costs arise per clinic instead of per product h_c ($c \in \hat{\mathcal{C}}$). It follows that running the ALNS, the reorder point algorithm is not executed.

Table 3.5 shows the consolidated results of these instances. Detailed results can be found in Table C.2 in Appendix C.2. The first column describes the number of considered surrounding clinics, and the next column the proven optimal solution by Archetti et al. (2007). Columns three and four present our best found solution of five runs and the average found solution. Columns five and six give information on the number of solved instances to optimality and the average gap to optimality (Δ). Last, column seven shows the gap from best to average (σ). We chose a run time of 60 minutes for running the ALNS.

		Our ALNS				
$\lvert\mathcal{C}\rvert$	Opt. costs	Best costs	Avg. costs	Opt	Δ [%]	σ [%]
5	5538.02	5538.02	5572.80	5/5	0.00	0.67
10	8872.41	8903.47	9197.99	2/5	0.35	3.18
15	11721.83	11811.86	12114.40	0/5	0.78	2.47
20	14863.85	15006.32	15219.32	0/5	0.95	1.40
25	17170.81	17479.36	17768.22	0/5	1.81	1.63
30	20657.29	20923.60	21243.02	0/5	1.27	1.53
Avg	13137.37	13277.10	13519.29	7/30	0.86	1.81

Table 3.5: Performance analysis for benchmark instances of Archetti et al. (2007).

Findings: Our ALNS solves 7 of the 30 instances to optimality with an average gap of 0.86%. Moreover, we observe that the solution is stable with an average σ of 1.81%. Especially the performance does not decrease monotonously with a larger number of considered clinics. These results show the performance, especially since our ALNS was not designed for this operational problem setting that has large differences, as mentioned above, but for a tactical problem setting with multiple products and stochastic demands that also includes the optimization of reorder points for cyclic delivery patterns.

3.6.2.3 Stability tests

In this section, we demonstrate the stability of the solutions of our ALNS. For this, we compare the routing for ten instances for the location of clinics as in our case study. We choose a number of 100 varying scenarios and one product of each product category. Thus, the instances only vary in their demand scenarios. The number of scenarios is sufficient as a maximum desired deviation of 10% is not exceeded for a confidence interval of 95%. It is tested for the total costs, number of emergency

deliveries, and average amount of reorder points. The ALNS is executed five times with a run time limit of 60 minutes in each run, as the solution is used for a tactical planning problem (Rave et al. 2023b). Table 3.6 presents for each instance the best routing found on the corresponding day, the best costs, the average costs, and the deviation from average to best costs (σ). The routing always starts and ends with the central clinic. The driving order equals the order of the numbered clinics in the squared brackets. If a second route is on the same weekday, the routing is presented in a second row.

	Best found routing at weekdays							
Instance	Mo.	Tu.	We.	Th.	Fr.	Best costs	Avg. costs	σ [%]
1				[8]-[3]-[5]	[1]-[6]-[2]-[4]-[9]	167.70	168.52	0.49
				[7]				
2				[8]-[3]-[5]-[7]	[1]-[6]-[2]-[4]-[9]	167.78	168.53	0.44
3				[8]-[3]-[5]	[7]-[1]-[6]-[2]	171.58	172.58	0.58
				[4]-[9]				
4				[8]-[3]-[5]	[7]-[1]-[6]-[2]-[4]-[9]	166.48	167.81	0.79
5				[8]-[3]-[5]	[7]-[1]-[6]-[2]	172.77	173.58	0.46
				[4]-[9]				
6				[8]-[3]-[5]-[7]	[1]-[6]-[2]-[4]-[9]	171.84	173.08	0.72
7				[9]-[8]-[3]-[5]-[7]	[1]-[6]-[2]-[4]	170.43	171.51	0.63
8				[8]-[3]-[5]-[7]	[1]-[6]-[2]-[4]-[9]	166.63	167.74	0.67
9				[8]-[3]-[5]	[7]-[1]-[6]-[2]	173.63	174.69	0.61
				[4]-[9]				
10				[8]-[3]-[5]-[7]	[1]-[6]-[2]-[4]-[9]	167.43	168.19	0.45

Table 3.6: Performance analysis for large instances.

Findings: The results are stable in costs as σ always has values below 1%, and each clinic is visited once, either on Thursday or on Friday. The supply is just after the weekly demand peak in clinics to prevent additional emergency delivery costs at the weekend. Clinics [8],[3], and [5] are always visited in the same order and day. The same holds for clinics [1], [6], and [2]. Clinics [4], [7], and [9] are added to different routes, or even new routes, in the instances under consideration. However, this variation does not lead to large cost differences. Clinic [7] is mainly visited on Thursday, and [4] and [9] mainly on Friday. The results appear very satisfactory as the costs are stable, and the best routing has little variation.

3.6.3 Numerical results

In this section, we present the results of the case study and multiple sensitivity analysis.

3.6.3.1 Case study

We demonstrate the advantages of an optimization of reorder points and routing compared to the status quo of clinic supply. The status quo is as follows: Each surrounding clinic determines its delivery days and reorder points on its own. There are in total about 250 emergency deliveries per year, as emergency deliveries are avoided if possible due to their extra costs. Subsequently, the central clinic plans the routing on the respective days and its own inventory management based on the given information.

Our integrated approach not only optimizes the inventory of all clinics consolidated but also the routing simultaneously. Therefore, in the following, first, the reorder points for the central clinic and the surrounding clinics are optimized for the same routing as the status quo, and then the results are compared to the status quo. This is done by applying our reorder point algorithm to the routing of the status quo. Second, additionally, the routing is optimized, and the results are again compared to the status quo. This is done by executing the ALNS. For both, we consider 50 instances á one product of each product category, 100 scenarios, and the clinic location as in our case study, and we set the run time limit of the ALNS again to 60 minutes. We obtain the status quo results by running the reorder point algorithm that chooses reorder points so that there are 250 emergency deliveries for surrounding clinics per year.

The following KPIs are compared in Table 3.7 all in comparison to the status quo in percent: total costs for the central clinic and for surrounding clinics (1. row), the average number of standard delivery visits per week for the surrounding clinics (2. row), the average number of emergency deliveries per week for surrounding clinics (3. row), and last the reorder points for each product category. Each KPI consolidates all nine surrounding clinics.

	Inventory optimization [%]		Inventory & routing optimization [%]	
	Central clinic	Surrounding clinics	Central clinic	Surrounding clinics
Costs	− 16.0	− 45.7	− 15.9	− 58.4
# Standard del.		± 0.0		− 47.1
# Emergency del.		+ 185.9		+ 160.9
Reorder points				
Product category 1	+ 3.7	− 9.7	+ 46.6	− 1.9
Product category 2	+ 4.6	− 42.4	+ 19.8	− 32.4
Product category 3	+ 3.8	− 64.4	+ 16.8	− 56.7
Product category 4	− 14.0	− 76.6	+ 4.5	− 64.1
Product category 5*	− 60.0	− 99.2	− 59.3	− 88.9
Product category 6*	− 53.6	− 100.0	− 41.7	− 100.0
Product category 7*	− 100.0	− 100.0	− 100.0	− 100.0

Table 3.7: Percentage change from status quo with cost-optimal inventory (2nd and 3rd column) and with simultaneous route and inventory optimization (4th and 5th column).
* Smaller clinics do not have any inventory of this product category already in the status quo.

Findings: The inventory optimization leads to cost savings of 16.0% for the central clinic and 45.7% for the surrounding clinics, as demand peaks are eliminated. Additional cost savings of 12.7 percentage points can be reached for the surrounding clinics if the routing is planned simultaneously. However, this additional routing optimization does not impact costs for the central clinic.

The cost savings are mainly achieved by applying the following: First, clinics make use of pooling effects, i.e., less inventory to be stored in surrounding clinics but more in the central clinic. The following applies in particular: The more expensive a product, the stronger the pooling effect. Even after inventory optimization, the reorder points for product category 7 are set to zero for all clinics, which means that all demand is satisfied via emergency deliveries. Storing more in the central clinic may not even be necessary when only split drugs are transported. Second, surrounding

clinics decrease the number of standard deliveries to one visit per clinic per week but increase the number of emergency deliveries by 185.9% or 160.9%, respectively.

3.6.3.2 Value of multi-product optimization

In this section, we compare our multi-product approach, where reorder points for multiple products and the routing are optimized simultaneously, to the following sequential procedure: we first determine order intervals and reorder points for each product individually and, second, the routing that covers all products. Thus, our ALNS is executed for the single-product case in the first step. In the second step, we use the resulting reorder points for all product categories as input parameters and optimize the routing by executing our ALNS without the reorder point algorithm. Table 3.8 presents the percentage change of this sequential procedure to the multi-product approach in percent.

	Separated reorder point and routing optimization [%]	
	Central clinic	Surrounding clinic
Costs	+ 5.3	+ 2.2
# Standard del.		± 0.0
# Emergency del.		+ 9.5
Reorder points		
Product category 1	− 19.4	+ 4.7
Product category 2	− 19.9	+ 0.7
Product category 3	+ 0.5	− 4.0
Product category 4	− 11.5	− 28.9
Product category 5	± 0.0	− 59.5
Product category 6	− 18.4	± 0.0
Product category 7	± 0.0	± 0.0

Table 3.8: Percentage change from the multi-product approach when optimizing reorder points for each product separately.

Findings: We observe that costs increase for both the central clinic and the surrounding clinics significantly by 5.3% and 2.2% on average. This is mainly caused by a variation of reorder points and resulting in an increase in emergency deliveries. For surrounding clinics, the reorder points increase for product categories 1 and 2 and decrease for product categories 3 to 5. For product categories 6 and 7, there is no change as the reorder points are already zero when considering all products consolidated. In contrast, for the central clinic, nearly all reorder points decrease. The changes in reorder points can be predominantly attributed to the adjusted capacity ratios for each product in standard and emergency delivery, which have a direct impact on the transportation cost per delivery.

3.6.3.3 Impact of drone delivery

In this section, the influence of drone delivery as instant replenishment orders on total costs and inventory pooling effects is analyzed. Thus, in Table 3.9, we compare the results for the case if the emergency delivery is carried out by drones to the results for the case if the emergency delivery is carried out by the same vans as for standard delivery. Van delivery, on the one hand, has higher costs than drone delivery, but on the other hand, it has an unlimited capacity such that there is at

maximum one emergency delivery per clinic per day. We first consider costs for drone delivery as in our case study (Columns 52%), and second, drone delivery costs are reduced by a factor of two (Columns 76%).

	Cost advantage of emergency delivery by drones			
	52% [%]		76% [%]	
	Central clinic	Surrounding clinics	Central clinic	Surrounding clinics
Costs	− 0.6	− 29.8	− 0.6	− 49.8
# Standard del.		− 0.7		− 0.7
# Emergency del.		+ 22.5		+ 53.5
Reorder points				
Product category 1	− 0.2	− 1.7	− 3.0	− 9.3
Product category 2	− 0.1	− 12.0	− 4.5	− 36.1
Product category 3	− 0.5	− 30.7	− 1.8	− 48.2
Product category 4	− 4.9	− 33.3	− 22.2	− 67.2
Product category 5	− 10.9	− 63.2	− 4.7	− 100.0
Product category 6	+ 2.1	− 100.0	+ 6.3	− 100.0
Product category 7	± 0.0	± 0.0	± 0.0	± 0.0

Table 3.9: Percentage change from van delivery as an emergency delivery option with drone delivery when drone delivery is 52% and 76% more cost efficient.

Findings: Drones as emergency delivery options lead to cost savings of 29.8% for surrounding clinics but have nearly no impact on the costs for the central clinic. The cost savings for surrounding clinics increase to 49.8% when drone delivery is more cost-efficient. These cost savings can be achieved by reducing the stored inventory at the surrounding clinic if emergency deliveries are used more frequently instead. Once again, the more expensive a product, the stronger the pooling effects. This has no effect on product category 7, as this already has a reorder point of 0 at van delivery for all clinics. For each product category, the pooling effects are stronger if the emergency delivery is more cost-efficient. The inventory of the central clinic also decreases slightly for some product categories, as there is an increase in the delivery of only individual consumer units to surrounding clinics so that whole packs are not stored, and the increased use of emergency deliveries leads to a distribution of delivery quantities over several days, thus avoiding demand peaks.

3.6.3.4 Impact of limited vehicle fleet

In this section, we show the impact of limiting the vehicle fleet for standard and emergency delivery as in Constraints (3.41) and (3.42). For this, we first limit the number of vans for standard delivery to one per day ($n^S = 1$, $n^{em.} = \infty$), and in a second analysis, we additionally limit the number of drone flights to five per day ($n^S = 1, n^{em.} = 5$). Table 3.10 shows the percentage change considering the limited fleet to the case when the vehicle fleet is unrestricted.

Findings: We observe that limiting the number of vans in standard delivery to one has no significant impact on the solution. The number of visits increases slightly on average, and emergency deliveries decrease. These changes result in a cost increase of 1.1% for surrounding clinics but, on the other hand, a minor cost reduction of 0.2% for the central clinic. There are only small changes

as the final found solution previously only contains multiple routes per day on rare occasions.

Limiting also the number of drone deliveries results in significant changes in costs, routing, number of emergency deliveries, and reorder points. The number of visits in standard delivery increases by 5.7%, but the number of emergency deliveries decreases by 7.4%. More products are stored in surrounding clinics with a reorder point increase of up to 17.7% (except product category 6, where nothing was stored previously), but fewer products are stored in the central clinic with a reorder point decrease of up to 17.9%. These changes result in a cost increase of 6.7% for surrounding clinics. However, costs for the central clinic are slightly reduced by 0.8%. This can be explained by the reduced use of pooling effects at the central clinic. It follows that limiting the number of emergency deliveries via drones has a greater impact on the solution than limiting the number of van routes in standard delivery.

	$n^S = 1, n^{em.} = \infty$ [%]		$n^S = 1, n^{em.} = 5$ [%]	
	Central clinic	Surrounding clinics	Central clinic	Surrounding clinics
Costs	− 0.2	+ 1.1	− 0.8	+ 6.7
# Standard Del.		+ 1.2		+ 5.7
# Emergency Del.		− 1.5		− 7.4
Reorder points				
Product category 1	− 1.0	+ 1.2	− 10.6	+ 11.3
Product category 2	+ 1.8	+ 0.6	− 11.3	+ 15.5
Product category 3	+ 2.1	+ 0.1	− 9.4	+ 17.3
Product category 4	+ 0.4	+ 0.3	− 6.2	+ 17.7
Product category 5	+ 1.8	+ 25.6	+ 2.3	+ 6.3
Product category 6	± 0.0	± 0.0	− 17.9	$+\infty$
Product category 7	± 0.0	± 0.0	± 0.0	± 0.0

Table 3.10: Percentage change from an unlimited vehicle fleet, when there is one van, and when there are in addition just five drone flights per day.

3.7 Conclusion

This paper considers a cyclic routing planning combined with inventory policies and drones as emergency delivery options for recourse decision for the medical supply of clinics. We introduce a two-echelon IRP that takes a cyclic $(\mathcal{T}_c, s_{p,c}, n_{p,c} \cdot q_p)$ inventory policy for surrounding clinics in the second echelon and a $(s_{p,\hat{c}}, Q_p)$ policy for the central clinic in the first echelon into account. We present the problem as a two-stage stochastic program and develop a specialized ALNS that determines local-optimal reorder points $s_{p,c}$ in each iteration. In a performance analysis, we show the solution quality and stability of the ALNS on IRP instances of Archetti et al. (2007).

The case study shows that the use of pooling effects leads to total cost savings of 16.0% for the central clinic and 45.7% for surrounding clinics. The cost savings for surrounding clinics can even be increased by additional 12.7 percentage points if the routing is optimized simultaneously. We have also analyzed that a multi-product optimization significantly decreases costs. The study also shows that drones as a more cost-efficient emergency delivery option reduce costs for surrounding

clinics by 29.8% compared to an emergency delivery option via van. However, drones have nearly no impact on the costs of the central clinic.

Future research could include possible transshipments between the surrounding clinics. The transshipments are, for example, a pick-up of medications at one clinic during standard delivery and taken to the next or an emergency delivery launched from a closer surrounding clinic. Extensions of our problem setting, like consolidating multiple clinics in one tour in the emergency delivery, can be considered. This, however, leads to a VRP in the recourse, such that the ALNS presented in this paper needs to be adjusted to solve a VRP in the recourse as well. Further, shelf life can be considered. This is relevant when the routing and reorder points of, e.g., blood with an expiration date of some days instead of medication need to be planned. Moreover, it can also be examined what the best fleet mix for emergency deliveries might look like, taking into account fixed costs and weather-related flight bans for drones.

Acknowledgments

The authors gratefully acknowledge the scientific and financial support of the Federal Ministry for Digital and Transport, Germany, for the research project MEDinTime reported in this paper.

Contribution 4 - Drone fleet planning and battery allocation for emergency resupply of pharmacies and ambulances

4 Drone fleet planning and battery allocation for emergency resupply of pharmacies and ambulances

Alexander Rave, Pirmin Fontaine, Heinrich Kuhn

Abstract For patients' treatments, pharmacies and ambulances are equipped with multiple drugs. If there is a medication shortage, pharmacies are replenished via emergency deliveries, and ambulances transport the patient to a nearby hospital. These processes result in delays in patients' treatments, high costs, and emissions and can be improved by aerial drones as a new transport vehicle for emergency delivery. Drones have great potential as only a few medications need to be transported, and drones can travel fast at low variable costs and emissions.

We consider a wholesaler who is the supplier of multiple pharmacies and plans to integrate drones for emergency delivery of medicines to serve both pharmacies and ambulances. We determine the most economical and ecological number of drones, batteries, transport boxes, and the location of spare batteries for emergency resupply, guaranteeing a certain supply rate and service level.

Based on a case study, we apply a management decision support framework proposed in the literature to define and solve our drone fleet planning and spare battery allocation problem. We perform a discrete-event simulation optimization that accounts for stochastic seasonal demands, weather conditions, and daylight-dependent flight bans for drones. With unchanged demand, cost savings of up to 19.6% are achieved with a supply rate and service level of at least 90%. If, on the other hand, demand increases and drone properties are improved, costs can be reduced by up to 51.7% with a supply rate and service level of more than 99%.

URL (Working Paper): `https://papers.ssrn.com/sol3/papers.cfm?abstract_id=4569199`

4.1 Introduction

Pharmacies and ambulances must have an extensive selection of medical goods available at all times. This makes it necessary that pharmacies and ambulances are appropriately equipped with various medical goods to provide patients care (e.g., Volland et al. 2017). If a pharmacy has a medication shortage, these drugs are replenished in an emergency delivery. For a pharmacy of a medium-sized clinic, this results in, on average, one emergency delivery per week (Rave et al. 2023a). This emergency delivery is typically a road-based transport and is especially inefficient, as a van is loaded with only a single drug for a commuting tour. As a result, high costs, emissions, and delays due to road binding occur. In case of medication shortages in ambulances at service, the ambulance transports the patient to a hospital, and the patient's treatment takes place there, leading to a decisive delay in the patient's treatment that could threaten the patient's welfare. Now, aerial drones have the opportunity to improve patient care, as drones might transport a few medications fast, environmentally friendly, and cost-efficient (e.g., Otto et al. 2018). Drone delivery improves the patients' service as each pharmacy or ambulance supplied by drones will be treated faster. When ambulances place an order for the medical supplies expected to be needed while still en route to the scene of the accident, it follows that ambulances also have the full range of medications available for patients' treatment.

We consider a wholesaler who is responsible for delivering medication to multiple pharmacies in case of emergency and plans to integrate aerial drones for this delivery. In this way, the wholesaler, on the one hand, improves the existing emergency delivery to pharmacies and, on the other hand, opens up a new business model with direct deliveries to ambulances at service. The service of ambulances requires a reliable delivery system, provided that external conditions (e.g., weather) allow drones to fly. Integrating drones raises the question of how many drones, spare batteries, and transport boxes to purchase and at which location to store spare batteries to guarantee a certain supply rate or service level while being cost- and ecologically efficient. These are conflicting goals as the acquisition of drones is associated with high fixed costs and causes CO_2 equivalents (CO_2 eq.).

Based on a real case of the project MEDinTime, where the pharmacy of a large German hospital serves as a wholesaler for clinics' pharmacies, we evaluate the drone fleet by applying the GUEST framework of Perboli and Rosano (2019), which is a lean business approach. This GUEST framework allows to give detailed insights on the connection between stakeholders, the delivery process, and the simulation optimization in a structured way. We perform a discrete-event simulation study and evaluate different drone fleets by comparing economic, ecological, and service-oriented key performance indicators (KPIs). In addition, we use this simulation in a simulation-optimization framework to determine the most economical or ecological drone fleet while guaranteeing a certain supply rate and service level. This choice is driven by the stochasticity and seasonality of order arrivals and flight bans for drones that impact both the utilization and availability of the drone fleet components. This further leads to additional waiting times or unavailability of drones, which must be compensated by standard truck deliveries. As a result, a formulation as a mixed-integer linear program (MILP) is not capable of reflecting this complexity, and similar to other problem settings, we choose the simulation as methodology (e.g., Cao et al. 2023, Zhang et al. 2020). On the

contrary, a simple averaging method would neglect these components and lead to incorrect results.

We contribute to the literature as follows: First, we introduce a discrete-event simulation optimization framework to determine the optimal drone fleet considering seasonal demands and flight bans and also show the value added by the simulation. Second, we generate multiple managerial insights for the case study based on the pharmacy of a large German hospital and in general by varying the network structure, demands and drone properties, and prices. Third, we transfer the GUEST framework to the drone fleet and spare battery allocation, identify stakeholders in the delivery system of the emergency supply of clinics, ambulance depots, and ambulances at service, and draw a business connection between them. Fourth, we present and analyze the supply chains for emergency deliveries.

The structure of our paper is the following: In Section 4.2, we describe the problem setting in detail. Second, we present the most relevant literature to differentiate our paper (Section 4.3). Then, we describe the GUEST framework in Section 4.4. In Section 4.4.1, we show the relevant stakeholders, and in Section 4.4.2, we draw their business connection and competition. In Section 4.4.3, we present our chosen KPIs and give detailed information on relevant parameter settings. The supply chain of clinics, ambulance depots, and ambulances at service is analyzed in Section 4.4.4. In Section 4.5, we show multiple managerial insights for our case study, test certain assumptions, and perform a sensitivity analysis. Last, Section 4.6 summarizes our results.

4.2 Problem setting

Network structure - status quo A wholesaler supplies multiple pharmacies regularly and in case of emergency with medication. The wholesaler is the contracted sole supplier of the pharmacies. In the status quo, ambulances are not supplied by the wholesaler. In case of medication shortage, an ambulance transports the patient to a nearby clinic instead.

Network structure - new emergency delivery network The wholesaler plans to integrate aerial drones as an alternative transportation mode for emergency delivery to serve pharmacies. Additionally, these drones shall serve ambulances. However, suppose the drone is unavailable or cannot perform a flight due to weather or daylight-dependent flight bans, the deliveries are as in the status quo: pharmacies are served via road-based transport, and ambulances are not served at all. In the delivery context, there is an additional aerial-based delivery mode for pharmacy supply and a new delivery mode for ambulance supply.

A drone can be used if a charged battery and a transport box suitable for the required medication are also available - a distinction is made here between transport boxes with and without a cooling function (Quantum Systems 2020). Drones can be made operational again more quickly if their batteries are changed instead of being charged. Thus, storing extra batteries at the wholesaler or the travel destination might be reasonable.

Figure 4.1 presents an example emergency delivery system for the status quo (left) and the new emergency delivery network (right) for the supply of pharmacies and ambulances when the wholesaler has one drone and sufficient batteries and transport boxes for delivery. The times show

when an emergency order is placed at the one day considered. While in the status quo, all pharmacies are supplied via road-based transport in case of emergency, but no ambulance is served at all; in the new delivery network, a pharmacy and two ambulances can be served via drones. A second pharmacy and a third ambulance cannot be supplied by drones since the drone is not available at that time. For the supply of the second pharmacy, this means that it is served via road-based transport instead. This results in opportunity costs due to the drone's unused economic, ecological, and delivery time advantages.

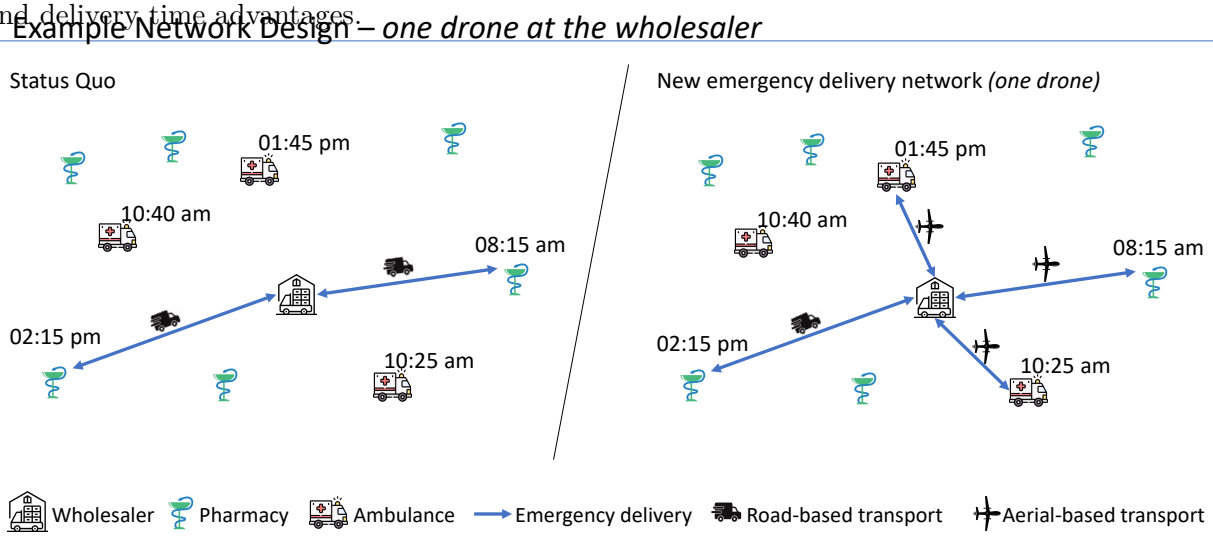

Figure 4.1: Example supply for one day as in status quo (left) and after integrating one drone (right).

Decision problem We decide on the most economical or ecological drone fleet and spare battery locations that guarantee a certain supply rate and service level. In detail, we evaluate variations of the following decisions on the drone network:

1. Vehicle fleet decision: How many drones, batteries, and different transport boxes to locate at the wholesaler?
2. Location decision: At which pharmacies to store additional spare batteries?

Assumptions We consider real flight conditions for drones:

- Demand and supply:
  - Pharmacies and ambulances have an independent stochastic demand in medication (e.g., Niakan and Rahimi 2015), and thus, stochasticity is also in their emergency order arrival with a daily and weekly season. We show the impact of this seasonality in Section 4.5.2.3
  - Orders are not consolidated.
  - The wholesaler always has sufficient medication in stock.
- Deliveries:

  - The location of ambulances is generally uncertain and just known after an order is placed and thus modeled via a stochastic flight duration.
  - Drones only serve ambulances within a certain flight-time range. On the other hand, the considered pharmacies are all in range of drones.
  - Drones can only perform a flight if they are ready to launch within 30 minutes after the order arrives.
  - There is a preparation time before the transport starts.
  - If a drone is not available for delivery, the trip is performed by a road-based transport instead (pharmacy) or rejected (ambulance).

- Batteries:
  - Batteries are charged when drones return to the wholesaler. We assume a sufficient number of available battery chargers so that no waiting times occur until the charging process for the drones starts.
  - Placing an additional battery is only considered at the wholesaler and remotely located pharmacies since one battery charge is otherwise sufficient for the return flight.
  - Batteries are used if fully charged to ensure that no batteries with a too-low capacity are used. Additionally, batteries need to have a rest capacity of at least 65% for the return flight for legal reasons. Note that the battery always has sufficient rest capacity for the flight-time range of serving ambulances.

- Transport boxes:
  - Transport box without a cooling function: This transport box has a larger payload, but only temperature-insensitive medicine can be transported.
  - Transport box with a cooling function: This transport box has a smaller payload, but also temperature-sensitive medication can be transported.

- Flight bans:
  - There are weather-related flight bans, i.e., precipitation, fog, and wind (Ranquist et al. 2017). The weather is stochastic but known by the weather forecast and thus assumed to be known for the full execution time of a delivery. In Section 4.5.2.2, we analyze the impact of flight bans.
  - There are daylight-dependent flight bans, i.e., no flights during the night. If the return flight is at night, the drone waits at the served pharmacy until the flight conditions fit again. The daylight has a yearly season. We show the impact of this seasonality in Section 4.5.2.3.

- Prioritization:
  - Drone delivery is prioritized compared to road-based transport.

- Orders are processed following a first-come-first-serve (FCFS) rule. We vary this assumption in Section 4.5.2.4 and prioritize ambulances and far-located pharmacies.
- The transport box, which results in lower costs, is prioritized if the drug fits.

4.3 Literature review

Drone delivery is a much-considered area in academia, with the focus of most publications on operational route planning when trucks and drones interact (e.g., Sacramento et al. 2019). In addition, tactical issues related to fleet planning in parcel delivery were studied by, e.g., Rave et al. (2023b). However, the biggest expense in drone delivery problems is the consideration of routing, which is not present in our problem setting. We, therefore, focus on the following on comparable drone applications in healthcare and network design settings. We recommend the literature review of Wang and Demeulemeester (2023) for an overview of simulation studies with application in healthcare planning and the literature review of Otto et al. (2018) for an overview of civil drone applications.

Drones as additional service option Chu et al. (2021) analyze the impact of drones transporting defibrillators in case of an out-of-the-hospital heart attack. For this, the authors develop a machine-learning-based dispatching rule. For the same case study, Boutilier and Chan (2022) present an integrated location-queuing model that decides on the locations of drone bases, secondarily also considering the total number of drones in the system.

Drones replacing road-based transports Asadi et al. (2022) present a Markov decision process for a stochastic scheduling and allocation problem with the use case of the Zipline project in Rwanda, Africa, where a central warehouse serves multiple hospitals with medication via drones. Dhote and Limbourg (2020) formulate a mixed-integer linear program (MILP) for a deterministic pick-up and delivery problem focusing on the transport of drugs based on a case study in Brussels. The authors decide on the location of the origin base of the drones as well as recharging stations in case the travel time exceeds the drone's maximum endurance. Otero Arenzana et al. (2020) present a deterministic facility location problem in the form of a MILP with integrated drone number selection for blood transports between blood banks and hospitals based on a case study in London. Rave et al. (2023a) model a cyclic inventory routing problem with stochastic demand and inventory control policies with drones as emergency delivery options for clinic resupply in case of shortages. Compared to our paper, the authors assume an unlimited drone fleet and do not include the supply of ambulance depots and ambulances at service.

Network design settings in public transport and freight planning Sa et al. (2020) consider a long-term airplane fleet planning problem, explore the stochastic demand in a Monte-Carlo simulation, and determine the optimal fleet via a MILP, including assigning passenger flows between airports.

Militão and Tirachini (2021) optimize the vehicle size and the fleet size of human-driven and automated vehicles in public transport. The authors present a simulation framework that minimizes

operator and user costs. Perboli and Rosano (2019) analyze freight transportation with traditional and green vehicles in urban areas. For this, the authors simulate and evaluate different fleet mixes considering ecological and service-oriented KPIs. Fehn et al. (2023) combine parcel delivery and a ride-pooling system. In a simulation study, the authors compare two integration approaches to the status quo. Zwick et al. (2022) simulate ride-pooling systems considering driver shifts and evaluate the efficiency of this public transport system by comparing it to on-demand systems. On-demand systems are simulated and analyzed by Nguyen-Phuoc et al. (2023), where the authors evaluate three stages of automation.

	Assumptions			Decisions		Methodology	
Paper	Drone delivery considered	Flight bans	Different KPIs evaluated	Location planning	Fleet planning	MILP	Simulation
Dhote and Limbourg (2020)	✓	✓*	✓*	✓		✓	
Otero Arenzana et al. (2020)	✓			✓	✓	✓	
Chu et al. (2021)	✓						
Asadi et al. (2022)	✓				✓		
Boutilier and Chan (2022)	✓			✓	✓	✓	✓
Rave et al. (2023a)	✓					✓	
Perboli and Rosano (2019)			✓		✓		✓**
Sa et al. (2020)			✓		✓	✓	✓
Militão and Tirachini (2021)					✓		✓
Zwick et al. (2022)			✓				✓
Fehn et al. (2023)			✓		✓		✓
Nguyen-Phuoc et al. (2023)			✓		✓		✓
Our paper	✓	✓	✓	✓***	✓****		✓**

Table 4.1: Comparison of relevant literature.
* Only verbally in a SWOT analysis, ** GUEST framework,
*** location of spare batteries, **** including required and additional hardware.

Table 4.1 distinguishes taken assumptions, the problem setting, and the methodology of our paper from the literature discussed previously. Our contribution differs in particular by weather- and daylight-dependent flight bans and a more detailed focus on the drone fleet, which is evaluated using various KPIs in a simulation study. Moreover, regarding the network, we are the first to look at the supply of both pharmacies and ambulances.

4.4 GUEST framework

We use the GUEST decision support framework to define and solve our drone fleet and spare battery allocation problem for emergency resupply. Initially introduced by Perboli and Rosano (2019), the GUEST framework is ideal for this purpose, as it allows to present detailed insights of the delivery process and the stakeholders involved in a structured manner in a simulation study (e.g., Perboli and Rosano 2019). A simulation study is useful to model the complex and stochastic processes in the emergency supply of clinics (Wang and Demeulemeester 2023). The individual letters of GUEST stand for process steps, which can be described as follows:

Go We give a detailed analysis of stakeholders that are relevant to the emergency delivery system (Section 4.4.1). We also present a business model canvas (BMC) for the wholesaler, which can be found in Appendix D.1.

Uniform We represent the stakeholders considered in a social business network and draw their business connection and competition to each other (Section 4.4.2).

Evaluate We introduce relevant KPIs and give detailed information on parameter values that are relevant for the emergency delivery process (Section 4.4.3).

Solve We draw the supply chain for the delivery to pharmacies and ambulance services that we consider in a discrete-event simulation study (Section 4.4.4).

Test We analyze the results, test taken assumptions, and present further results to generalize our findings (Section 4.5).

We use this GUEST framework for the case study of the MEDinTime project, in which the pharmacy of a large German hospital serves as a wholesaler and is to be equipped with aerial drones. The network structure and the generated insights can then be transferred to other wholesalers for medical supplies.

Within the GUEST framework, we apply a discrete-event simulation study including a simulation optimization to determine the drone fleet with the largest cost or emission savings that guarantees a certain supply rate for pharmacies and service level for ambulances. The model accounts for stochastic seasonal demands and weather conditions, as well as daylight-dependent flight bans for drones. We chose the methodology of a simulation study because the utilization and availability of drones, transport boxes, and spare batteries depend on the stochasticity and seasonality of order arrivals and flight bans for drones. This leads to additional waiting times for drones and thus to extended order delivery times or unavailability of drones, which must be compensated by standard truck deliveries. A simple averaging method would neglect these additional waiting times for drones and lead to incorrect results. Therefore, a deterministic optimization approach would lead to inaccurate results, which is particularly problematic in the healthcare sector, as this area is highly intolerant of faults (Young 2005). We show in Section 4.5.2.1 the necessity of a simulation and further in Section 4.5.2.3 that seasonality impacts the drone fleet and the KPIs.

4.4.1 Go - detailed analysis of all stakeholder

The wholesaler, pharmacies, ambulances, and the truck service provider are stakeholders in the emergency delivery system.

Wholesaler The wholesaler, the Ingolstadt Hospital's pharmacy in our case study, is responsible for supplying pharmacies of surrounding clinics and ambulance depots and plans to supply ambulances. On the other hand, the wholesaler is served by the medication manufacturer.

The wholesaler plans to operate a drone fleet for emergency deliveries but is not equipped with a road-based vehicle fleet. For this, the wholesaler accesses a truck service provider instead because it is cheaper to outsource transport due to unevenly distributed delivery trips on weekdays.

A detailed analysis in the form of a BMC for the wholesaler can be found in Appendix D.1. We have not created a BMC for the other stakeholders as it does not provide relevant additional information.

Pharmacies Nine surrounding clinics' pharmacies are supplied cyclically once or twice a week by the wholesaler (e.g., every Tuesday and Friday) (Rave et al. 2023a). Additionally, there are three ambulance depots' pharmacies whose stock is replenished irregularly.

Ambulances Eleven ambulances (nine cars, one boat, and one helicopter) belong to the ambulance depots served by the wholesaler, except the helicopter that launches directly at the wholesaler's location. The ambulances do not belong to clinics but to support organizations, e.g., the fire department or the Bavarian Red Cross. In case of emergency, an ambulance is launched from its depot located in the city center and travels to the incident scene. If necessary, initial care is provided at the destination of incidence for which medical equipment is required. Drone delivery may now occur when urgently needed medical goods are not sufficiently in stock in the ambulance. After the patient's care, the ambulance then transports the patient to a hospital if necessary, hands the patient off to hospital staff, and then returns to its base station. However, it may be that no transport is required. In this case, the ambulance returns directly to its base station, ready for the next call (Henderson and Mason 2004). At the base station inventory of the ambulance is replenished.

Truck service provider The truck service provider takes over standard and emergency delivery to pharmacies. There is a heterogeneous fleet of vehicles with different capacities for these transports. Smaller transport vehicles or even passenger cars can be chosen for emergency deliveries, while larger transport vehicles are used for standard medication delivery that includes many drugs. We assume that for emergency delivery, electric-powered vehicles are chosen.

A key advantage of the truck service provider is that medicines can be transported reliably and cost-effectively, as there are demand peaks in deliveries. Therefore, an extensive fleet of vehicles is required, including personnel provided for this purpose. However, the truck service provider must travel to the wholesaler before a transport is carried out. Consequently, there is a delay in delivery time.

4.4.2 Uniform - social business network

The stakeholders introduced are commercially connected, and some compete with each other. Figure 4.2 presents these connections and competitions in the form of a social business network before (blue lines) and after integrating drone delivery (blue and red lines). Bold arcs represent a stronger connection or competition.

Business connection The wholesaler is commercially connected to all stakeholders introduced. The business connection with ambulances is weaker than pharmacies because drone delivery is just an additional service option for them. The wholesaler commissions the truck service provider. Thus, the truck service provider has no direct connection to pharmacies.

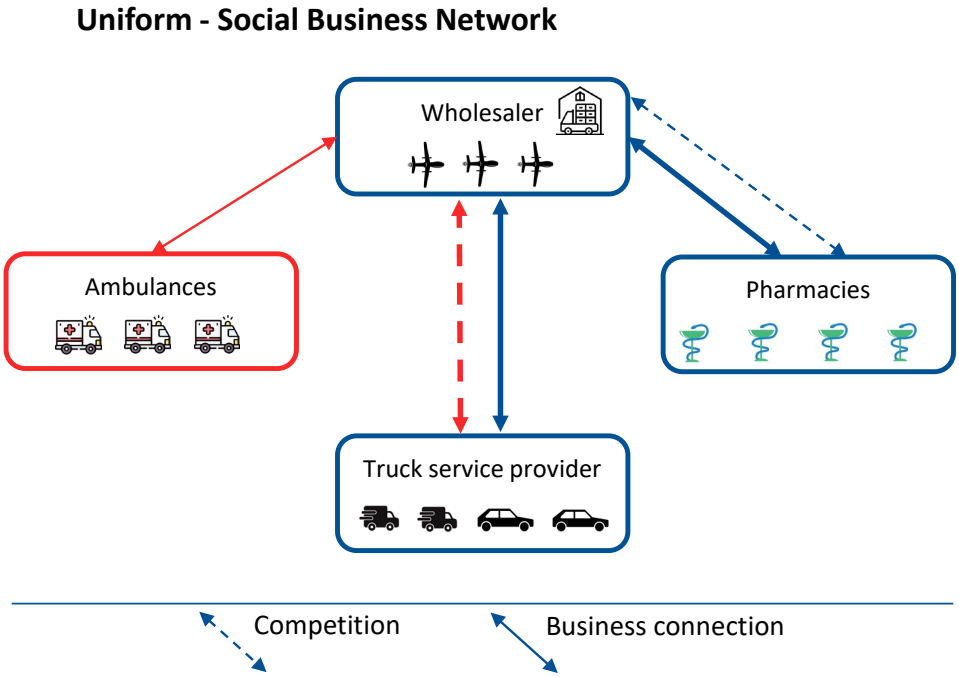

Figure 4.2: Social Business Network. Bold arcs represent a stronger connection or competition. Blue lines indicate the network before integrating drones, and both blue and red lines the network after integrating drones.

Competition The competition between the wholesaler and the truck service provider arises after integrating drones as each emergency delivery performed by the drone is one less transport performed by the truck service provider. It follows that the utilization of the truck service provider gets lower when integrating drone delivery. This lower utilization may in turn lead to an adjustment of delivery prices by the truck service provider. We analyze this possible adjustment in a sensitivity analysis in Section 4.5.3.3.

In our case, the wholesaler and the clinics' pharmacies are competitors, as the wholesaler itself is a clinic. Therefore, a patient treated at one clinic results in lost revenue at another clinic. Although clinics maximize profits arising from patients' treatments, patient care is a top priority. In addition, a fundamental overload of clinics and ambulances in Germany ensures that competition is far less prominent than in other industries. As a result, competition is weak.

To sum up, integrating drones leads to additional business connections with ambulances, but also new competition arises between the wholesaler and the truck service provider.

4.4.3 Evaluate – definition of KPIs and analysis of relevant properties

This section gives detailed information on the cost and CO_2 eq. structure, present the chosen economic, ecological, and service-oriented KPIs, and provides further details on the road- and aerial-based transport properties, the order arrivals of medication, flight bans, and delivery times.

Cost structure Drones, batteries, and boxes have high fixed costs, but only low variable costs arise per traveled km, as the drone flies autonomously (e.g., Rave et al. 2023b). On the other

hand, road-based delivery only leads to high costs per taken-over delivery since an external service provider is commissioned for delivery. The road-based delivery costs depend on the travel distance, but there is also a fixed component per delivery.

The dedicated drone is the Trinity F90+ (Quantum Systems 2023), a vertical takeoff and landing tilt-rotor drone that can fly silently. This medium-sized drone perfectly fits the purpose of drug delivery, as it can transport drugs quickly, efficiently, safely (Darvishpoor et al. 2020), and autonomously while being out of humans' sight. In addition, a transport box with a cooling function has been developed that only fits this drone. The relatively low transport capacity of the drone does not pose a problem due to the volume of demand in emergency deliveries (Quantum Systems 2020). This drone costs without battery and transport boxes 14,760€ to purchase and is expected to be used for 500 complete emergency transports or up to three years. Both transport boxes cost 500€ to purchase, but the normal transport box can be used for 500 deliveries or three years, and the box with cooling function only for 100 deliveries or 1.5 years. A battery costs 640€ and can be used for 1.5 years, or 150 charging cycles, which means it can be loaded 150 times. In addition, insurance costs per year are approximated at 5% of the purchase price of the drone. Per minute traveled, the drone incurs electricity costs of 0.0045€ if loaded (outbound flight) and 0.0044€ if unloaded (return flight). A detailed calculation of variable costs can be found in Appendix D.2. To generalize the findings, i.e., if a different drone is chosen, we vary the drone's costs in Section 4.5.3.3.

CO_2 equivalents The drone is made of different materials, which causes CO_2 eq. during their production and processing, resulting in 14.49kg for a drone (without battery and box), 2.70kg for each battery, 0.033kg for each standard transport box, and 0.165kg of CO_2 eq. for a transport box with cooling function. More detailed information and the derivation on the CO_2 eq. in drone production can be found in Appendix D.3. Each flight results in no CO_2 eq. since the clinics receive only green electricity. This contrasts with road transport, which causes 0.136kg/km (Arar 2010). Due to the low transport load of one medication package in emergency transport, no distinction is made between outbound and return flights. From these data, it follows that drones are already profitable from an ecological point of view after only a few tours.

KPIs We compare the following KPIs when introducing drones to the supply chain:

1. Cost savings of pharmacy supply compared to the status quo:
   $\Delta^{cost} = 1 - \frac{\check{C}^{fix}_{drone} + \check{C}^{var}_{drone} + \check{C}_{truck}}{C_{truck}}$

2. CO_2 eq. savings compared to the status quo:
   $\Delta^{CO2} = 1 - \frac{\check{E}^{fix}_{drone} + \check{E}_{truck}}{E_{truck}}$

3. Share of performed pharmacy supply by drones (supply rate via drones):
   $\alpha^{ph.} = \frac{\hat{Q}^{ph.}}{Q^{ph.}}$

4. Share of supplied ambulances (service level):
   $\alpha^{amb.} = \frac{\hat{Q}^{amb.}}{Q^{amb.}}$

For the computation of Δ^{cost}, we consider both fixed ($\check{C}^{fix}_{drone}$) and variable ($\check{C}^{var}_{drone}$) costs for drones but for truck delivery only costs that arise per delivery ($\check{C}_{truck}$). For the computation of Δ^{CO2}, we take CO_2 eq. during manufacture for drone hardware ($\check{E}^{fix}_{drone}$) and emissions per traveled km of the road-based transport ($\check{E}_{truck}$) into account. C_{truck} (E_{truck}) are the costs (CO_2 eq.) for truck delivery for the status quo, i.e., all pharmacy supply is carried out by truck. $Q^{ph.}$ and $Q^{amb.}$ quantify the total number of orders for emergency resupply by pharmacies and ambulances, respectively, that can be performed by drones if the external flight conditions fit for drone delivery. $\hat{Q}^{ph.}$ and $\hat{Q}^{amb.}$ define the deliveries actually performed by drones for emergency resupply to pharmacies or ambulances, respectively.

For the status quo (no drones), it holds $\Delta^{cost} = \Delta^{CO2} = \alpha^{ph.} = \alpha^{amb.} = 0$. On the contrary, if there is an unlimited number of drones, then $\alpha^{ph.} = \alpha^{amb.} = 1$. Depending on fixed costs and CO_2 eq. of drones, Δ^{cost} and Δ^{CO2} might be negative, which means there is an increase in costs or CO_2 eq., respectively, when using drones. Note that the closer the values of the KPIs are to 1, the higher are the savings (Δ^{cost} and Δ^{CO2}), the supply rate ($\alpha^{ph.}$), and the service level ($\alpha^{amb.}$).

Within the network, all participating pharmacies and ambulances are interested in being supplied with drones whenever suitable, i.e., prefer a higher supply rate or service level because of the drones' significant travel time savings. This, however, leads to a conflict between these KPIs in purchasing drones, batteries, and transport boxes. On the one hand, an increased number of drones, batteries, or transport boxes can reduce the number of rejections for drone supply, as a drone is on the air for up to multiple hours for just one delivery. On the other hand, the more drones, batteries, and transport boxes are in the system, the higher the costs and CO_2 eq. So, with an increasing drone fleet, the supply rate and the service level rise monotonously, but the savings only to a certain extent and then decrease. In particular, the cost savings are much more likely to fall due to the data on costs and CO_2 eq. It follows that in the simulation optimization, we either maximize Δ^{cost} or Δ^{CO2} subject to $\alpha^{ph.} > a^{ph.}$ and $\alpha^{amb.} > a^{amb.}$, where $a^{ph.}$ is the target supply rate and $a^{amb.}$ the target service level, e.g., $a^{ph.} = a^{amb.} = 90\%$.

Order arrivals There are, on average, 250 emergency orders from surrounding clinics, 15 from ambulance depots, and 100 from ambulances per year. We model the arrivals via a schedule such that the arrival rate, i.e., the probability of order arrivals at each time unit, changes with intervals of 15 minutes.

Order arrivals of surrounding clinics Orders from pharmacies of surrounding clinics are subject to a daily and weekly season. Figure 4.3 shows the probability of an order arrival for one surrounding clinic that is supplied regularly on Tuesday and Friday. The probability that an order will arrive is largest in the early afternoon (daily season). Emergency orders also include unpacked or unordered but still required medications directly after a standard supply took place. As a result, emergency deliveries are usually made a few hours after the standard delivery, which is in the afternoon. Vice versa, an emergency delivery does typically not arise close (24 hours) before a standard delivery as this needed medication - except in case of severe emergency - is transported in this standard delivery. This is considered by a 25% reduced probability of order arrivals. Additionally, a weekly

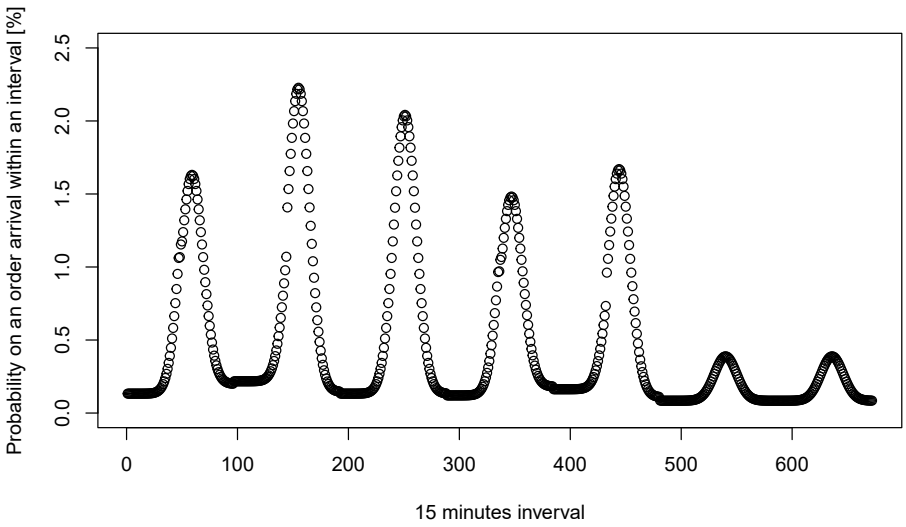

Figure 4.3: Probability of an order arrival for one surrounding clinic within a week, Monday to Sunday, that is supplied regularly on Tuesday and Friday.

season arises due to the fluctuation of bed occupancy in clinics. In Germany, patients typically go to the hospital at the beginning of a week and leave before the weekend (Rave et al. 2023a). We consider this by multiplying the probability by seasonal factors for the week (Monday: 1.1, Tuesday: 1.2, Wednesday: 1.1, Thursday: 1.0, Friday: 0.9, Saturday: 0.7, Sunday: 0.7). Additionally, clinics place orders during weekends on vary rare occasions as their pharmacy is sparsely staffed, i.e., during weekends the probability of an order arrival is just 25% compared to weekdays.

Order arrivals of ambulance depots Unlike clinics, ambulance depots are not served in a cyclic repeating standard delivery but are only served with medication via standard delivery as needed. In addition, we assume there is no weekly season but still a daily season with a higher probability (15 minutes interval) for an order arrival in the early afternoon.

Order arrivals of ambulances The probability of emergency calls is normally distributed throughout the day, with the peak in the early afternoon. Thus, there is a daily season for the order arrivals of ambulances. Again, there is no weekly season (Henderson and Mason 2004).

Weather and daylight dependent flight bans Drone delivery is not permitted if the weather is too bad, i.e., precipitation or wind with maximum speeds of more than 9 m/s. We differentiate here between "sunny days" (53.93% of all days), where the drone can fly the whole day, "rainy days" (29.23% of all days), where the drone cannot fly the whole day, and "changeable days" (16.84% of all days), where the drone cannot fly in certain areas of the operation to a 50% chance. In case of changeable days, the flight ban for each destination changes continuously. The probability values are based on analyzing weather data in Bavaria for four years. No significant change within the year can be observed (Bayerisches Landesamt für Umwelt 2022). Thus, the same probabilities are assumed on each day.

Drone delivery is not permitted during the night. The drone can launch earliest after dawn and must arrive latest before dusk. As daylight varies significantly within the year, we consider a yearly season for daylight. The time change is neglected.

Transport boxes The payload of the transport box without cooling function is assumed to be sufficiently large so that emergency deliveries always fit, as in emergency deliveries, only single pills and not complete packages are transported (Rave et al. 2023a). On the other hand, the transport box with the cooling function does not always fit the total requested demand as there is little space left due to the cooling function. We assume that 20% exceeds the payload of the transport box with cooling function and 30% need to be transported with cooling function.

Delivery time The considered drones travel at a speed of $17 m/s$ for up to 90 minutes per battery load in an Euclidean path that we correct by a detour factor as drones have to avoid certain obstacles, e.g., settlements. The pharmacies have a (corrected) distance from 3 to 90 km to the wholesaler. The battery load time lasts up to one hour, depending on the discharge state. Before the drone returns, the battery needs a load of at least 65%. Thus, there are four clinics where the battery must either be loaded or swapped with a loaded battery. We assume that a drone is used for deliveries if it can be launched within 30 minutes for the supply of pharmacies or three minutes for the supply of ambulances.

		Road-based transport		Aerial-based transport		
Travel destination	Average number of emergency orders [*year*]	Variable costs [€]	CO_2 eq. [*kg*]	Variable costs [€]	Delivery time* [*min.*]	Time savings ** [%]
Pharmacy (C)-1	43	86.30	13.69	0.42	40.3	48
Pharmacy (C)-2	21	53.00	6.67	0.19	28.9	51
Pharmacy (C)-3	25	48.00	4.05	0.11	22.6	60
Pharmacy (C)-4	21	74.90	9.64	0.29	34.2	53
Pharmacy (C)-5	48	53.00	5.86	0.17	26.7	55
Pharmacy (C)-6	2	29.50	1.76	0.03	14.3	68
Pharmacy (C)-7	33	142.20	25.97	0.82	98.4	12
Pharmacy (C)-8	12	83.30	13.74	0.42	45.3	41
Pharmacy (C)-9	46	110.20	23.95	0.75	78.3	16
Pharmacy (AD)-1	5	29.50	1.76	0.03	13.9	68
Pharmacy (AD)-2	5	27.30	1.54	0.03	13.1	69
Pharmacy (AD)-3	5	51.50	6.62	0.19	31.6	46
Ambulances	100	-	-	0.04 - 0.13	10 - 30	-

Table 4.2: Detailed information on demand, variable costs, CO_2 eq., and delivery times for each clinic's pharmacy supply (C), ambulance depot's pharmacy supply (AD), and ambulance supply.
* Including drone preparation time , ** total time savings for drone delivery compared to road-based transport.

Compared to road-based delivery, the drone has two advantages in delivery time: First, it is already on site and only needs to be set up (approximately 10 minutes). Transport via delivery truck requires the supplier to arrive first (about 20 - 30 minutes). Second, the drone flies independently of roads and traffic. On the contrary, a drone might have a lower speed than a delivery truck traveling

on a highway.

Table 4.2 shows for clinic supply (C), ambulance depot supply (AD), and ambulance supply the demand, the costs for serving, delivery times, and CO_2 eq. for the road- and aerial-based transport in detail. For ambulances, there is a range, as the travel destination varies. The average time savings in clinic deliveries demonstrate the advantage of the drone in terms of time. These refer to non-rush-hour times for road-based transport, so the time savings could even be much greater due to the drone's independence from traffic.

4.4.4 Solve - analysis of the supply chains

In this section, we describe the emergency supply chain that starts with order placement and ends with the release of drones, transport boxes, and batteries for the supply of pharmacies (Section 4.4.4.1) and ambulances (Section 4.4.4.2). The supply chains describe the emergency delivery process after integrating drones. We simulate these supply chains for one week, starting on Monday and ending on Sunday.

The times of dusk and dawn are determined once per week, as sunrise and sunset times only differ slightly within a week. At the beginning of each day, it is determined if drone delivery is permitted in the next 24 hours always ("sunny day"), never ("rainy day"), or with a chance of 50% ("changeable day"). If the drone needs to return from a pharmacy, but the flight is restricted due to weather and daylight-dependent flight bans, it is checked once per hour to see if the flight conditions fit for drone flights.

4.4.4.1 Supply of pharmacies

From the wholesaler's perspective, the complete emergency supply chain for one pharmacy is modeled in Figure 4.4. This model is repeated for each pharmacy served with the same resource pools to represent the resupply of all pharmacies. It starts with an order of a drug and ends either with the release of the used battery when a drone has been sent or with the dispatching of a road-based transport. The colored background indicates where the process takes place.

After a drug is ordered, it is checked whether there is a drone, a transport box that fits the medicine, and a battery available within a certain time limit. Whenever a standard box is suitable for the medicine, this box is used first. Otherwise, the box with the cooling function is used. Moreover, it is checked if the weather and the remaining time till dusk fit. Otherwise, the medicine is transported via road-based transport.

If a drone carries out the delivery, the drone delivers the medicine to the pharmacy. In the next step, it is checked if the battery has sufficient rest capacity for the return flight. If the capacity is insufficient, the battery is either loaded or swapped depending on whether the pharmacy is equipped with a spare battery. If the battery is loaded, this results in a longer presence time at that pharmacy. Then, it is checked if weather and daylight enable drone flights, else the drone waits until the weather brightens up or until dawn before the drone returns to the wholesaler. Arriving at the wholesaler, the drone and the transport box are released directly, and the battery after it is fully loaded.

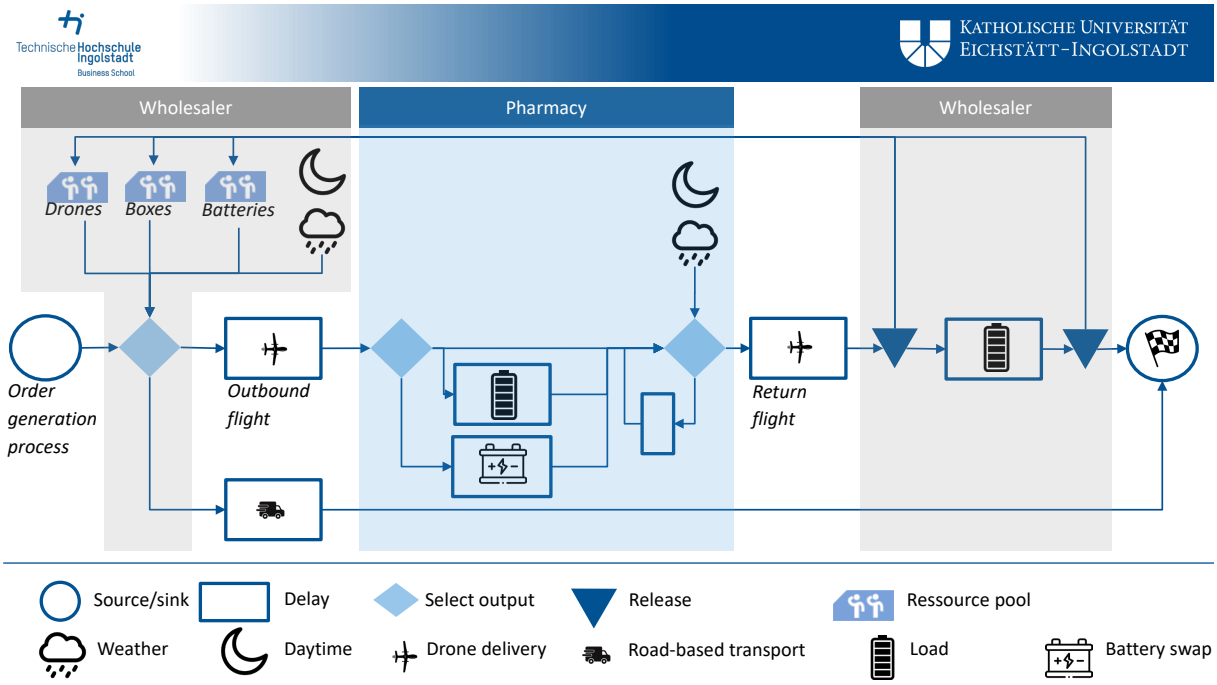

Figure 4.4: Detailed representation of the supply chain of emergency deliveries to pharmacies.

4.4.4.2 Supply of ambulances

The supply chain for ambulance resupply is modeled in Figure 4.5. This supply is similar to that of pharmacies with the following simplifications: First, there is neither battery swapping nor loading at the ambulance since ambulances are always in range for a complete outbound and return flight. Second, there is no alternative road-based delivery process. If the drone cannot transport the medication, clinic, which once and must fit for both the outbound and return flights.

Technische Hochschule Ingolstadt
Business School
Katholische Universität Eichstätt-Ingolstadt

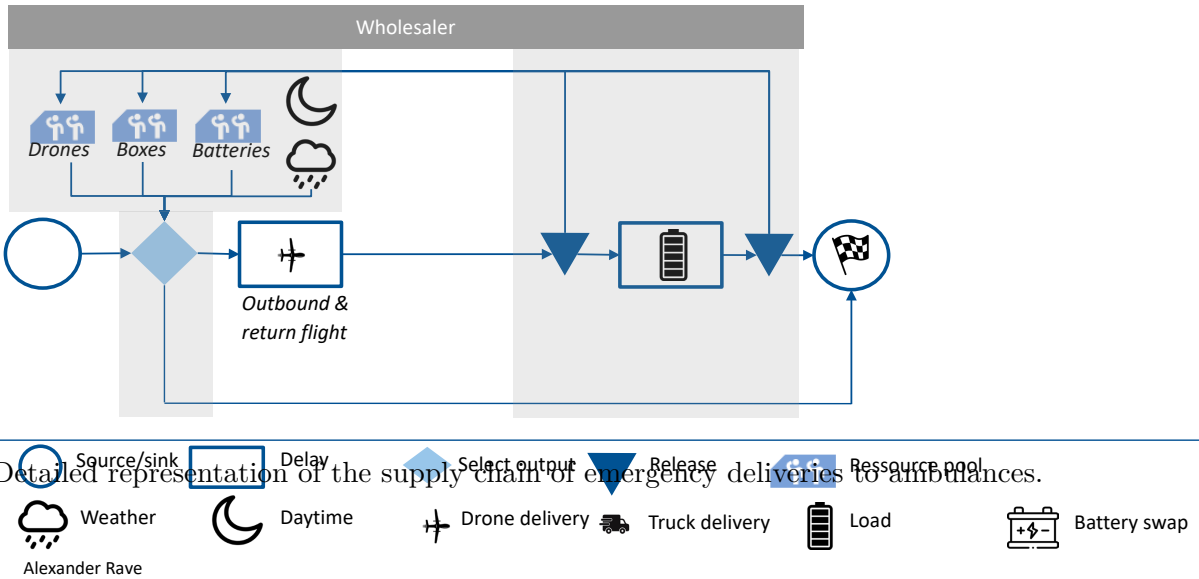

Figure 4.5: Detailed representation of the supply chain of emergency deliveries to ambulances.

4.5 Test – verification and analysis of results

In this section, we present the results of our case study, i.e., the pharmacy of a large German hospital serves both pharmacies and ambulances. The simulation is implemented in AnyLogic version 8.8.1, and one week and 520 replications are analyzed. According to a sequential test, the number of replications is sufficient as a maximum desired deviation of 5% for all KPIs is not exceeded for a confidence interval of 95%. Due to the problem setting (night flight ban, low demand at night, low demand on weekends, low variable costs per flight), the simulation has no warm-up phase. Only on very rare occasions a drone would not be located at the wholesaler on Monday mornings.

In Section 4.5.1, we present the results of the case study. In Section 4.5.2, we test the impact of certain assumptions on the drone fleet and the KPIs. Last, we generalize our findings in Section 4.5.3.

4.5.1 Case results

In the following, we present the cost- and CO_2 eq.-optimal drone fleet and spare battery locations to guarantee a supply rate and service level of 90%. For further analysis, we demonstrate the impact of different drone fleets on the defined KPIs. Table 4.3 presents these results. The first column shows the number of drones, batteries, standard boxes, and boxes with cooling function in the complete supply chain. The drone fleets that are found in the simulation optimization process are gray-shaded. The last four columns show the expected values for the economic, ecologic, supply rate, and service level related KPIs.

The table only reports reasonable combinations since the drone fleet has various design options. In particular, the following holds: There is at least the same number of batteries and total transport boxes as there are drones. Transport boxes with cooling functions fit more medicine on average, and thus, there is at least the same number compared to standard transport boxes. If surrounding pharmacies are equipped with a spare battery, all four surrounding pharmacies that are too far away for a direct return flight have a spare battery each (noted with $*/4$ in the table). We start with the most simple reasonable system of one drone, one battery, one standard transport box, and one transport box with a cooling function, and we stop at three drones, as a supply rate and service level of nearly 100% are reached. Additional hardware would, therefore, only have a negative impact on the economic and ecological KPIs without increasing the supply rate or service level.

Findings The cost-optimal drone fleet that guarantees a supply rate and service level of at least 90% is $(1, 2, 1, 1)$. This drone fleet reduces total delivery costs by 19.6%. On the contrary, significantly more drones, batteries, and boxes are required with $(3, 4, 2, 2)$ for the CO_2 eq.-optimal drone fleet. This fleet reduces total CO_2 eq. for delivery by 48.9% which is only slightly larger than a fleet of $(1, 2, 1, 1)$ has. A supply rate and service level of nearly or even 100% are achieved with a fleet $(3, 4, 2, 2)$ or $(3, 4/4, 2, 2)$, respectively. If the wholesaler targets a higher supply rate and service level of 95%, a drone fleet of at least $(2, 2, 1, 1)$ needs to be chosen, resulting in a significant reduction and nearly elimination of all cost benefits.

We find that the major decision for the drone fleet is the number of drones, as this decision varies,

Drone fleet	KPIs			
(#Drones, #Batteries, #Std. Boxes, #Cool Boxes)	Δ^{cost} [%]	Δ^{CO2} [%]	$\alpha^{ph.}$ [%]	$\alpha^{amb.}$ [%]
$(1, 1, 1, 1)$	18.4	44.7	89.2	87.5
$(1, 2, 1, 1)$	**19.6**	46.6	92.8	91.4
$(1, 2/4, 1, 1)$	10.9	46.6	94.5	91.2
$(2, 2, 1, 1)$	1.9	47.8	97.6	97.6
$(2, 3, 1, 1)$	-0.4	47.8	97.8	98.0
$(2, 3, 1, 2)$	-0.8	48.6	99.1	98.3
$(2, 3/4, 1, 1)$	-8.4	47.8	98.1	97.7
$(3, 4, 1, 2)$	-22.0	48.2	99.1	98.5
$(3, 4, 2, 2)$	-21.3	**48.9**	**99.9**	99.8
$(3, 4/4, 1, 2)$	-30.1	48.1	99.4	98.5
$(3, 4/4, 2, 2)$	-29.9	48.8	99.8	**100.0**

Table 4.3: KPIs for different drone fleets. The found fleets in simulation optimization are gray shaded and the best values for KPIs are in bold. Note that a negative value for Δ^{cost} means that there is an increase in costs.
$*/4$ One battery is located at four surrounding pharmacies each.

e.g., the cost savings, by nearly 20 percentage points per drone. However, the aligned decision on the number of boxes and batteries and the location of batteries might also have a significant impact. So, for example, cost savings might decrease by up to eight percentage points if spare batteries are added at surrounding clinics.

In Table 4.3, expected values for the KPIs are reported. The variance, on the other hand, increases for Δ^{cost} and Δ^{CO2} or decreases for $\alpha^{ph.}$ and $\alpha^{amb.}$, when drones, batteries, or boxes are added to the system. So, the variance for Δ^{cost} by a factor of up to 5.2 comparing $(1, 1, 1, 1)$ to $(3, 4/4, 2, 2)$ because the number of emergency deliveries per week and the number of deliveries taken over by drone vary significantly in each replication, but the fixed costs stay the same. Thus, a fleet of $(1, 2, 1, 1)$ is, on average, more cost-efficient than $(1, 1, 1, 1)$ but at higher risks. Contrarily, the variance for both the supply rate and the service level is reduced by nearly 100% when considering more extensive fleets.

If we consider the most economic fleet of $(1, 2, 1, 1)$ in more detail, drones lead to a cost reduction of emergency deliveries to pharmacies of 4,063 € annually. Then, a supply of ambulances costs 42.70 € per trip on average. In total, CO_2 eq. can be reduced by 1.668t per year.

4.5.2 Impact of assumptions

In this section, we test the impact of assumptions on the drone fleet and the KPIs.

4.5.2.1 Comparison to simple averaging

Given the data, the average share of flight bans can be computed based on the order arrival: the drone cannot fly in 37.7% of all cases due to bad weather and in 17.7% of all cases due to the night flight ban. Considering in total 365 orders per year, the drone can perform an average of 188.7 flights, resulting in cost savings of 24.8% for a $(1, 1, 1, 1)$ fleet. These are higher than our results from the simulation since the number of drone flights is overestimated by 20.8%. This has

multiple reasons like no consideration of waiting times, which might shift a flight into a night flight ban, or no consideration of annual cycles of night flight bans. However, the main reason for this overestimation is the unknown availability of the drone. The supply rate and the service level are, therefore, difficult to estimate, resulting in an assumption to be set as 100%. This might be a reasonable assumption since, on average, less than one order is placed per day. It follows that a larger fleet only results in higher costs since the supply rate and the service level are always 100%. Using simple averaging, the waiting times of drones are neglected, so their availability is overestimated compared to real-world conditions.

4.5.2.2 Impact of external flight conditions

Ignoring weather-related and daylight-dependent flight bans for drones, then a fleet of $(2, 3, 1, 1)$ has significantly better KPI values (all KPIs) than $(1, 2, 1, 1)$, with expected cost savings of $\Delta^{cost} = 47.3\%$. As a result, a fleet of $(2, 3, 1, 1)$ is Pareto-superior to a fleet of $(1, 2, 1, 1)$, which is not the case when considering these flight bans. Thus, weather and daylight-dependent flight bans significantly influence the drone fleet and the KPIs.

4.5.2.3 Impact of seasonality

We analyze the impact of the seasonality of order arrivals (daily and weekly seasonality) and daylight-dependent flight bans (annual seasonality).

Daily/weekly seasonality When ignoring the seasonality of order arrivals, i.e., all orders arrive uniformly within the day and week, the cost-optimal drone fleet is $(1, 1, 1, 1)$ with lower cost savings of 6.1% and CO_2 eq. savings of 30.6%. Contrary, $\alpha^{ph.}$ and $\alpha^{amb.}$ increase to 95.5% and 92.7%, respectively. The orders are more likely to arrive during the night, but on the other hand, the orders arrive less aggregated within the day and week. It follows that drone delivery is more rejected due to daylight-dependent flight bans but less rejected due to unavailable hardware. Fewer drone deliveries have a negative impact on Δ^{cost} and Δ^{CO2}. But fewer rejected orders due to unavailable hardware positively impact $\alpha^{ph.}$ and $\alpha^{amb.}$. It follows that the daily and weekly seasonality of order arrivals have a large influence on the KPIs and the chosen drone fleet itself.

Annual seasonality When considering the seasonality of the daylight-dependent flight bans, i.e., dusk and dawn arise at different times within a year, drone utilization in summer is higher than in winter. For a fleet of $(1, 2, 1, 1)$, this results in 15% more rejected drone deliveries in summer compared to winter, and, thus, the supply rate and service level in summer are lower than in winter. When ignoring this annual seasonality, the cost-optimal drone fleet stays $(1, 2, 1, 1)$ with slightly increased Δ^{cost} and Δ^{CO2} but lower supply rate and service level, as the number of orders that arrive during daylight increases by 4.2%. On the other hand, drone utilization within the year does not vary. It follows that a fleet of $(1, 1, 1, 1)$ is in greater competition in terms of costs compared to a fleet of $(1, 2, 1, 1)$. Thus, the annual seasonality of daylight-dependent flight bans has a minor influence on the KPIs and the drone fleet.

4.5.2.4 Impact of priorities

While previously, all orders are served in an FCFS rule, we now relax this assumption and prioritize orders from pharmacies according to the distance to the wholesaler. Additionally, ambulances are in the first position, as they are most urgent in supply. This distance-based prioritization is chosen as it might increase cost savings as far-located pharmacies are costlier to be served by road-based transport.

Considering a $(1, 2, 1, 1)$ fleet, we find that this prioritization, however, does not lead to any change in values for the KPIs. This can be explained by the rare occasion of orders of, on average, about seven per week and the maximum time (30 minutes for pharmacy supply, three minutes for ambulances) until a drone has to launch. It follows that prioritizing certain pharmacies does not impact the drone fleet and the KPIs.

4.5.3 Generalization of findings

In this section, we give managerial insights on the drone fleet when varying the network structure, number of orders and drone properties, and cost structure.

4.5.3.1 Varying network structure

We present the cost-optimal drone network (Table 4.4) without any service level and supply rate constraints, and the cost-optimal drone network that guarantees a supply rate and service level of at least 95% (Table 4.5) when varying the network structure, i.e., the average traveled distance to a pharmacy is reduced or increased. The distance of ambulances is not varied. While the traveled distances and thus also the variable costs for drone flights are reduced linearly, the costs for road-based transport are only partly reduced, as the price of each road-based transport has a fixed term. Considering large distances, we assume in this analysis that all pharmacies are still within range of the drone.

Average distance	Cost-optimal drone fleet	KPIs			
		Δ^{cost} [%]	Δ^{CO2} [%]	$\alpha^{ph.}$ [%]	$\alpha^{amb.}$ [%]
9.5	$(1, 1, 1, 1)$	-19.6	46.7	97.7	92.4
19.0	$(1, 1, 1, 1)$	4.1	47.5	94.3	91.2
28.6	$(1, 2, 1, 1)$	13.9	46.8	94.1	91.4
38.1 (basic scenario)	$(1, 2, 1, 1)$	19.6	46.6	92.8	91.4
57.1	$(1, 2, 1, 1)$	25.0	44.8	89.0	87.5
76.2	$(1, 2, 1, 1)$	27.7	44.0	85.3	87.8

Table 4.4: Cost-optimal drone fleets and KPIs for different distances. Note that the average distance of 38.1 is as in the case study.

Findings Table 4.4 shows that integrating drones becomes more profitable with increasing distance to pharmacies, but CO_2 eq. savings, the supply rate, and the service level decrease as drones are not available for longer times. To counteract this, one battery is added to the drone fleet. It follows that cost savings of up to 27.7% can be achieved with the largest average distance to travel. On

the contrary, if the average distance to travel is too low, any drone fleet is not profitable. In this case, drones take over most deliveries with even the smallest reasonable drone fleet, but the low costs of road-based transport only offset their fixed costs.

When providing a supply rate and service level of at least 95% (Table 4.5), a second drone and, for the largest distance, a second transport box with a cooling function must be deployed. It follows that the cost savings are significantly lower and not even profitable when the average distance to travel is 28.6km or less. For larger distances, the utilization of the second drone rises, and thus, the cost savings are not reduced that strongly. Additionally, the CO_2 eq. savings are higher if a supply rate and a service level of 95% is targeted than if the cost-optimal drone fleet is chosen.

Average distance	Cost-optimal drone fleet with $\alpha^{ph.}, \alpha^{amb.} \geq 95\%$	KPIs			
		Δ^{cost} [%]	Δ^{CO2} [%]	$\alpha^{ph.}$ [%]	$\alpha^{amb.}$ [%]
9.5	$(2, 2, 1, 1)$	-70.7	46.7	99.3	99.6
19.0	$(2, 2, 1, 1)$	-27.5	48.8	98.3	98.3
28.6	$(2, 2, 1, 1)$	-9.7	47.0	97.5	97.4
38.1 (basic scenario)	$(2, 2, 1, 1)$	1.9	47.8	97.6	97.6
57.1	$(2, 2, 1, 1)$	14.6	47.8	96.8	96.6
76.2	$(2, 2, 1, 2)$	21.3	48.4	96.3	95.9

Table 4.5: Cost-optimal drone fleets that provide a supply rate and a service level of at least 95% and KPIs for different distances. Note that the average distance of 38.1 is as in the case study.

4.5.3.2 Increased number of orders and improved drone properties

We analyze how the drone fleet varies when the number of emergency orders increases and drone properties are improved. The number of emergency orders from pharmacies and ambulances is expected to increase. For example, Rave et al. (2023a) have shown that hospitals can achieve substantial cost savings by reducing inventory if, instead, the number of emergency deliveries increases. Additionally, drones may become more and more weather-resistant, reliable, and safer to fly at night. Thus, we demonstrate both the effect of increased medication orders for both pharmacies and ambulances and improved drone parameters. We compare the following four scenarios:

Scenario 1: Total order arrivals are (uniformly) increased by 100% to 530 deliveries per year and of ambulances to 200 per year on average. Drone parameters remain unchanged.

Scenario 2: Total order arrivals of pharmacies are (uniformly) increased by 200% to 795 deliveries per year and of ambulances to 300 per year on average. Drone parameters remain unchanged.

Scenario 3: Order arrivals as in Scenario 2, but drones are 50% more weather resistant, i.e., there are 50% fewer weather-related delivery losses and can fly during dusk and dawn.

Scenario 4 Order arrivals as in Scenario 2, but drone flights are independent of the weather and are able to fly during the night.

Table 4.6 shows the cost-optimal drone fleet for the basic scenario as in the case study and for Scenarios 1-4. Moreover, the expression of each of the four KPIs is reported.

Scenario	Drone fleet	KPIs			
		Δ^{cost} [%]	Δ^{CO2} [%]	$\alpha^{ph.}$ [%]	$\alpha^{amb.}$ [%]
Basic scenario	$(1, 2, 1, 1)$	19.6	46.6	92.8	91.4
Scenario 1	$(2, 3, 1, 1)$	21.8	48.0	95.4	95.2
Scenario 2	$(3, 4, 2, 2)$	22.8	50.3	99.3	98.9
Scenario 3	$(3, 4, 2, 2)$	37.2	73.8	99.2	99.0
Scenario 4	$(3, 4/4, 2, 2)$	51.7	98.8	99.5	99.5

Table 4.6: Cost-optimal drone fleet and KPIs for the considered scenarios. The basic scenario is as in the case study.
$*/4$ One battery is located at four surrounding pharmacies each.

Findings With increased demand and improved drone properties, the cost-optimal numbers of drones, batteries, and boxes increase. Especially, storing spare batteries at surrounding clinics is profitable from an economic point of view from Scenario 4 on, from a service-oriented point of view, always anyway. In Scenario 1 and Scenario 2, the cost savings that can be achieved are slightly higher compared to the basic scenario because about half of all trips are still inefficient road-based transports. In contrast, Δ^{cost} increases significantly by up to 32.1 percentage points if drones become more weather-resistant. The same applies to CO_2 eq. savings of nearly 100% in Scenario 4. Thus, to reduce emergency delivery costs, drone properties should be improved rather than convincing clinics (e.g., by using pooling effects) to order more frequently, provided that there is a certain basic demand for emergency delivery.

4.5.3.3 Variation of cost structure

As in Section 4.4.2 analyzed, the wholesaler competes with the truck service provider by building up its own drone fleet. This competition could make cooperation more difficult. As a result, there are two possible scenarios: On the one hand, lower utilization of the truck service provider's fleet could lead to a price increase per trip. On the other hand, competition between the wholesaler and the truck service provider leads to a decrease in the price per road-based transport. On the contrary, fixed costs for drones might sink as well if a more affordable drone is chosen.

To analyze the variation of costs on the drone fleet, the costs of road-based transport are multiplied by the cost factor δ. The costs are affected linearly, including the case if drone costs vary. The cost structure does not have an influence on the supply chain, but only the resulting KPI for cost savings, so the supply rate, the service level, and the CO_2 eq. savings do not vary and are the same as in Table 4.3. We can observe that drones are cost-efficient if $\delta > 0.54$ with $(1, 2, 1, 1)$, i.e., drones are cost-efficient, as long as the truck service provider does not nearly halve their prices. The drone fleet $(1, 2, 1, 1)$ is the cost-optimal drone fleet as long as $\delta < 9.43$, switching to $(2, 3, 1, 2)$. If $\delta < 0.39$, $(1, 1, 1, 1)$ would be the cost-optimal drone fleet. In this case, however, drones are costlier than road-based transport.

4.6 Conclusion

This paper considers the drone fleet planning and spare battery allocation for emergency supply of pharmacies and ambulances at service with medication. We use the GUEST framework by Perboli and Rosano (2019) and give detailed insights on relevant stakeholders within the considered supply chain and their business connection to each other. We implement a discrete-event simulation study and evaluate different fleets with conflicting economic, ecological, and service-oriented KPIs. In a simulation optimization, we determine the cost-optimal fleet that guarantees a certain supply rate and service level. Last, we test assumptions and give multiple managerial insights for a real-life case study. We find that the assumptions of seasonality and flight bans significantly impact the fleet and the KPIs.

In the case study, we show that the drone fleet of one drone and two batteries can lead to cost savings of 19.6% compared to the status quo with a supply rate and service level of at least 90%. Contrary, if a supply rate and service level of at least 95% is targeted, nearly all cost benefits vanish. In a sensitivity analysis, we show that drone delivery becomes more cost-efficient if pharmacies are far located. Moreover, considering an increase in orders and drone parameters, cost savings of up to 51.7% and emissions savings of as much as 98.8% can be achieved while maintaining a supply rate for pharmacies and a service level for ambulances of more than 99%. Placing spare batteries at surrounding clinics is only relevant from an economic point of view if both demand increases and the drones become more resistant regarding weather and daylight-dependent flight bans.

Further research could examine the additional positioning of drones at some pharmacies to allow pharmacies to supply each other, which increases the speed of resupply and, thus, the patients' service. However, this requires the simultaneous consideration of inventories of medication, as these are not always sufficiently available at surrounding small pharmacies. In addition, inventory optimization of ambulances could also be considered, as they always have access to a complete pharmacy due to the high service level provided by drone deliveries.

Acknowledgments

The authors gratefully acknowledge the scientific and financial support of the Federal Ministry for Digital and Transport, Germany, for the research project MEDinTime reported in this paper. We also gratefully thank Harry Wagner from Technical University Ingolstadt of Applied Sciences for the scientific support.

Literaturverzeichnis

Accorsi, L., Vigo, D., 2020. A hybrid metaheuristic for single truck and trailer routing problems. Transportation Science 54 (5), 1351–1371.

Agatz, N., Bouman, P., Schmidt, M., 2018. Optimization approaches for the traveling salesman problem with drone. Transportation Science 52 (4), 965–981.

Aksen, D., Kaya, O., Sibel Salman, F., Özge Tüncel, 2014. An adaptive large neighborhood search algorithm for a selective and periodic inventory routing problem. European Journal of Operational Research 239 (2), 413–426.

Arar, J. I., 2010. New directions: The electric car and carbon emissions in the us. Atmospheric Environment 44, 733–734.

Archetti, C., Bertazzi, L., Hertz, A., Speranza, M. G., 2012. A hybrid heuristic for an inventory routing problem. INFORMS Journal on Computing 24 (1), 101–116.

Archetti, C., Bertazzi, L., Laporte, G., Speranza, M. G., 2007. A branch-and-cut algorithm for a vendor-managed inventory-routing problem. Transportation Science 41 (3), 382–391.

Archetti, C., Ljubić, I., 2022. Comparison of formulations for the inventory routing problem. European Journal of Operational Research 303 (3), 997–1008.

Arslan, O., 2021. The location-or-routing problem. Transportation Research Part B: Methodological 147, 1–21.

Asadi, A., Nurre Pinkley, S., Mes, M., 2022. A markov decision process approach for managing medical drone deliveries. Expert Systems with Applications 204, 117490.

Aurambout, J.-P., Gkoumas, K., Ciuffo, B., 2019. Last mile delivery by drones: an estimation of viable market potential and access to citizens across european cities. European Transport Research Review 11, 1–21.

Bayerisches Landesamt für Umwelt, 2022. Jahresgrafik Veitshöchheim. World Wide Web, last access: November 02, 2022.
URL `https://www.gkd.bayern.de/de/meteo/niederschlag/kelheim/ingolstadt-2409/jahreswerte`

Baykasoğlu, A., Subulan, K., Taşan, A. S., Dudaklı, N., 2019. A review of fleet planning problems in single and multimodal transportation systems. Transportmetrica A: Transport Science 15 (2), 631–697.

BDEW, 2022. BDEW-Strompreisanalyse Dezember 2022. World Wide Web, last access: January 25, 2023.
URL `https://www.bdew.de/service/daten-und-grafiken/bdew-strompreisanalyse/`

Bell, W. J., Dalberto, L. M., Fisher, M. L., Greenfield, A. J., Jaikumar, R., Kedia, P., Mack, R. G., Prutzman, P. J., 1983. Improving the distribution of industrial gases with an on-line computerized routing and scheduling optimizer. INFORMS Journal on Applied Analytics 13 (6), 4–23.

Bouman, P., Agatz, N., Schmidt, M., 2018. Instances for the TSP with Drone (and some solutions) (v1.2). World Wide Web, last access: February 14, 2023.
URL `https://doi.org/10.5281/zenodo.1204676`

Boutilier, J. J., Chan, T. C. Y., 2022. Drone network design for cardiac arrest response. Manufacturing & Service Operations Management 24 (5), 2407–2424.

Boysen, N., Fedtke, S., Schwerdfeger, S., 2021. Last-mile delivery concepts: a survey from an operational research perspective. OR Spectrum 43 (1), 1–58.

Boysen, N., Schwerdfeger, S., Weidinger, F., 2018. Scheduling last-mile deliveries with truck-based autonomous robots. European Journal of Operational Research 271 (3), 1085–1099.

Campbell, A., Clarke, L., Kleywegt, A., Savelsbergh, M., 1998. The inventory routing problem. In: Fleet Management and Logistics. Kluwer Academic Publishers, pp. 95–113.

Campbell, A. M., Savelsbergh, M. W. P., 2004. A decomposition approach for the inventory-routing problem. Transportation Science 38 (4), 488–502.

Campbell, A. M., Wilson, J., 2014. Forty years of periodic vehicle routing. Networks 63 (1), 2–15.

Campbell, J. F., Sweeney II, D. C., Zhang, J., 2017. Strategic design for delivery with trucks and drones. Tech. Rep. Supply Chain & Analytics Report - SCMA-2017-0201, College of Business Administration, University of Missouri – St. Louis, One University Blvd, St. Louis, MO 63121, USA, April 17, 2017.

Cao, N., Marcus, A., Altarawneh, L., Kwon, S., 2023. Priority-based replenishment policy for robotic dispensing in central fill pharmacy systems: A simulation-based study. Health Care Management Science 26, 344–362.

Caraballo, L., Díaz-Báñez, J., Maza, I., Ollero, A., 2017. The block-information-sharing strategy for task allocation: A case study for structure assembly with aerial robots. European Journal of Operational Research 260 (2), 725–738.

Cavani, S., Iori, M., Roberti, R., 2021. Exact methods for the traveling salesman problem with multiple drones. Transportation Research Part C: Emerging Technologies 130, 103280.

Çetinkaya, S., Bookbinder, J. H., 2003. Stochastic models for the dispatch of consolidated shipments. Transportation Research Part B: Methodological 37 (8), 747–768.

Chauhan, D., Unnikrishnan, A., Figliozzi, M., 2019. Maximum coverage capacitated facility location problem with range constrained drones. Transportation Research Part C: Emerging Technologies 99, 1–18.

Chen, C., Demir, E., Huang, Y., 2021. An adaptive large neighborhood search heuristic for the vehicle routing problem with time windows and delivery robots. European Journal of Operational Research 294 (3), 1164–1180.

Chu, J., Leung, K. B., Snobelen, P., Nevils, G., Drennan, I. R., Cheskes, S., Chan, T. C., 05 2021. Machine learning-based dispatch of drone-delivered defibrillators for out-of-hospital cardiac arrest. Resuscitation 162, 120–127.

Clemence, C., 2019. Leaders Emerge In The Aluminium Industry's Race To Zero Carbon. World Wide Web, last access: January 23, 2023.
URL https://aluminiuminsider.com/leaders-emerge-in-the-aluminium-industrys-race-to-zero-carbon/.

Coelho, L. C., Cordeau, J.-F., Laporte, G., 2014. Thirty years of inventory routing. Transportation Science 48 (1), 1–19.

Cui, Z., Long, D. Z., Qi, J., Zhang, L., 2023. The inventory routing problem under uncertainty. Operations Research 71 (1), 378–395.

D'Andrea, R., 2014. Guest editorial can drones deliver? IEEE Transactions on Automation Science and Engineering 11 (3), 647–648.

Darvishpoor, S., Roshanian, J., Raissi, A., Hassanalian, M., 2020. Configurations, flight mechanisms, and applications of unmanned aerial systems: A review. Progress in Aerospace Sciences 121, 100694.

Dell'Amico, M., Montemanni, R., Novellani, S., 2021a. Benchmark instances and optimal solutions for the traveling salesman problem with drone. arXiv preprint arXiv:2107.13275.

Dell'Amico, M., Montemanni, R., Novellani, S., 2021b. Drone-assisted deliveries: New formulations for the flying sidekick traveling salesman problem. Optimization Letters 15, 1617–1648.

Dhote, J., Limbourg, S., 2020. Designing unmanned aerial vehicle networks for biological material transportation – the case of brussels. Computers & Industrial Engineering 148, 106652.

El-Adle, A. M., Ghoniem, A., Haouari, M., 2021. Parcel delivery by vehicle and drone. Journal of the Operational Research Society 72 (2), 398–416.

Euchi, J., Sadok, A., 2021. Hybrid genetic-sweep algorithm to solve the vehicle routing problem with drones. Physical Communication 44, 101236.

Fehn, F., Engelhardt, R., Dandl, F., Bogenberger, K., Busch, F., 2023. Integrating parcel deliveries into a ride-pooling service — An agent-based simulation study. Transportation Research Part A: Policy and Practice 169, 103580.

Fontaine, P., Crainic, T. G., Jabali, O., Rei, W., 2021. Scheduled service network design with resource management for two-tier multimodal city logistics. European Journal of Operational Research 294 (2), 558–570.

Frank, M., Ostermeier, M., Holzapfel, A., Hübner, A., Kuhn, H., 2021. Optimizing routing and delivery patterns with multi-compartment vehicles. European Journal of Operational Research 293 (2), 495–510.

Freitas, J. C., Penna, P. H. V., Toffolo, T. A., 2023. Exact and heuristic approaches to truck–drone delivery problems. EURO Journal on Transportation and Logistics 12, 100094.

Gartner, J., 2016. JD.com's Drone Delivery Program Takes Flight in Rural China. World Wide Web, last access: May 17, 2022.
URL https://jdcorporateblog.com/jd-coms-drone-delivery-program-takes-flight-in-rural-china/.

Ha, Q. M., Deville, Y., Pham, Q. D., Hà, M. H., 2018. On the min-cost traveling salesman problem with drone. Transportation Research Part C: Emerging Technologies 86, 597–621.

Heimfarth, A., Ostermeier, M., Hübner, A., 2022. A mixed truck and robot delivery approach for the daily supply of customers. European Journal of Operational Research 303 (1), 401–421.

Hemmelmayr, V. C., Cordeau, J. F., Crainic, T. G., 2012. An adaptive large neighborhood search heuristic for two-echelon vehicle routing problems arising in city logistics. Computers & Operations Research 39 (12), 3215–3228.

Henderson, S. G., Mason, A. J., 2004. Ambulance service planning: Simulation and data visualisation. In: Brandeau, M. L., Sainfort, F., Pierskalla, W. P. (Eds.), Operations Research and Health Care: A Handbook of Methods and Applications. Springer US, Boston, MA, pp. 77–102.

Higginson, J. K., Bookbinder, J. H., 1995. Markovian decision processes in shipment consolidation. Transportation Science 29 (3), 242–255.

Jafarkhan, F., Yaghoubi, S., 2018. An efficient solution method for the flexible and robust inventory-routing of red blood cells. Computers & Industrial Engineering 117, 191–206.

Jeswani, H., Krüger, C., Russ, M., Horlacher, M., Antony, F., Hann, S., Azapagic, A., 2021. Life cycle environmental impacts of chemical recycling via pyrolysis of mixed plastic waste in comparison with mechanical recycling and energy recovery. Science of The Total Environment 769, 144483.

Joerss, M., Neuhaus, F., Schröde, J., 2016. How customer demands are reshaping last-mile delivery. The McKinsey Quarterly, 17, 1–5.

URL https://www.mckinsey.com/~/media/McKinsey/Industries/Travel%20Transport%20and%20Logistics/Our%20Insights/How%20customer%20demands%20are%20reshaping%20last%20mile%20delivery/How-customer-demands-are-reshaping-last-mile-delivery.ashx

Johansson, L., Sonntag, D. R., Marklund, J., Kiesmüller, G. P., 2020. Controlling distribution inventory systems with shipment consolidation and compound poisson demand. European Journal of Operational Research 280 (1), 90–101.

Keeney, T., 2015. Amazon drones could deliver a package in under thirty minutes for one dollar. World Wide Web, last access: August 25, 2021.
URL https://ark-invest.com/articles/analyst-research/drone-delivery-amazon/

Kim, S., Moon, I., 2019. Traveling salesman problem with a drone station. IEEE Transactions on Systems, Man, and Cybernetics: Systems 49 (1), 42–52.

Kim, S. J., Lim, G., Cho, J., Côté, M. J., 2017. Drone-aided healthcare services for patients with chronic diseases in rural areas. Journal of Intelligent & Robotic Systems 88, 163–180.

Kitjacharoenchai, P., Min, B.-C., Lee, S., 2020. Two echelon vehicle routing problem with drones in last mile delivery. International Journal of Production Economics 225, 107598.

Kitjacharoenchai, P., Ventresca, M., Moshref-Javadi, M., Lee, S., Tanchoco, J. M., Brunese, P. A., 2019. Multiple traveling salesman problem with drones: Mathematical model and heuristic approach. Computers & Industrial Engineering 129, 14–30.

Li, H., Chen, J., Wang, F., Bai, M., 2021. Ground-vehicle and unmanned-aerial-vehicle routing problems from two-echelon scheme perspective: A review. European Journal of Operational Research 294 (3), 1078–1095.

Lin, S.-W., Yu, V. F., Chou, S.-Y., 2009. Solving the truck and trailer routing problem based on a simulated annealing heuristic. Computers & Operations Research 36 (5), 1683–1692, selected papers presented at the Tenth International Symposium on Locational Decisions (ISOLDE X).

Luo, Z., Liu, Z., Shi, J., 2017. A two-echelon cooperated routing problem for a ground vehicle and its carried unmanned aerial vehicle. Sensors 17 (5).

Malicki, S., Minner, S., 2021. Cyclic inventory routing with dynamic safety stocks under recurring non-stationary interdependent demands. Computers & Operations Research 131, 105247.

McKay, M. D., Beckman, R. J., Conover, W. J., 1979. A comparison of three methods for selecting values of input variables in the analysis of output from a computer code. Technometrics 21 (2), 239–245.

Melin, H. E., 2019. Analysis of the climate impact of lithium-ion batteries and how to measure it. Circular Energy Storage-Research and Consulting, 1–17.

Mercedes-Benz AG, 2022. Technical data, weights and measures of the Sprinter Panel Van. World Wide Web, last access: December 01, 2022.
URL https://www.mercedes-benz.ie/vans/en/sprinter/panel-van/technical-data

Militão, A. M., Tirachini, A., 2021. Optimal fleet size for a shared demand-responsive transport system with human-driven vs automated vehicles: A total cost minimization approach. Transportation Research Part A: Policy and Practice 151, 52–80.

Miller, C. E., Tucker, A. W., Zemlin, R. A., 1960. Integer programming formulation of traveling salesman problem. Journal of the ACM 7 (4), 326–329.

Mims, C., 2022. Amazon, Alphabet and Others Are Quietly Rolling Out Drone Delivery Across America. World Wide Web, last access: May 17, 2022.
URL https://www.wsj.com/articles/amazon-alphabet-and-others-are-quietly-rolling-out-drone-delivery-across-america-11648872022.

Mühlbauer, F., Fontaine, P., 2021. A parallelised large neighbourhood search heuristic for the asymmetric two-echelon vehicle routing problem with swap containers for cargo-bicycles. European Journal of Operational Research 289 (2), 742–757.

Murray, C. C., Chu, A. G., 2015. The flying sidekick traveling salesman problem: Optimization of drone-assisted parcel delivery. Transportation Research Part C: Emerging Technologies 54, 86–109.

Murray, C. C., Raj, R., 2020. The multiple flying sidekicks traveling salesman problem: Parcel delivery with multiple drones. Transportation Research Part C: Emerging Technologies 110, 368–398.

Nguyen-Phuoc, D. Q., Zhou, M., Hong Chua, M., Romano Alho, A., Oh, S., Seshadri, R., Le, D.-T., 2023. Examining the effects of automated mobility-on-demand services on public transport systems using an agent-based simulation approach. Transportation Research Part A: Policy and Practice 169, 103583.

Niakan, F., Rahimi, M., 2015. A multi-objective healthcare inventory routing problem; a fuzzy possibilistic approach. Transportation Research Part E: Logistics and Transportation Review 80, 74–94.

Nicholson, L., Vakharia, A. J., Selcuk Erenguc, S., 2004. Outsourcing inventory management decisions in healthcare: Models and application. European Journal of Operational Research 154 (1), 271–290.

Nolz, P. C., Absi, N., Feillet, D., 2014. A bi-objective inventory routing problem for sustainable waste management under uncertainty. Journal of Multi-Criteria Decision Analysis 21 (5-6), 299–314.

Ostermeier, M., Heimfarth, A., Hübner, A., 2022. Cost-optimal truck-and-robot routing for last-mile delivery. Networks 79 (3), 364–389.

Osterwalder, A., Pigneur, Y., 2010. Business Model Generation: A Handbook for Visionaries, Game Changers, and Challengers. Vol. 1. John Wiley & Sons.

Otero Arenzana, A., Escribano Macias, J. J., Angeloudis, P., 2020. Design of hospital delivery networks using unmanned aerial vehicles. Transportation Research Record 2674 (5), 405–418.

Otto, A., Agatz, N., Campbell, J., Golden, B., Pesch, E., 2018. Optimization approaches for civil applications of unmanned aerial vehicles (UAVs) or aerial drones: A survey. Networks 72 (4), 411–458.

Perboli, G., Rosano, M., 2019. Parcel delivery in urban areas: Opportunities and threats for the mix of traditional and green business models. Transportation Research Part C: Emerging Technologies 99, 19–36.

Pisinger, D., Ropke, S., 2007. A general heuristic for vehicle routing problems. Computers & Operations Research 34 (8), 2403–2435.

Poikonen, S., Wang, X., Golden, B., 2017. The vehicle routing problem with drones: Extended models and connections. Networks 70 (1), 34–43.

Quantum Systems, 2020. Long-range drones to deliver emergency medication to hospitals – project MEDin-Time. World Wide Web, last access: December 01, 2022.
URL `https://www.quantum-systems.com/category/medintime/`

Quantum Systems, 2023. Trinity f90+ mapping drone. World Wide Web, last access: January 18, 2023.
URL `https://www.quantum-systems.com/project/trinityf90plus-mapping-drone/`

Raa, B., Aouam, T., 2023. A shortfall modelling-based solution approach for stochastic cyclic inventory routing. European Journal of Operational Research 305 (2), 674–684.

Rahimi, M., Baboli, A., Rekik, Y., 2017. Multi-objective inventory routing problem: A stochastic model to consider profit, service level and green criteria. Transportation Research Part E: Logistics and Transportation Review 101, 59–83.

Ranquist, E., Steiner, M., Argrow, B., 01 2017. Exploring the range of weather impacts on UAS operations. 18th Conference on Aviation, Range, and Aerospace Meteorology, 22–27 January 2017, Seattle, WA, USA, American Meteorological Society, J3.1.

Rave, A., Fontaine, P., Kuhn, H., 2023a. Cyclic stochastic inventory routing with reorder points and recourse decision for an application in medical supply. Available at SSRN 4421477.

Rave, A., Fontaine, P., Kuhn, H., 2023b. Drone location and vehicle fleet planning with trucks and aerial drones. European Journal of Operational Research 308 (1), 113–130.

Roberti, R., Ruthmair, M., 2021. Exact methods for the traveling salesman problem with drone. Transportation Science 55 (2), 315–335.

Rohmer, S., Claassen, G., Laporte, G., 2019. A two-echelon inventory routing problem for perishable products. Computers & Operations Research 107, 156–172.

Roldán, R. F., Basagoiti, R., Coelho, L. C., 2017. A survey on the inventory-routing problem with stochastic lead times and demands. Journal of Applied Logic 24, 15–24.

Ropke, S., Pisinger, D., 2006. An adaptive large neighborhood search heuristic for the pickup and delivery problem with time windows. Transportation Science 40 (4), 455–472.

Sa, C. A., Santos, B. F., Clarke, J.-P. B., 2020. Portfolio-based airline fleet planning under stochastic demand. Omega 97, 102101.

Sacramento, D., Pisinger, D., Røpke, S., 2019. An adaptive large neighborhood search metaheuristic for the vehicle routing problem with drones. Transportation Research. Part C: Emerging Technologies 102, 289–315.

Schermer, D., Moeini, M., Wendt, O., 2019. A matheuristic for the vehicle routing problem with drones and its variants. Transportation Research Part C: Emerging Technologies 106, 166–204.

Scott, J. E., Scott, C. H., 2017. Drone delivery models for healthcare. In: Hawaii International Conference on System Sciences (HICSS).

Seifried, K., 2019. The traveling salesman problem with one truck and multiple drones. Available at SSRN 3389306.

Shavarani, S. M., Mosallaeipour, S., Golabi, M., İzbirak, G., 2019. A congested capacitated multi-level fuzzy facility location problem: An efficient drone delivery system. Computers & Operations Research 108, 57–68.

Simoni, M. D., Kutanoglu, E., Claudel, C. G., 2020. Optimization and analysis of a robot-assisted last mile delivery system. Transportation Research Part E: Logistics and Transportation Review 142, 102049.

Stenius, O., Karaarslan, A. G., Marklund, J., de Kok, A. G., 2016. Exact analysis of divergent inventory systems with time-based shipment consolidation and compound poisson demand. Operations Research 64 (4), 906–921.

Tamke, F., Buscher, U., 2021. A branch-and-cut algorithm for the vehicle routing problem with drones. Transportation Research Part B: Methodological 144, 174–203.

Taube, F., Minner, S., 2018. Data-driven assignment of delivery patterns with handling effort considerations in retail. Computers & Operations Research 100, 379–393.

Tiniç, G. O., Karasan, O. E., Kara, B. Y., Campbell, J. F., Ozel, A., 2023. Exact solution approaches for the minimum total cost traveling salesman problem with multiple drones. Transportation Research Part B: Methodological 168, 81–123.

Toth, P., Vigo, D., 2014. Vehicle Routing: Problems, Methods, and Applications, 2nd Edition. Society for Industrial and Applied Mathematics, Philadelphia, PA.

Troudi, A., Addouche, S.-A., Dellagi, S., Mhamedi, A. E., 2018. Sizing of the drone delivery fleet considering energy autonomy. Sustainability 10 (9).

Vidal, T., Crainic, T. G., Gendreau, M., Prins, C., 2013. A hybrid genetic algorithm with adaptive diversity management for a large class of vehicle routing problems with time-windows. Computers & Operations Research 40 (1), 475–489.

Voigt, S., Frank, M., Fontaine, P., Kuhn, H., 2022. Hybrid adaptive large neighborhood search for vehicle routing problems with depot location decisions. Computers & Operations Research 146, 105856.

Volland, J., Fügener, A., Schoenfelder, J., Brunner, J. O., 2017. Material logistics in hospitals: A literature review. Omega 69, 82–101.

Wang, D., Hu, P., Du, J., Zhou, P., Deng, T., Hu, M., 2019. Routing and scheduling for hybrid truck-drone collaborative parcel delivery with independent and truck-carried drones. IEEE Internet of Things Journal 6 (6), 10483–10495.

Wang, K., Pesch, E., Kress, D., Fridman, I., Boysen, N., 2022. The piggyback transportation problem: Transporting drones launched from a flying warehouse. European Journal of Operational Research 296 (2), 504–519.

Wang, L., Demeulemeester, E., 2023. Simulation optimization in healthcare resource planning: A literature review. IISE Transactions 55 (10), 985–1007.

Wang, X., Poikonen, S., Golden, B., 2016. The vehicle routing problem with drones: Several worst-case results. Optimization Letters 11 (4), 679–697.

Wankmüller, C., Truden, C., Korzen, C., Hungerländer, P., Kolesnik, E., Reiner, G., Feb 2020. Optimal allocation of defibrillator drones in mountainous regions. OR Spectrum 42 (3), 785—814.

Wingcopter GmbH, 2020. Wingcopter 198. World Wide Web, last access: November 25, 2021.
URL `https://wingcopter.com/wingcopter-198`

Yadollahi, E., Aghezzaf, E.-H., Raa, B., 2017. Managing inventory and service levels in a safety stock-based inventory routing system with stochastic retailer demands. Applied Stochastic Models in Business and Industry 33 (4), 369–381.

Young, T., 2005. An agenda for healthcare and information simulation. Health Care Management Science 8, 189–196.

Zhang, H., Best, T., Chivu, A., Meltzer, D., 03 2020. Simulation-based optimization to improve hospital patient assignment to physicians and clinical units. Health Care Management Science 23, 117–141.

Zheng, X., Yin, M., Zhang, Y., 2019. Integrated optimization of location, inventory and routing in supply chain network design. Transportation Research Part B: Methodological 121, 1–20.

Zipline, 2022. Impact evaluation: Drone delivery improves health access and equity. World Wide Web, last access: March 31, 2022.
URL `https://flyzipline.com/ghana-impact-evaluation`

Zwick, F., Kuehnel, N., Hörl, S., 2022. Shifts in perspective: Operational aspects in (non-)autonomous ride-pooling simulations. Transportation Research Part A: Policy and Practice 165, 300–320.

Anhang A

Appendix for Drone location and vehicle fleet planning with trucks and aerial drones

A.1 Large instances

Scenario	T	D^T	D^M	D^{CDC}	used microdepots				C^{best}	C^{avg}	σ[%]
54.5.15	1	2	0	0					216.8	216.8	0.02
56.5.13	1	3	0	0					215.5	215.9	0.16
59.5.14	1	3	1	0			M_3		230.8	232.0	0.55
61.5.16	1	2	1	0			M_3		227.9	229.7	0.77
66.5.15	1	2	2	0		M_2		M_5	248.6	249.3	0.29
78.5.20	1	1	2	0		M_2		M_5	240.9	242.6	0.73
81.5.20	1	0	2	1		M_2		M_5	280.2	280.2	0.00
83.5.23	1	0	2	1		M_2		M_5	266.0	266.0	0.00
96.5.26	1	0	2	1		M_2		M_5	279.2	279.4	0.10
97.5.25	1	0	2	1		M_2		M_5	291.1	291.1	0.00
105.5.19	1	0	2	1		M_2		M_5	295.1	295.2	0.03
110.5.27	1	0	2	1		M_2		M_5	303.1	303.1	0.00
112.5.32	1	0	2	1		M_2		M_5	287.7	288.1	0.15
116.5.22	1	0	3	1		M_2	M_3	M_5	281.8	281.8	0.00
123.5.26	1	0	3	1		M_2	M_3	M_5	290.3	290.4	0.01
125.5.30	2	0	3	1	M_1	M_2		M_5	353.3	355.0	0.47
132.5.30	2	0	4	0	M_1	M_2	M_3	M_5	379.7	379.7	0.00
139.5.28	2	0	4	1	M_1	M_2	M_3	M_5	365.0	365.1	0.03
141.5.38	2	0	4	0	M_1	M_2	M_3	M_5	366.3	366.3	0.00
142.5.31	2	0	4	0	M_1	M_2	M_3	M_5	383.1	383.1	0.00
147.5.31	2	0	4	0	M_1	M_2	M_3	M_5	367.2	367.2	0.00
153.5.31	2	0	4	0	M_1	M_2	M_3	M_5	356.5	357.0	0.12
157.5.30	2	0	4	0	M_1	M_2	M_3	M_5	357.8	359.3	0.40
163.5.36	2	0	4	0	M_1	M_2	M_3	M_5	372.7	373.8	0.29
171.5.46	2	0	4	0	M_1	M_2	M_3	M_5	430.7	431.2	0.12
177.5.50	2	0	4	0	M_1	M_2	M_3	M_5	454.8	457.2	0.52
180.5.51	2	0	4	1	M_1	M_2	M_3	M_5	464.1	467.5	0.72
185.5.38	2	0	4	1	M_1	M_2	M_3	M_5	429.4	429.4	0.00
194.5.42	2	0	4	1	M_1	M_2	M_3	M_5	414.1	414.2	0.04
196.5.45	2	0	4	1	M_1	M_2	M_3	M_5	425.1	428.0	0.67

Table A.1: Results for our numerical setup with varying demand of large instances.

A.2 VRPD benchmark

Demand	**Sacramento et al. (2019)**			**Euchi and Sadok (2021)**			**Own results**			
class	C^{best}	C^{avg}	σ[%]	C^{best}	C^{avg}	σ[%]	C^{best}	C^{avg}	σ[%]	σ^{BKS}[%]
6.5.1	1.0982	1.0982	0.00	1.0982	1.0982	0.00	1.0982	1.0982	0.00	0.00
6.5.2	0.8422	0.8422	0.00	0.8422	0.8422	0.00	0.8422	0.8422	0.00	0.00
6.5.3	1.2114	1.2114	0.00	1.2114	1.2114	0.00	1.2114	1.2114	0.00	0.00
6.5.4	0.9460	0.9460	0.00	0.9460	0.9460	0.00	0.9460	0.9460	0.00	0.00
6.10.1	2.4061	2.4061	0.00	2.4061	2.4061	0.00	2.4061	2.4061	0.00	0.00
6.10.2	1.6793	1.6793	0.00	1.6793	1.6793	0.00	1.6793	1.6793	0.00	0.00

Continued on next page

Table A.2 – *Continued from previous page*

6.10.3	1.3255	1.3255	0.00	1.3255	1.3255	0.00	1.3255	1.3255	0.00	0.00
6.10.4	1.4431	1.4431	0.00	1.4431	1.4431	0.00	1.4431	1.4431	0.00	0.00
6.20.1	2.6776	2.6776	0.00	2.6776	2.6776	0.00	2.6776	2.6776	0.00	0.00
6.20.2	4.3196	4.3196	0.00	4.3196	4.3196	0.00	4.3196	4.3196	0.00	0.00
6.20.3	3.8248	3.8248	0.00	3.8248	3.8248	0.00	3.8248	3.8247	0.00	0.00
6.20.4	3.6787	3.6787	0.00	3.6787	3.6787	0.00	3.6787	3.6787	0.00	0.00
10.5.1	1.6556	1.6556	0.00	1.6556	1.6556	0.00	1.6556	1.6556	0.00	0.00
10.5.2	1.4519	1.4519	0.00	1.4519	1.4519	0.00	1.4519	1.4519	0.00	0.00
10.5.3	1.4736	1.4736	0.00	1.4736	1.4736	0.00	1.4736	1.4736	0.00	0.00
10.5.4	1.2849	1.2849	0.00	1.2849	1.2849	0.00	1.2849	1.2849	0.00	0.00
10.10.1	2.3265	2.3265	0.00	2.3265	2.3265	0.00	2.3265	2.3265	0.00	0.00
10.10.2	3.1586	3.1586	0.00	3.1586	3.1586	0.00	3.1586	3.1586	0.00	0.00
10.10.3	2.5527	2.5527	0.00	2.5527	2.5527	0.00	2.5527	2.5527	0.00	0.00
10.10.4	2.5393	2.5393	0.00	2.5393	2.5393	0.00	2.5393	2.5393	0.00	0.00
10.20.1	4.4524	4.4524	0.00	4.4524	4.4524	0.00	4.4524	4.4524	0.00	0.00
10.20.2	6.1678	6.1678	0.00	6.1678	6.1678	0.00	6.1678	6.1678	0.00	0.00
10.20.3	4.5463	4.5463	0.00	4.5463	4.5463	0.00	4.5463	4.5463	0.00	0.00
10.20.4	6.1536	6.1536	0.00	6.1536	6.1536	0.00	6.1536	6.1668	0.21	0.00
12.5.1	1.3738	1.3738	0.00	1.3738	1.3738	0.00	1.3738	1.3738	0.00	0.00
12.5.2	1.0590	1.0590	0.00	1.0590	1.0590	0.00	1.0590	1.0590	0.00	0.00
12.5.3	1.4477	1.4477	0.00	1.4477	1.4477	0.00	1.4477	1.4477	0.00	0.00
12.5.4	1.5810	1.5810	0.00	1.5810	1.5810	0.00	1.5810	1.5810	0.00	0.00
12.10.1	2.6810	2.6810	0.00	2.6810	2.6810	0.00	2.6810	2.6810	0.00	0.00
12.10.2	2.6842	2.6842	0.00	2.6842	2.6842	0.00	2.6842	2.6842	0.00	0.00
12.10.3	2.8805	2.8805	0.00	2.8805	2.8805	0.00	2.8805	2.8805	0.00	0.00
12.10.4	2.3142	2.3142	0.00	2.3142	2.3142	0.00	2.3142	2.3142	0.00	0.00
12.20.1	5.7776	5.7776	0.00	5.7776	5.7776	0.00	5.7776	5.7776	0.00	0.00
12.20.2	8.2725	8.2725	0.00	8.2725	8.2725	0.00	8.2725	8.2725	0.00	0.00
12.20.3	4.1669	4.1669	0.00	4.1669	4.1669	0.00	4.1669	4.1669	0.00	0.00
12.20.4	6.0886	6.0886	0.00	6.0886	6.0886	0.00	6.0886	6.0886	0.00	0.00
20.5.1	1.7935	1.7935	0.00	1.3585	1.5789	13.96	1.7935	1.7935	0.00	24.25
20.5.2	1.9540	1.9540	0.00	1.3579	1.5789	14	1.8221	1.8221	0.00	25.48
20.5.3	1.4866	1.4866	0.00	1.5789	1.5893	0.65	1.4866	1.4866	0.00	0.00
20.5.4	1.3789	1.3789	0.00	1.3079	1.5811	17.32	1.3789	1.3789	0.00	5.15
20.10.1	3.2525	3.2525	0.00	2.9814	3.2816	9.15	3.2525	3.2525	0.00	8.34
20.10.2	3.0894	3.0894	0.00	3.0600	3.0600	0.00	3.0894	3.0894	0.00	0.95
20.10.3	3.7023	3.7258	0.63	3.2981	3.2981	0.00	3.7023	3.7023	0.00	10.92
20.10.4	3.3089	3.3137	0.14	3.0981	3.0981	0.00	3.1966	3.1966	0.00	3.08
20.20.1	7.3445	7.3512	0.09	6.6428	7.0600	5.91	7.3230	7.3291	0.08	9.29
20.20.2	7.5489	7.5489	0.00	7.6000	7.8702	3.43	7.5489	7.5607	0.16	0.00
20.20.3	7.4610	7.4746	0.18	7.4110	7.4957	1.13	7.4610	7.4610	0.00	0.67
20.20.4	7.0133	7.0133	0.00	6.9043	6.9043	0.00	7.0133	7.0133	0.00	1.55
50.10.1	5.8613	5.8613	0.00	5.7342	5.8923	2.68	5.8614	5.9408	1.34	2.17
50.10.2	5.5849	5.6210	0.64	5.4416	5.4743	0.60	5.5849	5.5849	0.00	2.57
50.10.3	5.4224	5.4255	0.06	5.1802	5.2755	1.81	5.4888	5.7062	3.81	5.62
50.10.4	5.2083	5.3526	2.70	5.0731	5.1981	2.41	5.1405	5.4827	6.24	1.31
50.20.1	10.4553	10.4564	0.01	10.0822	10.2636	1.77	10.4566	10.6110	1.46	3.58
50.20.2	10.0561	10.0561	0.00	10.0289	10.0461	0.17	10.0561	10.0820	0.26	0.27
50.20.3	10.5425	10.6570	1.07	10.5087	10.5567	0.45	10.5425	10.7049	1.52	0.32
50.20.4	10.6642	11.0008	3.06	9.3591	9.7042	3.56	11.0395	11.1409	0.91	15.22
50.30.1	15.8179	15.8179	0.00	15.7235	15.7380	0.09	15.8179	15.9497	0.83	0.60
50.30.2	15.0148	15.4636	2.90	14.9088	14.9926	0.56	14.9795	15.0286	0.33	0.47
50.30.3	16.7690	16.7713	0.01	16.1284	16.4681	2.06	16.7796	16.8633	0.50	3.88
50.30.4	18.2875	18.2875	0.00	18.3802	18.9568	3.04	18.2875	18.3780	0.49	0.00
50.40.1	20.3751	21.1771	3.79	20.3019	20.3019	0.00	20.0882	21.2848	5.62	-1.06
50.40.2	20.6262	20.6262	0.00	20.5623	20.5623	0.00	20.6262	20.6790	0.26	0.31
50.40.3	22.6452	22.7053	0.26	22.6328	22.9932	1.57	22.6657	22.9102	1.07	0.15
50.40.4	22.3371	22.7891	1.98	22.3481	22.9461	2.61	22.3371	22.3371	0.00	0.00
100.10.1	6.8574	6.8902	0.48	6.3633	6.3859	0.35	6.8931	7.0288	1.93	7.69

Continued on next page

Table A.2 – *Continued from previous page*

100.10.2	7.5851	7.6781	1.21	7.3796	7.4512	0.96	7.5547	7.6083	0.70	2.32
100.10.3	7.1835	7.3055	1.67	8.1195	8.2266	1.30	7.2405	7.3730	1.80	0.79
100.10.4	7.4568	7.5459	1.18	6.8926	7.0440	2.15	7.4689	7.5310	0.82	7.72
100.20.1	13.6067	13.7946	1.36	12.5410	13.2443	5.31	13.9798	13.9986	0.13	10.29
100.20.2	14.1340	14.5375	2.78	14.0118	14.5979	4.01	14.1667	14.4054	1.66	1.09
100.20.3	13.7099	13.7672	0.42	12.4879	12.5325	0.36	14.0065	14.4508	3.07	10.84
100.20.4	13.8494	14.1976	2.45	12.1350	12.2157	0.66	13.6085	13.8257	1.57	10.83
100.30.1	22.5882	23.6364	4.43	23.4927	23.4929	0.00	22.1278	22.3138	0.83	-2.08
100.30.2	22.3143	22.3846	0.31	22.0396	22.1350	0.43	22.6947	22.8905	0.86	2.89
100.30.3	23.7195	23.9094	0.79	23.2988	23.5033	0.87	23.3769	23.5578	0.77	0.33
100.30.4	22.3701	22.6585	1.27	22.1495	22.5052	1.58	22.7022	22.9554	1.10	2.43
100.40.1	29.1397	30.1807	3.45	29.1397	29.5463	1.38	28.9907	29.3766	1.31	-0.51
100.40.2	30.9900	31.2092	0.70	30.3610	30.4129	0.17	31.1576	31.3523	0.62	2.56
100.40.3	29.0248	29.6653	2.16	29.0112	29.0635	0.18	29.3583	30.1569	2.65	1.18
100.40.4	28.9735	29.2049	0.79	28.5904	28.6360	0.16	29.2673	29.4952	0.77	2.31
150.10.1	8.7903	8.9351	1.62	8.5865	9.6364	10.90	8.8329	9.0109	1.98	2.79
150.10.2	8.2591	8.4160	1.87	8.1462	10.9009	25.27	8.3217	8.4821	1.89	2.11
150.10.3	8.4960	9.0207	5.82	9.7052	9.8430	1.40	8.4138	8.6962	3.25	-0.98
150.10.4	8.8373	9.0398	2.24	10.8302	10.9725	1.30	8.8469	8.9152	0.77	0.11
150.20.1	17.3194	17.5964	1.57	17.0099	17.6175	3.45	17.4518	17.7115	1.47	2.53
150.20.2	16.6341	17.4507	4.68	16.1837	16.6333	2.70	16.6581	16.7896	0.78	2.85
150.20.3	17.4058	18.3447	5.12	16.9830	16.9830	0.00	17.6484	18.2769	3.44	3.77
150.20.4	16.8752	17.4774	3.45	16.8102	16.8102	0.00	16.8430	17.0358	1.13	0.19
150.30.1	25.9854	26.5488	2.12	25.8524	25.8524	0.00	25.5617	25.7346	0.67	-1.14
150.30.2	26.2055	26.7411	2.00	26.1370	26.1370	0.00	27.0083	27.4973	1.78	3.23
150.30.3	25.3164	26.1137	3.05	25.0101	25.0101	0.00	25.5945	26.2195	2.38	2.28
150.30.4	26.1027	27.2923	4.36	25.9812	25.9812	0.00	25.9322	26.1393	0.79	-0.19
150.40.1	34.0121	35.4534	4.07	29.4683	29.8651	1.33	33.8560	34.1849	0.96	12.96
150.40.2	36.5616	38.2965	4.53	35.2343	45.9885	23.38	37.3489	39.7175	5.96	5.66
150.40.3	36.6574	38.2955	4.28	36.8769	36.8769	0.00	36.2182	36.4779	0.71	-1.21
150.40.4	35.0156	36.0662	2.91	35.5854	35.7586	0.48	34.8401	35.3078	1.32	-0.50
200.10.1	10.0945	10.4050	2.98	10.0956	10.1574	0.61	9.8962	9.9743	0.78	-2.00
200.10.2	10.4226	10.6149	1.81	10.2855	10.5303	2.33	10.0557	10.1145	0.58	-2.29
200.10.3	9.7990	9.9235	1.25	9.1050	9.1050	0.00	9.7359	9.8236	0.89	6.48
200.10.4	10.3553	10.6400	2.68	10.1251	10.1251	0.00	10.3061	10.3850	0.76	1.76
200.20.1	21.2151	21.4601	1.14	21.2185	21.2185	0.00	20.9326	21.2115	1.31	-1.35
200.20.2	21.4585	22.0461	2.67	21.0193	21.1948	0.83	21.6359	21.7961	0.73	2.85
200.20.3	20.8522	21.0604	0.99	19.0312	19.0312	0.00	20.8347	20.9688	0.64	8.66
200.20.4	19.2350	20.1804	4.68	18.8840	19.1840	1.56	19.2561	19.6779	2.14	1.93
200.30.1	30.3602	31.7826	4.48	30.0730	30.6830	1.99	29.9292	30.2124	0.94	-0.48
200.30.2	32.8128	33.2164	1.22	32.0915	32.0915	0.00	31.5970	31.8373	0.75	-1.57
200.30.3	32.2535	32.7373	1.48	32.0835	32.0967	0.04	31.1024	31.3947	0.93	-3.15
200.30.4	32.0931	32.7638	2.05	32.0375	32.0375	0.00	31.7090	33.3396	4.89	-1.04
200.40.1	41.4980	42.3048	1.91	41.2954	41.5796	0.68	41.9058	44.9005	6.67	1.46
200.40.2	43.2502	44.2211	2.20	43.0717	43.1256	0.13	42.9621	43.5546	1.36	-0.26
200.40.3	43.3375	44.2613	2.09	43.1857	43.1857	0.00	43.6542	44.2726	1.40	1.07
200.40.4	42.0579	43.3370	2.95	42.0313	42.0313	0.00	39.7972	40.1223	0.81	-5.61

Table A.2: Detailed results of VRPD instances from Sacramento et al. (2019).

Anhang B

Appendix for Two-indexed formulation of the traveling salesman problem with multiple drones performing sidekicks and loops

B.1 Benchmark results for instances of Murray and Chu (2015)

The following two tables present results for the instances of Murray and Chu (2015) for the endurance of $e = 20$ and $e = 40$. The instance names are similar to Dell'Amico et al. (2021a).

	$m = 1$			$m = 3$			$m = \infty$		
Instance	τ^*	CPU [s]	Gap	τ^*	CPU [s]	Gap	τ^*	CPU [s]	Gap
20140810T123437v1	54.3926	12	-	51.3825	2	-	51.3825	2	-
20140810T123437v2	51.6111	12	-	51.6111	7	-	51.6111	6	-
20140810T123437v3	54.0684	15	-	52.8225	10	-	52.8225	8	-
20140810T123437v4	66.8684	9	-	65.6225	11	-	65.6225	8	-
20140810T123437v5	45.3353	326	-	32.0655	10	-	24.4390	2	-
20140810T123437v6	43.9153	210	-	28.9400	7	-	24.0264	1	-
20140810T123437v7	46.5813	18	-	43.2069	9	-	39.8664	7	-
20140810T123437v8	59.3813	34	-	57.7700	12	-	53.1454	7	-
20140810T123437v9	39.2035	821	-	24.9912	6	-	21.8536	1	-
20140810T123437v10	36.9077	343	-	25.7710	11	-	21.9720	2	-
20140810T123437v11	39.3002	107	-	33.7779	7	-	32.3077	2	-
20140810T123437v12	51.5645	61	-	47.7507	8	-	45.1077	3	-
20140810T123440v1	46.4304	52	-	43.8455	6	-	43.8455	6	-
20140810T123440v2	49.3737	56	-	46.2455	11	-	46.2455	14	-
20140810T123440v3	53.6616	13	-	51.6277	8	-	51.6277	7	-
20140810T123440v4	66.4616	14	-	64.4277	6	-	64.4277	10	-
20140810T123440v5	39.7498	115	-	32.2263	3	-	31.6066	1	-
20140810T123440v6	40.3790	91	-	34.0066	2	-	34.0066	1	-
20140810T123440v7	43.3126	21	-	40.7304	2	-	40.7304	2	-
20140810T123440v8	55.7960	20	-	53.5304	2	-	53.5304	1	-
20140810T123440v9	35.5331	14	-	31.6066	1	-	31.6066	0	-
20140810T123440v10	36.0764	10	-	34.0066	1	-	34.0066	1	-
20140810T123440v11	40.7304	4	-	40.7304	1	-	40.7304	1	-
20140810T123440v12	53.5304	7	-	53.5304	1	-	53.5304	1	-
20140810T123443v1	69.5865	8	-	69.5865	4	-	69.5865	7	-
20140810T123443v2	72.0639	5	-	71.7473	3	-	71.5839	3	-
20140810T123443v3	76.1447	4	-	76.0673	1	-	75.9039	1	-
20140810T123443v4	89.1839	2	-	88.8673	2	-	88.7039	2	-
20140810T123443v5	54.7521	236	-	42.2634	3	-	39.7845	3	-
20140810T123443v6	55.1268	112	-	45.0943	11	-	43.9992	5	-
20140810T123443v7	62.2491	36	-	60.8333	5	-	60.8333	5	-
20140810T123443v8	80.0971	34	-	76.3401	27	-	73.8724	5	-
20140810T123443v9	41.9314	749	-	27.6100	1	-	24.5760	1	-
20140810T123443v10	42.9348	153	-	30.9760	1	-	30.9760	1	-
20140810T123443v11	51.4056	17	-	43.7760	3	-	43.7760	2	-
20140810T123443v12	62.6175	9	-	56.5760	1	-	56.5760	1	-

Table B.1: Results for instances of Murray and Chu (2015) with an endurance of 20.

	$m = 1$			$m = 3$			$m = \infty$		
Instance	τ^*	CPU [s]	Gap	τ^*	CPU [s]	Gap	τ^*	CPU [s]	Gap
20140810T123437v1	49.1189	3369	-	35.5186	23	-	33.8109	8	-
20140810T123437v2	46.3113	442	-	35.3759	29	-	32.6510	7	-
20140810T123437v3	52.6868	248	-	49.2858	87	-	40.9090	28	-
20140810T123437v4	65.4868	272	-	62.5748	112	-	54.5333	56	-
20140810T123437v5	42.8354	2663	-	28.4013	31	-	24.4390	2	-
20140810T123437v6	41.6015	1344	-	28.4688	10	-	24.0264	3	-
20140810T123437v7	43.3913	173	-	36.4363	13	-	35.8290	8	-
20140810T123437v8	56.1913	267	-	50.5161	13	-	48.6273	7	-
20140810T123437v9	37.8082	3600	12.2%	24.9912	12	-	21.8536	1	-
20140810T123437v10	36.9077	635	-	25.7710	15	-	21.9720	2	-
20140810T123437v11	39.3002	312	-	29.3975	19	-	26.4022	1	-
20140810T123437v12	51.2536	115	-	40.7507	7	-	37.3724	1	-
20140810T123440v1	45.1029	686	-	35.5331	29	-	32.3895	1	-
20140810T123440v2	44.4461	866	-	37.2360	60	-	34.0066	1	-
20140810T123440v3	52.3083	421	-	45.3532	16	-	45.3532	7	-
20140810T123440v4	66.3969	581	-	58.9284	14	-	58.1532	7	-
20140810T123440v5	39.7498	310	-	32.2263	3	-	31.6066	0	-
20140810T123440v6	39.6581	207	-	34.0066	1	-	34.0066	1	-
20140810T123440v7	43.3126	58	-	40.7304	1	-	40.7304	1	-
20140810T123440v8	55.7960	40	-	53.5304	1	-	53.5304	1	-
20140810T123440v9	35.5331	13	-	31.6066	1	-	31.6066	1	-
20140810T123440v10	36.0764	9	-	34.0066	1	-	34.0066	1	-
20140810T123440v11	40.7304	5	-	40.7304	1	-	40.7304	1	-
20140810T123440v12	53.5304	5	-	53.5304	1	-	53.5304	1	-
20140810T123443v1	54.0129	1121	-	37.5843	7	-	37.4695	2	-
20140810T123443v2	56.5729	2149	-	38.5950	11	-	35.1953	1	-
20140810T123443v3	66.1746	298	-	54.6474	11	-	47.4513	1	-
20140810T123443v4	81.4603	350	-	69.2538	13	-	65.6295	3	-
20140810T123443v5	49.0759	3600	25.0%	31.2183	19	-	24.2916	0	-
20140810T123443v6	48.4864	2640	-	35.0597	12	-	30.0160	0	-
20140810T123443v7	56.8793	777	-	44.3748	3	-	42.8160	0	-
20140810T123443v8	68.3988	225	-	56.5760	1	-	55.6160	0	-
20140810T123443v9	41.9314	3600	6.3%	27.6100	3	-	23.6160	0	-
20140810T123443v10	42.9348	240	-	30.9760	1	-	30.0160	0	-
20140810T123443v11	51.3950	38	-	42.8160	0	-	42.8160	0	-
20140810T123443v12	62.6175	7	-	55.6160	0	-	55.6160	0	-

Table B.2: Results for instances of Murray and Chu (2015) with an endurance of 40.

B.2 Benchmark results for instances of Bouman et al. (2018)

The following five tables present the results for the instances of Bouman et al. (2018). The instance names are similar to El-Adle et al. (2021) and the results are split up for each considered number of nodes.

$\lvert\mathcal{I}_0\rvert = 16$									
	$m = 1$			$m = 3$			$m = \infty$		
Instance	τ^*	CPU [s]	Gap	τ^*	CPU [s]	Gap	τ^*	CPU [s]	Gap
Uniform-61-n20	347.0919	74	-	346.9223	27	-	346.9223	75	-
Uniform-62-n20	353.7019	2	-	353.7019	2	-	353.7019	4	-
Uniform-63-n20	372.9289	2	-	370.1349	2	-	370.1349	1	-
Uniform-64-n20	357.9113	10	-	357.9113	11	-	357.9113	9	-
Uniform-65-n20	368.6511	5	-	368.6511	4	-	368.6511	4	-
Uniform-66-n20	426.5167	2	-	426.5167	2	-	426.5167	2	-
Uniform-67-n20	372.7803	2	-	372.7803	1	-	372.7803	1	-
Uniform-68-n20	423.3365	2	-	423.3365	2	-	423.3365	3	-
Uniform-69-n20	363.4143	7	-	363.4143	6	-	363.4143	5	-
Uniform-70-n20	410.1439	8	-	410.1439	4	-	410.1439	8	-

Table B.3: Results for instances of Bouman et al. (2018) with 16 nodes.

$\lvert\mathcal{I}_0\rvert = 20$									
	$m = 1$			$m = 3$			$m = \infty$		
Instance	τ^*	CPU [s]	Gap	τ^*	CPU [s]	Gap	τ^*	CPU [s]	Gap
Uniform-61-n20	351.5212	588	-	351.4622	1526	-	351.4622	399	-
Uniform-62-n20	374.1195	431	-	374.1195	481	-	374.1195	1308	-
Uniform-63-n20	394.5000	34	-	391.7060	31	-	391.7060	78	-
Uniform-64-n20	368.7314	575	-	368.7314	506	-	368.7314	581	-
Uniform-65-n20	390.5601	224	-	381.0652	52	-	381.0652	67	-
Uniform-66-n20	436.2728	166	-	435.1632	62	-	433.3361	101	-
Uniform-67-n20	391.4744	46	-	391.4744	34	-	391.4744	53	-
Uniform-68-n20	435.6068	25	-	435.6068	29	-	435.6068	36	-
Uniform-69-n20	380.4329	336	-	380.4329	181	-	380.4329	525	-
Uniform-70-n20	422.6549	42	-	422.6549	84	-	422.6549	42	-

Table B.4: Results for instances of Bouman et al. (2018) with 20 nodes.

$\lvert\mathcal{I}_0\rvert = 24$									
	$m = 1$			$m = 3$			$m = \infty$		
Instance	τ^*	CPU [s]	Gap	τ^*	CPU [s]	Gap	τ^*	CPU [s]	Gap
Uniform-71-n50	415.8466	1059	-	415.8466	1449	-	415.8466	1219	-
Uniform-72-n50	410.1562	28	-	410.1562	30	-	410.1562	29	-
Uniform-73-n50	394.5155	495	-	391.3396	324	-	391.3564	316	-
Uniform-74-n50	467.6828	865	-	467.6828	502	-	467.6828	552	-
Uniform-75-n50	463.6015	1072	-	463.6015	863	-	463.6015	1742	-
Uniform-76-n50	394.2924	3600	2.7%	394.2924	3600	4.8%	394.2924	3600	2.8%
Uniform-77-n50	458.7309	565	-	452.9030	98	-	452.9030	106	-

Continued on next page

Continued from previous page

Uniform-78-n50	412.8484	1428	-	410.8227	1263	-	410.8227	1217	-
Uniform-79-n50	412.1437	554	-	412.1437	1460	-	412.1437	1492	-
Uniform-80-n50	397.2048	3600	4.6%	391.7442	3600	2.8%	391.7442	3600	2.7%

Table B.5: Results for instances of Bouman et al. (2018) with 24 nodes.

$\lvert\mathcal{I}_0\rvert = 28$									
	$m = 1$			$m = 3$			$m = \infty$		
Instance	τ^*	CPU [s]	Gap	τ^*	CPU [s]	Gap	τ^*	CPU [s]	Gap
Uniform-71-n50	446.9016	3600	6.7%	441.6016	3600	4.8%	441.6016	3600	3.2%
Uniform-72-n50	449.6584	541	-	449.6584	645	-	449.6584	412	-
Uniform-73-n50	449.0387	3600	2.6%	445.8796	3600	2.6%	445.8628	3600	1.2%
Uniform-74-n50	470.8468	3600	1.0%	470.8405	3600	1.3%	470.8468	3600	1.7%
Uniform-75-n50	473.0050	3600	4.0%	473.0050	3600	5.9%	473.0050	3600	6.8%
Uniform-76-n50	407.7456	3600	9.2%	407.4875	3600	8.8%	407.7456	3600	9.5%
Uniform-77-n50	485.5172	3600	2.6%	480.5688	3600	1.0%	480.5687	3159	-
Uniform-78-n50	462.1742	3600	1.5%	459.4857	3600	1.2%	459.4857	3600	2.1%
Uniform-79-n50	447.7367	3600	7.9%	447.7367	3600	8.6%	447.7367	3600	10.3%
Uniform-80-n50	454.8248	3600	9.1%	450.3997	3600	8.4%	449.3641	3600	8.9%

Table B.6: Results for instances of Bouman et al. (2018) with 28 nodes.

$\lvert\mathcal{I}_0\rvert = 32$									
	$m = 1$			$m = 3$			$m = \infty$		
Instance	τ^*	CPU [s]	Gap	τ^*	CPU [s]	Gap	τ^*	CPU [s]	Gap
Uniform-71-n50	483.6558	3600	7.5%	478.3559	3600	7.7%	478.3559	3600	6.5%
Uniform-72-n50	493.0942	3600	3.4%	493.0942	3600	3.6%	493.0942	3600	3.6%
Uniform-73-n50	497.0019	3600	7.5%	490.4027	3600	6.9%	490.4758	3600	7.3%
Uniform-74-n50	484.4209	3600	15.1%	479.3757	3600	14.1%	492.1320	3600	17.6%
Uniform-75-n50	502.6546	3600	12.5%	502.5212	3600	12.0%	504.6453	3600	12.6%
Uniform-76-n50	494.6067	3600	19.5%	474.7205	3600	15.6%	483.1039	3600	19.0%
Uniform-77-n50	521.4612	3600	7.2%	511.1739	3600	4.9%	511.1739	3600	4.7%
Uniform-78-n50	507.7490	3600	7.3%	504.8168	3600	5.3%	505.4795	3600	5.5%
Uniform-79-n50	483.3885	3600	16.1%	452.3963	3600	10.4%	459.7861	3600	12.1%
Uniform-80-n50	473.7993	3600	21.9%	445.4466	3600	16.9%	451.4449	3600	19.0%

Table B.7: Results for instances of Bouman et al. (2018) with 32 nodes.

Anhang C

Appendix for Cyclic stochastic inventory routing with reorder points and recourse decision for an application in medical supply

C.1 Small instances

				CPLEX			ALNS				
Inst.	$\lvert\hat{\mathcal{C}}\rvert$	$p \in \mathcal{P}$	$\lvert\Omega\rvert$	Costs	Gap [%]	Time [s]	Best costs	Avg. costs	σ [%]	Time [s]	Δ [%]
M-1	4	1	5	2.4330	-	37	2.4330	2.4330	-	27	-
R1-2	4	1	5	2.9737	-	43	2.9737	2.9737	-	1	-
R2-3	4	1	5	2.1938	-	1	2.1938	2.1938	-	0	-
R3-4	4	1	5	2.7103	-	1	2.7103	2.7103	-	28	-
M-5	4	2	5	5.9270	-	841	5.9271	5.9564	0.49	300	-
R1-6	4	2	5	3.8962	-	41	3.8962	3.8962	-	35	-
R2-7	4	2	5	4.5830	-	3	4.5830	4.6248	0.90	120	-
R3-8	4	2	5	4.8799	-	6	4.8799	4.8869	0.14	173	-
M-9	4	3	5	4.6614	-	3	4.6614	4.6621	0.01	63	-
R1-10	4	3	5	7.0386	-	2	7.0386	7.0386	-	7	-
R2-11	4	3	5	5.6938	-	3	5.6938	5.7741	1.39	181	-
R3-12	4	3	5	6.3950	-	5	6.3950	6.3950	-	0	-
M-13	4	1,2	5	10.2422	28	3600	9.8354	9.8354	-	300	-3.97
R1-14	4	1,2	5	7.8025	-	2052	7.8025	7.8117	0.12	179	-
R2-15	4	1,2	5	7.2629	-	118	7.2629	7.2629	-	0	-
R3-16	4	1,2	5	8.1623	-	91	8.1623	8.1900	0.34	253	-
M-17	4	1,2,3	5	17.2051	21	3600	16.2412	16.2412	-	300	-5.6
R1-18	4	1,2,3	5	16.9167	27	3600	16.9167	16.9430	0.15	300	-
R2-19	4	1,2,3	5	14.6688	-	377	14.6688	14.6688	-	0	-
R3-20	4	1,2,3	5	18.0214	14	3600	18.1574	18.1712	0.08	300	0.75
M-21	7	1	2	3.9107	29	3600	3.7736	3.7736	-	300	-3.51
R1-22	7	1	2	5.5495	12	3600	5.3368	5.3368	-	300	-3.83
R2-23	7	1	2	4.7262	20	3600	4.6513	4.6523	0.02	300	-1.58
R3-24	7	1	2	6.4221	30	3600	6.1125	6.1125	-	300	-4.82
M-25	7	2	2	6.3795	-	657	6.3795	6.3795	-	0	-
R1-26	7	2	2	7.6421	19	3600	7.6421	7.6421	-	300	-
R2-27	7	2	2	4.7228	-	24	4.7228	4.7240	0.03	142	-
R3-28	7	2	2	7.9691	15	3600	7.9691	7.9691	-	300	-
M-29	7	3	2	7.2791	-	397	7.2791	7.2791	-	0	-
R1-30	7	3	2	4.3390	-	2	4.3390	4.3390	-	0	-
R2-31	7	3	2	6.8301	-	127	6.8301	7.0485	3.10	240	-
R3-32	7	3	2	9.5096	-	476	9.5628	9.6539	0.94	300	0.56
M-33	7	1,2	2	16.3952	57	3600	12.2557	12.2603	0.04	300	-25.25
R1-34	7	1,2	2	15.1775	55	3600	12.9558	12.9743	0.14	300	-14.64
R2-35	7	1,2	2	10.9020	37	3600	10.3046	10.3046	-	300	-5.48
R3-36	7	1,2	2	15.3906	20	3600	14.4562	14.4833	0.19	300	-6.07
M-37	7	1,2,3	2	33.9267	64	3600	22.4928	22.5572	0.29	300	-33.7
R1-38	7	1,2,3	2	51.5159	78	3600	21.7242	21.8438	0.55	300	-57.83
R2-39	7	1,2,3	2	22.0797	40	3600	19.7454	19.7859	0.20	300	-10.57
R3-40	7	1,2,3	2	53.5479	70	3600	27.4347	27.5259	0.33	300	-48.77
M-41	10	1	1	5.1196	-	342	5.1196	5.1196	-	3	-
R1-42	10	1	1	5.7673	44	3600	4.8426	4.8524	0.20	300	-16.03
R2-43	10	1	1	4.5026	16	3600	4.5026	4.5127	0.22	300	-
R3-44	10	1	1	5.7289	20	3600	5.7289	5.7289	-	300	-
M-45	10	2	1	7.6590	22	3600	7.6201	7.6244	0.06	300	-0.51
R1-46	10	2	1	7.0747	17	3600	7.0747	7.0747	-	300	-
R2-47	10	2	1	5.3971	-	33	5.3971	5.3971	-	0	-
R3-48	10	2	1	8.1021	38	3600	7.7737	7.7737	-	300	-4.05
M-49	10	3	1	9.5964	20	3600	9.5964	9.6423	0.48	300	-
R1-50	10	3	1	4.8449	-	5	4.8449	4.8449	-	22	-
R2-51	10	3	1	5.4927	-	7	5.4927	5.4927	-	0	-
R3-52	10	3	1	10.3821	-	128	10.3821	10.3821	-	51	-
M-53	10	4	1	7.4996	-	6	7.4996	7.6642	2.15	198	-
R1-54	10	4	1	13.2423	-	325	13.2423	13.2423	-	112	-

Continued on next page

Continued from previous page

R2-55	10	4	1	12.4876	8	3600	12.4876	12.4876	-	300	-
R3-56	10	4	1	16.1072	-	63	16.1071	16.4444	2.05	218	-
M-57	10	5	1	13.7504	-	5	13.7504	13.7504	-	25	-
R1-58	10	5	1	11.7721	-	2	11.7721	11.7721	-	84	-
R2-59	10	5	1	11.6002	-	2	11.6002	11.6002	-	39	-
R3-60	10	5	1	13.6624	-	3	13.6624	13.6624	-	0	-
M-61	10	6	1	17.6657	-	23	17.6657	18.0118	1.92	184	-
R1-62	10	6	1	24.8828	-	23	24.8828	24.8828	-	27	-
R2-63	10	6	1	9.5174	-	1	9.5174	9.5174	-	0	-
R3-64	10	6	1	21.4008	-	4	21.4008	21.4008	-	49	-
M-65	10	7	1	17.1729	-	1	17.1729	17.1729	-	47	-
R1-66	10	7	1	41.5341	-	4	41.5341	41.5341	-	29	-
R2-67	10	7	1	38.1420	28	3600	38.1420	38.1420	-	300	-
R3-68	10	7	1	28.1036	-	1	28.1036	28.1036	-	14	-
A-69	15	1	1	15.9818	-	1265	15.9818	15.9919	0.06	107	-
A-70	15	1	1	16.4826	-	761	16.4826	16.608	0.75	269	-
A-71	15	1	1	16.2164	6	3600	16.2164	16.4751	1.57	300	-
A-72	15	1	1	16.7131	4	3600	16.7131	17.3854	3.87	300	-
A-73	15	1	1	17.6030	4	3600	17.6030	17.6117	0.05	300	-
A-74	15	1	1	27.8470	42	3600	27.4362	27.6236	0.68	300	-1.50
A-75	15	1	1	27.3037	42	3600	26.6746	27.2452	2.09	300	-2.36
A-76	15	1	1	16.2097	5	3600	16.0320	16.3224	1.78	300	-1.11
A-77	15	1	1	27.9306	42	3600	27.4960	27.8916	1.42	300	-1.58
A-78	15	1	1	51.2633	70	3600	28.6530	28.9684	1.09	300	-78.91

Table C.1: Detailed performance analysis for small instances (* optimal solution). The clinics have the locations as in our case study ("M"), or three random locations ("R1","R2","R3"), or as in Archetti et al. (2007) ("A") for all clinics all with a hyphen separated consecutive numbering.

C.2 Large instances

			Our ALNS			
Instance name	$\|\mathcal{C}\|$	Opt. costs	Best costs	Avg. costs	σ [%]	GAP [%]
abs1n5.dat	5	5942.82	5942.82	5971.83	0.49	-
abs2n5.dat	5	5045.91	5045.91	5050.06	0.08	-
abs3n5.dat	5	6956.28	6956.28	6965.98	0.14	-
abs4n5.dat	5	5163.42	5163.42	5243.96	1.54	-
abs5n5.dat	5	4581.66	4581.66	4632.16	1.09	-
abs1n10.dat	10	8870.15	8953.86	9138.19	2.02	0.93
abs2n10.dat	10	8569.73	8634.30	8847.42	2.41	0.75
abs3n10.dat	10	8509.81	8509.81	8726.34	2.48	-
abs4n10.dat	10	8792.29	8792.29	9287.04	5.33	-
abs5n10.dat	10	9620.07	9627.07	9990.98	3.64	0.07
abs1n15.dat	15	12118.83	12228.00	12474.10	1.97	0.89
abs2n15.dat	15	11932.10	12107.00	12273.00	1.35	1.44
abs3n15.dat	15	13554.15	13569.20	14101.50	3.77	0.11
abs4n15.dat	15	10618.55	10686.50	10889.20	1.86	0.64
abs5n15.dat	15	10385.54	10468.60	10834.20	3.37	0.79
abs1n20.dat	20	14702.95	14775.10	14833.60	0.39	0.49
abs2n20.dat	20	14646.96	14870.50	14999.30	0.86	1.50
abs3n20.dat	20	14532.91	14606.70	14889.90	1.90	0.51

Continued on next page

Table C.2 – *Continued from previous page*

abs4n20.dat	20	14539.72	14777.30	15149.50	2.46	1.61
abs5n20.dat	20	15896.71	16002.00	16224.30	1.37	0.66
abs1n25.dat	25	15581.47	15908.80	16250.30	2.10	2.06
abs2n25.dat	25	16823.16	17044.70	17256.90	1.23	1.30
abs3n25.dat	25	18098.02	18222.60	18774.10	2.94	0.68
abs4n25.dat	25	16303.69	17042.20	17269.10	1.31	4.33
abs5n25.dat	25	19047.70	19178.50	19290.70	0.58	0.68
abs1n30.dat	30	23183.99	23507.40	23675.20	0.71	1.38
abs2n30.dat	30	20090.29	20382.00	20813.60	2.07	1.43
abs3n30.dat	30	23382.73	23679.20	24064.30	1.60	1.25
abs4n30.dat	30	17649.53	17941.20	18339.70	2.17	1.63
abs5n30.dat	30	18979.93	19108.20	19322.30	1.11	0.67

Table C.2: Detailed performance analysis for benchmark instances of Archetti et al. (2007). Instance names are as in Archetti et al. (2007).

Anhang D

Appendix for Drone fleet planning and battery allocation for emergency resupply of pharmacies and ambulances

D.1 Business Model Canvas

Developed by Osterwalder and Pigneur (2010), we present a BMC for the wholesaler, i.e., the pharmacy of a large German hospital (Figure D.1), to show in detail how the wholesaler generates, provides, and acquires value. The BMC includes both the status quo and the new business model with emergency resupply via drones ("New"). It shows the partners, activities, resources, its value creation, customer relationships and segments, and channels and also provides information on the wholesaler's costs and revenue structure.

<table>
<tr><th>Key Partners</th><th>Key Activities</th><th>Value Propositions</th><th>Customer Relationships</th><th>Customer Segments</th></tr>
<tr>
<td rowspan="2">• Manufacturer
• Wholesaler
(The pharmacy of Ingolstadt Hospital itself is served by a wholesaler to prevent shortages)
• Truck service provider
• Pharmacies of clinics
• Pharmacies of ambulance depots
• New: Ambulances at service</td>
<td>• Procurement, stocking, and distribution of drugs
• New: Drone operation and maintenance</td>
<td rowspan="2">• Efficient dispensing of medication for own patients and pharmacies to serve
• New: Fast and efficient emergency delivery</td>
<td>• Staff availability for resupply in case of emergency
• New: Fast resupply via drones in case of emergency</td>
<td rowspan="2">• Patients of their hospital
• Pharmacies of surrounding clinics
• Pharmacies of ambulance depots
• New: Ambulances at service</td>
</tr>
<tr>
<td>Key Resources
• Medical goods
• New: Drones, batteries, transport boxes</td>
<td>Channels
• Supply only of contractual partners
• Order digitally in the e-shop of the pharmacy, truck service provider is then commissioned by fax, phone, or mail</td>
</tr>
<tr><th colspan="2">Cost Structure</th><th colspan="3">Revenue Streams</th></tr>
<tr>
<td colspan="2">• Procurement and stocking of medication
• Insurance fees
• Transportation costs (road-based transport)
• New: Costs for drone usage</td>
<td colspan="3">• Sale of medication to pharmacies
• Fee for transportation (road-based transport)
• New: Price for drone delivery</td>
</tr>
</table>

Figure D.1: BMC for the wholesaler, i.e., a pharmacy of a large German hospital.

D.2 Variable costs for drone delivery

The approximated variable costs per minute for outbound and return flights are based on the formula of D'Andrea (2014) for variable costs per km, which has also been conducted by e.g., Dhote and Limbourg (2020). Variable costs are approximated by $\frac{c}{e} \cdot \left(\frac{m_p + m_v}{370 \cdot \eta \cdot r} + \frac{p}{v} \right)$, where

- $c = 0.3714$: costs in €$/kWh$ (BDEW 2022)
- $e = 0.8$: charging efficiency
- $m_p = 4.28$: mass of the considered drone in kg
- $m_v = 0.1$: avg. mass of a transported drug in kg
- $\eta = 0.5$: power transmission efficiency (motor and propeller)
- $r = 3$: lift-to-drag ratio
- $p = 0.1$: power consumption of electronics in kW
- $v = 61.2$: speed of the considered drone in km/h

We do not have information on e, η, r, and p for the considered drone, and thus, similar to Dhote and Limbourg (2020), we consider the same values as D'Andrea (2014) did. It follows that a loaded drone costs 0.0044€ per km and unloaded 0.0043€ per km, and thus with the considered drone speed 0.0045€ or 0.0044€ per minute, respectively.

D.3 CO_2 eq. in the life cycle of a drone

Table D.1 gives information on the used material for the drone and its components and the resulting CO_2 eq. during its life cycle. Based on the material and weight, the proportional CO_2 eq. are calculated. The drone, without its battery and transport box, weighs 2.930kg.

	Material	weight [kg]	CO_2 eq. [kg]
Drone	Different plastics (Jeswani et al. 2021)	1.660	7.770
	Metals & electronics (Clemence 2019)	1.270	6.716
	$\sum$	2.930	14.486
Battery	Lithium-Ion battery (Melin 2019)	1.150	2.697

Table D.1: Detailed information on CO_2 eq. of a drone and its battery.

The CO_2 eq. for the transport boxes are based on assumptions due to missing information. We consider that the transport box weighs 200g and is made of thin plastic. In contrast, the transport box with cooling function is made of thicker plastic, including electronics resulting in their assumed CO_2 eq. of 0.033kg and 0.165kg, respectively.

Ehrenwörtliche Erklärung

Hiermit versichere ich, dass ich die schriftliche Dissertationsleistung selbständig und ohne unerlaubte fremde Hilfe angefertigt habe. Ich habe keine anderen als die in der Arbeit angegebenen Schriften und Hilfsmittel benutzt und die den benutzten Werken wörtlich oder inhaltlich entnommenen Stellen kenntlich gemacht. Insbesondere versichere ich, dass ich nicht die Hilfe von Vermittlungs- oder Beratungsdiensten (Promotionsberater oder Promotionsberaterinnen oder andere Personen) in Anspruch genommen habe.
Weiterhin versichere ich, dass ich keine früheren Promotionsversuche unternommen, Promotionen abgeschlossen oder die Dissertation in gleicher oder anderer Form in einem anderen Versuch oder in einem anderen Prüfungsverfahren vorgelegt habe.

Ingolstadt, November 2023

(Alexander Rave)